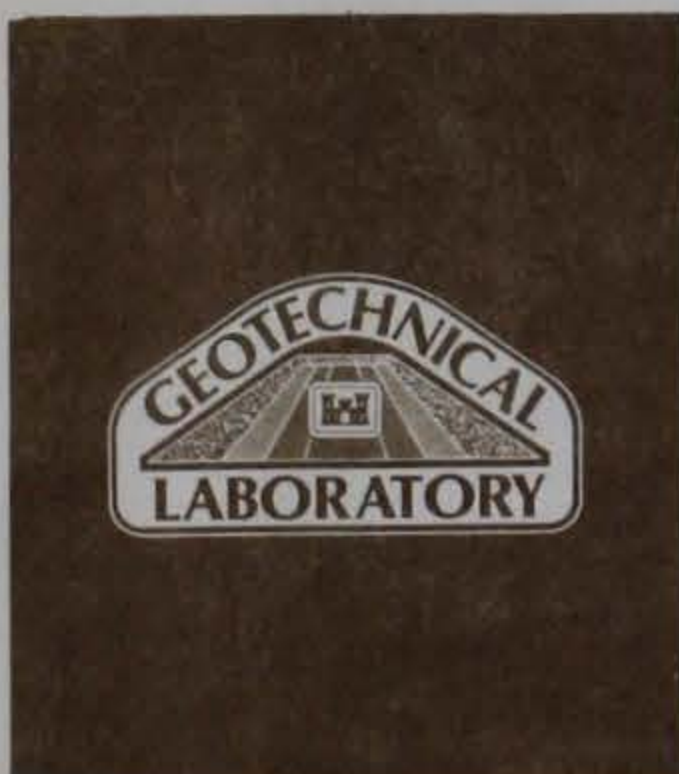
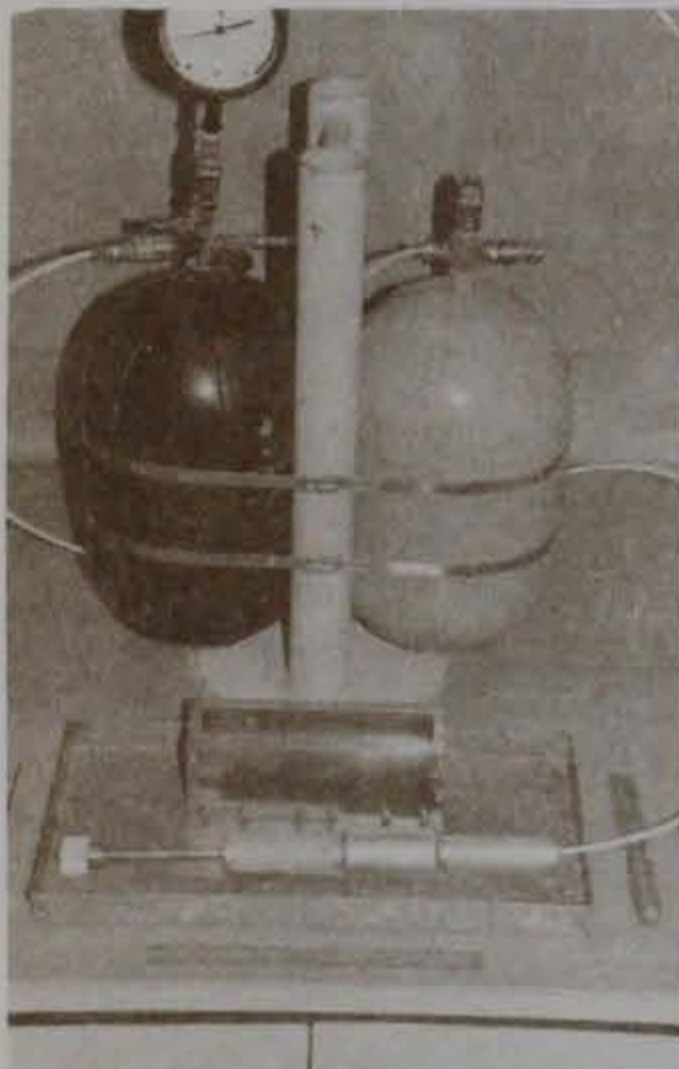
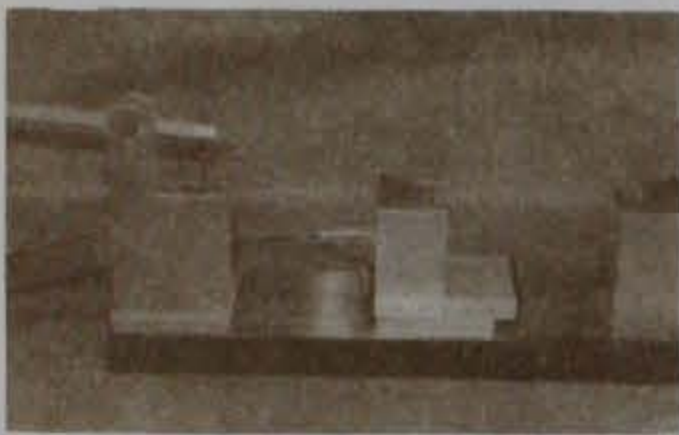
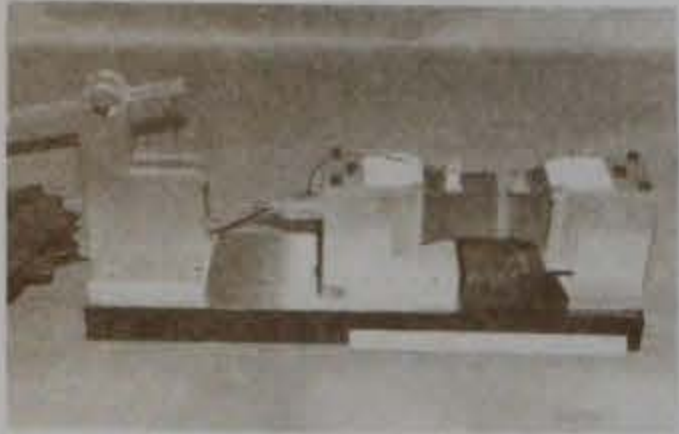


TA7
W34
no. GL-
87-10

ny Corps
ineers

REFERENCE



US-CE-C Property of the
United States Government

TECHNICAL REPORT GL-87-10

UNIAXIAL TENSILE TEST FOR SOIL

by

Daniel A. Leavell, John F. Peters

Geotechnical Laboratory

DEPARTMENT OF THE ARMY
Waterways Experiment Station, Corps of Engineers
PO Box 631, Vicksburg, Mississippi 39180-0631

BOOKS ARE ACCOUNTABLE PROPERTY CHARGED
TO AN INDIVIDUAL BY NAME. PLEASE DO
NOT LEND TO OTHERS WITHOUT CLEARING
YOURSELF.



April 1987

Final Report

Approved For Public Release; Distribution Unlimited

Library Branch
Technical Information Center
U.S. Army Engineer Waterways Experiment Station
Vicksburg, Mississippi

Prepared for DEPARTMENT OF THE ARMY
US Army Corps of Engineers
Washington, DC 20314-1000

Under CWIS Work Unit No. 31211

LSZK # 16376003

TA 7

W/34

no. GL-87-10

Unclassified
SECURITY CLASSIFICATION OF THIS PAGE

REPORT DOCUMENTATION PAGE				Form Approved OMB No. 0704-0188	
1a. REPORT SECURITY CLASSIFICATION Unclassified		1b. RESTRICTIVE MARKINGS			
2a. SECURITY CLASSIFICATION AUTHORITY		3. DISTRIBUTION / AVAILABILITY OF REPORT			
2b. DECLASSIFICATION / DOWNGRADING SCHEDULE		Approved for public release; distribution unlimited.			
4. PERFORMING ORGANIZATION REPORT NUMBER(S) Technical Report GL-87-10		5. MONITORING ORGANIZATION REPORT NUMBER(S)			
6a. NAME OF PERFORMING ORGANIZATION USAEWES Geotechnical Laboratory		6b. OFFICE SYMBOL (If applicable) WESGC	7a. NAME OF MONITORING ORGANIZATION		
6c. ADDRESS (City, State, and ZIP Code) PO Box 631 Vicksburg, MS 39180-0631		7b. ADDRESS (City, State, and ZIP Code)			
8a. NAME OF FUNDING / SPONSORING ORGANIZATION US Army Corps of Engineers		8b. OFFICE SYMBOL (If applicable)	9. PROCUREMENT INSTRUMENT IDENTIFICATION NUMBER		
8c. ADDRESS (City, State, and ZIP Code) Washington, DC 20314-1000		10. SOURCE OF FUNDING NUMBERS			
		PROGRAM ELEMENT NO. CWIS 31211	PROJECT NO.	TASK NO.	WORK UNIT ACCESSION NO.
11. TITLE (Include Security Classification) Uniaxial Tensile Test for Soil					
12. PERSONAL AUTHOR(S) Leavell, Daniel A.; Peters, John F.					
13a. TYPE OF REPORT Final		13b. TIME COVERED FROM 1981 TO 1984		14. DATE OF REPORT (Year, Month, Day) April 1987	15. PAGE COUNT 116
16. SUPPLEMENTARY NOTATION Available from National Technical Information Service, 5285 Port Royal Road, Springfield, VA 22161					
17. COSATI CODES			18. SUBJECT TERMS (Continue on reverse if necessary and identify by block number)		
FIELD	GROUP	SUB-GROUP	Brittle fracture Partially saturated soils		
			Compacted soils Q test		
			Critical state theory (Continued)		
19. ABSTRACT (Continue on reverse if necessary and identify by block number)					
<p>The tensile strength of soil is generally considered small for engineering applications. Yet there are a number of applications where even a small amount of tensile strength can have significant influence on computational results and actual structure performance. For example, the tensile strengths of clays are significant in problems involving low mean normal stresses. Motivation for studying tensile strength comes indirectly from the study of partially saturated soils, as the tensile strength is presumably derived from the suction potential of the soil. This report describes an apparatus for measuring strength of soil in direct tension. Data are presented for compacted Vicksburg silty clay for uniaxial tension and unconsolidated-undrained (Q) compression tests with a view toward proposing criteria to relate tensile and compressive strengths for partially saturated materials.</p> <p>The primary advantage of the apparatus is its ability to apply a uniaxial load through precisely aligned end-grips, which are restricted from rotations about the long axis of the</p>					
20. DISTRIBUTION / AVAILABILITY OF ABSTRACT <input checked="" type="checkbox"/> UNCLASSIFIED/UNLIMITED <input type="checkbox"/> SAME AS RPT. <input type="checkbox"/> DTIC USERS			21. ABSTRACT SECURITY CLASSIFICATION Unclassified		
22a. NAME OF RESPONSIBLE INDIVIDUAL			22b. TELEPHONE (Include Area Code)	22c. OFFICE SYMBOL	

18. SUBJECT TERMS (Continued).

Shear strength
Soil suction
Tensile strength
Triaxial test
Unconsolidated-undrained test

19. ABSTRACT (Continued).

specimen. This design is in contrast to tensile tests for rock and concrete that avoid applying moments to specimen ends by attaching the end-grips to a flexible pulling mechanism. A flexible loading mechanism was viewed as unsuitable for brittle low-strength compacted soils because of difficulties in achieving precise loading alignment. Precise alignment for the tensile device is achieved by mounting one of the end-grips on a commercially available slide table that restricts movement to one direction.

The testing program for compacted Vicksburg silty clay consisted of over 40 tensile tests on specimens having different molding water contents and compaction efforts. Other tests included Q, compaction, Atterberg limits, and suction potential. Comparisons were also made with tensile strengths previously determined for Vicksburg silty clay using the double punch, split cylinder, and hollow cylinder tests.

A major finding of the laboratory investigation was that of all methods used to determine tensile properties, the highest strength and stiffness was obtained from the direct tensile device. Strengths obtained from the hollow cylinder test were comparable to the direct tension test provided that the maximum stress at the interior wall of the cylinder was used as the basis of comparison. Research by other investigators are cited that show similar trends. A model is proposed that relates the strength derived from capillary tension to a fracture law. Using Griffith theory, the tensile strength is related to the cohesion intercept obtained from Q tests. The predicted correlation between compressive and tensile strengths was supported by the experimental data. Further, the strengths from compression and tension tests were correlated with water content relative to optimum, and dry density; however strength did not correlate with suction potential. If similar results are found for other clays, it would appear that the tensile strength of unsaturated soil cannot be viewed as a special case of the effective stress law in which the suction potential is simply treated as a negative pore pressure.

PREFACE

Laboratory investigation of the tensile properties of compacted partially saturated soil and its influence and role in the cracking of embankment dams was authorized by the Office, Chief of Engineers, US Army, under Civil Works Investigation Study (CWIS) Work Unit 31211, "Material Characterization and Analysis of Cracking in Embankment Dams." This investigation was conducted at the US Army Engineer Waterways Experiment Station (WES) during the period January 1981 to August 1984.

The laboratory testing was performed by Mrs. U. Sanders, Mr. D. A. Leavell, and Dr. J. F. Peters, Soils Research Center (SRC), Soil Mechanics Division (SMD), Geotechnical Laboratory (GL), WES. The uniaxial tension test device, laboratory testing procedures, data analysis, and theoretical concepts were developed by Mr. Leavell and Dr. Peters. Suction tests in support of this research were performed by Dr. L. D. Johnson, SMD.

This report was prepared by Mr. Leavell and Dr. Peters under the direct supervision of Mr. G. P. Hale, Chief, SRC, and the general supervision of Mr. C. L. McAnear, Chief, SMD, and Dr. W. F. Marcuson III, Chief, GL.

The Director and the Commander and Director of WES during the preparation and publication of this report were COL Allen F. Grum, USA, and COL Dwayne G. Lee, CE, respectively. Dr. Robert W. Whalin was Technical Director.

CONTENTS

	<u>Page</u>
PREFACE.....	1
CONVERSION FACTORS, NON-SI TO SI (METRIC) UNITS OF MEASUREMENT.....	4
PART I: INTRODUCTION.....	5
Background.....	5
Purpose and Scope.....	8
PART II: EXPERIMENTAL PROGRAM.....	9
Description of Equipment.....	9
Sample/Specimen Preparation.....	9
Testing Procedure.....	10
Commentary on Test Development.....	11
Compression Tests.....	14
PART III: MATERIAL TESTED.....	16
General Description.....	16
Compaction Characteristics.....	16
Suction-Water Content Relationship.....	19
PART IV: TEST RESULTS.....	22
Test Program.....	22
Strength Versus Suction.....	22
Strength Versus Kneading Pressure.....	22
Stress-Strain Characteristics.....	25
Triaxial Compression Test Data.....	27
Comparisons to Published Data.....	31
PART V: DISCUSSION OF RESULTS.....	33
Implications to Strength Theories.....	33
Correlation Between Effective Stress and Suction.....	35
Future Research.....	39
PART VI: SUMMARY AND CONCLUSIONS.....	44
Summary.....	44
Conclusions.....	44
REFERENCES.....	46
TABLES 1-4	
APPENDIX A: TENSILE TEST PROCEDURE.....	A1
Introduction.....	A1
Apparatus.....	A1
Sample/Specimen Preparation.....	A2
Apparatus Preparation.....	A8
Specimen Setup.....	A10
Data Presentation.....	A13
APPENDIX B: TENSILE TEST RESULTS.....	B1

Page

APPENDIX C: SUCTION DATA..... C1
APPENDIX D: TRIAXIAL COMPRESSION TEST DATA..... D1

CONVERSION FACTORS, NON-SI TO SI (METRIC)
UNITS OF MEASUREMENT

Non-SI units of measurement used in this report can be converted to SI (metric) units as follows:

<u>Multiply</u>	<u>By</u>	<u>To Obtain</u>
inches	2.54	centimetres
Fahrenheit degrees	5/9	Celsius degrees or Kelvin*
tons (force) per square foot	95.76052	kilonewtons per square metre
pounds (force) per square inch	6.89476	kilonewtons per square metre
pounds (force) per cubic foot	0.15709	kilonewtons per cubic metre

* To obtain Celsius (C) temperature readings from Fahrenheit (F) readings, use the following formula: $C = (5/9)(F - 32)$. To obtain Kelvin (K) readings, use: $K = (5/9)(F - 32) + 273.15$.

UNIAXIAL TENSILE TEST FOR SOIL

PART I: INTRODUCTION

Background

Test methods

1. Over the years different test configurations and methodologies have been used to determine the tensile strength of soil (Haefeli 1950; Al-Hussaini and Townsend 1973). However, most of this work did not consider the uniaxial stress-strain response of soil in tension. Also, the most common test methods involved loading configurations that created inhomogeneous stress conditions from which the tensile stress at failure had to be computed indirectly. These indirect tests suffer the disadvantages of (a) requiring a stress analysis for determining strength that in turn requires the stress-strain properties of the material and (b) creating mixed compression and tension that invokes a complex mode of failure.

2. The split cylinder (Brazilian) test is an example of an indirect test that is simple, quick, and easy to use. Total stress tensile strengths for soils have been obtained from the split cylinder test by Uchida and Matsumoto (1961), Hudson and Kennedy (1968), Townsend et al. (1969), Narain and Rawat (1970), Satyanarayana and Rao (1972), Al-Hussaini and Townsend (1974), Ramanathan and Raman (1974), Krishnayya and Eisenstein (1974), Krishnayya et al. (1974), Moore (1975), and Bai et al. (1982). Researchers have also used other indirect tests such as the double punch test (Fang and Hirst 1973; Al-Hussaini and Townsend 1974) and beam (flexure) test (Leonards and Narain 1963; Satyanarayana and Rao 1972; Ajaz and Parry 1975 and 1976; Ajaz 1980) to measure tensile strengths. A major disadvantage of these tests is that they employ a combination of tensile and compressive stresses with no direct way of measuring strains. With the exception of the flexure test by Ajaz and Parry (1975 and 1976), the tensile stress at failure is computed indirectly using linear elasticity, making its application to soil questionable and the development of an actual stress-strain relationship impossible.

3. The hollow cylinder test has been used to determine tensile stresses and strains in soil (Al-Hussaini and Townsend 1974; Bai et al. 1982). The

tensile strength at failure is assumed to be the tensile stress at the specimen's mean radius with this stress being computed from Lamé's solution of stresses in a thick-walled pressure cylinder. However, it is well known that the stress field through a cylinder wall is not uniform; to estimate the maximum tensile stress, the stress-strain response of the material must be known. The hollow cylinder test has the advantage that all stresses are tensile and the average stress in the specimen wall is directly related to the inner and outer pressure acting on the specimen.

4. The direct tensile test has the advantage that it is the only test where, in principle, all induced stresses and strains are homogeneous and can be computed from direct measurements without making assumptions on the material's stress-strain response. In practice, the test has the drawback that it is virtually impossible to apply a tensile stress to the specimen ends without inducing a nonuniform stress field. Thus, the major challenge in designing a direct tensile loading device is in developing a suitable end-gripping technique. Tschebotarioff et al. (1953), Hasegawa and Ikeuti (1964), and Ajaz and Parry (1974 and 1975) overcame some of the problems associated with this test and were able to give the complete stress-strain response for some compacted soils. Although similar tests were performed by Andrei (1961), Satyanarayana and Rao (1972), Lushnikov et al. (1973), and Bai et al. (1982), only ultimate tensile stresses were reported.

5. Tschebotarioff et al. (1953) appears to have been the first to carry out a systematic study of tensile strength for compacted soils. Stress-strain data were obtained from compacted clay specimens having a shape similar to the briquette used for testing mortar mixes in tension but with unwieldy dimensions: the length of the specimen being 132 cm with a reduced rectangular center section having dimensions of 15.2 by 7.6 by 40.7 cm. The specimen was tested horizontally and loaded through metal supports that encased the edges of its oversized bell-shaped ends. The center section of the specimen was supported by ball-bearing rollers to eliminate sagging. Axial deformations were obtained from extensometers attached to the reduced center section of the specimen.

6. The apparatus developed by Hasegawa and Ikeuti (1964) used compacted clay specimens that were 19 cm long with a reduced center section 2.0 by 2.0 by 5.0 cm. This test was also performed on a horizontal specimen; however loading was applied through small metal plates that were embedded in the

enlarged ends. The specimen was supported by a bed of mercury and had two small ceramic markers mounted in the gage length that were monitored with a cathetometer to determine displacements. It was found that most tests failed near the location of the embedded metal loading plates making their gripping technique only partially effective.

7. The test devised by Ajaz and Parry (1974) used a specimen that had a fairly complicated geometry but, generally speaking, had the same shape as those previously mentioned, i.e. enlarged bell-shaped ends with a reduced center section. The specimen was positioned vertically to eliminate any need for support of the center section. An optical device was used to measure displacements in the strain controlled tests. For load controlled tests, lead shot was embedded in one face of the specimen and monitored radiographically to determine the uniformity of the strain field throughout the specimen. Failure always occurred in the reduced section of the specimen where the strains were confirmed by radiographs to be uniform.

8. Direct tensile triaxial tests performed by Conlon (1966), Bishop and Garga (1969), and Parry and Nadarajah (1974) allowed specimens to be tested in either a drained or undrained condition. While this testing technique eliminated the end-gripping problem and allowed accurate measurement of tensile stresses, there was no provision for measuring accurate strains.

Failure laws

9. Despite the large number of investigations carried out on tensile strength, relatively little systematic theory has been developed on the failure of soils in tension. The majority of the tensile tests performed involved measurement of total stresses rather than effective stresses, making it difficult to develop a comprehensive theory. This deficiency comes in part from the interest in determining the tensile strength of partially saturated compacted materials. Thus, deficiencies in understanding tensile strength parallel deficiencies in understanding partially saturated materials.

10. Various researchers have attempted to predict the tensile strength of soil using failure criteria such as Mohr-Coulomb, Griffith, and modified Griffith as summarized by Lee (1968) and Obert and Duvall (1967). Most have found that Mohr-Coulomb overpredicts tensile strength, whereas Griffith predicts excessive curvature in the compressive region of the strength envelope. A more applicable approach outlined by Lee (1968) used the Griffith criteria with modifications by McClintock and Walsh, and Brace (modified Griffith

theory). Bishop and Garga (1969) and Shen (1982) used the modified Griffith failure criteria to predict the failure of blue London clay and lateritic clay, respectively, and found it to work quite well.

Purpose and Scope

11. The purpose of this study was to determine the uniaxial stress-strain response of compacted partially saturated soil in total stress tension and how this response compared to unconsolidated-undrained (Q) triaxial compression test data. The nature of this study required the development of an apparatus to test soil in uniaxial tension as well as special testing procedures and techniques. A chronology of the test's developmental phase, detailed description of the equipment, and testing procedures are presented. The test results are compared with published data for both direct and indirect tensile tests for soil.

PART II: EXPERIMENTAL PROGRAM

Description of Equipment

12. The direct tensile test equipment developed for this study consists of two gripping jaws, a rigid base, a slide table, a linear variable displacement transformer (LVDT), a load cell, and a loading mechanism. One of the gripping jaws is rigidly attached to the base while the other is attached to the slide table. The slide table provides a precise alignment of the pulling force along the longitudinal axis of the specimen. The LVDT is mounted along a reduced section of the specimen at a gage length of 5.0 cm and provides a means of measuring axial displacements. The load cell is attached to the jaw that is mounted on the slide table ensuring that the load measured is that which is actually applied to the specimen. Loading of the specimen is accomplished through a deadweight pulley system; however other loading systems (pneumatic or displacement) are readily adaptable to the device. The assembled test device with its loading system is shown in Figure 1.

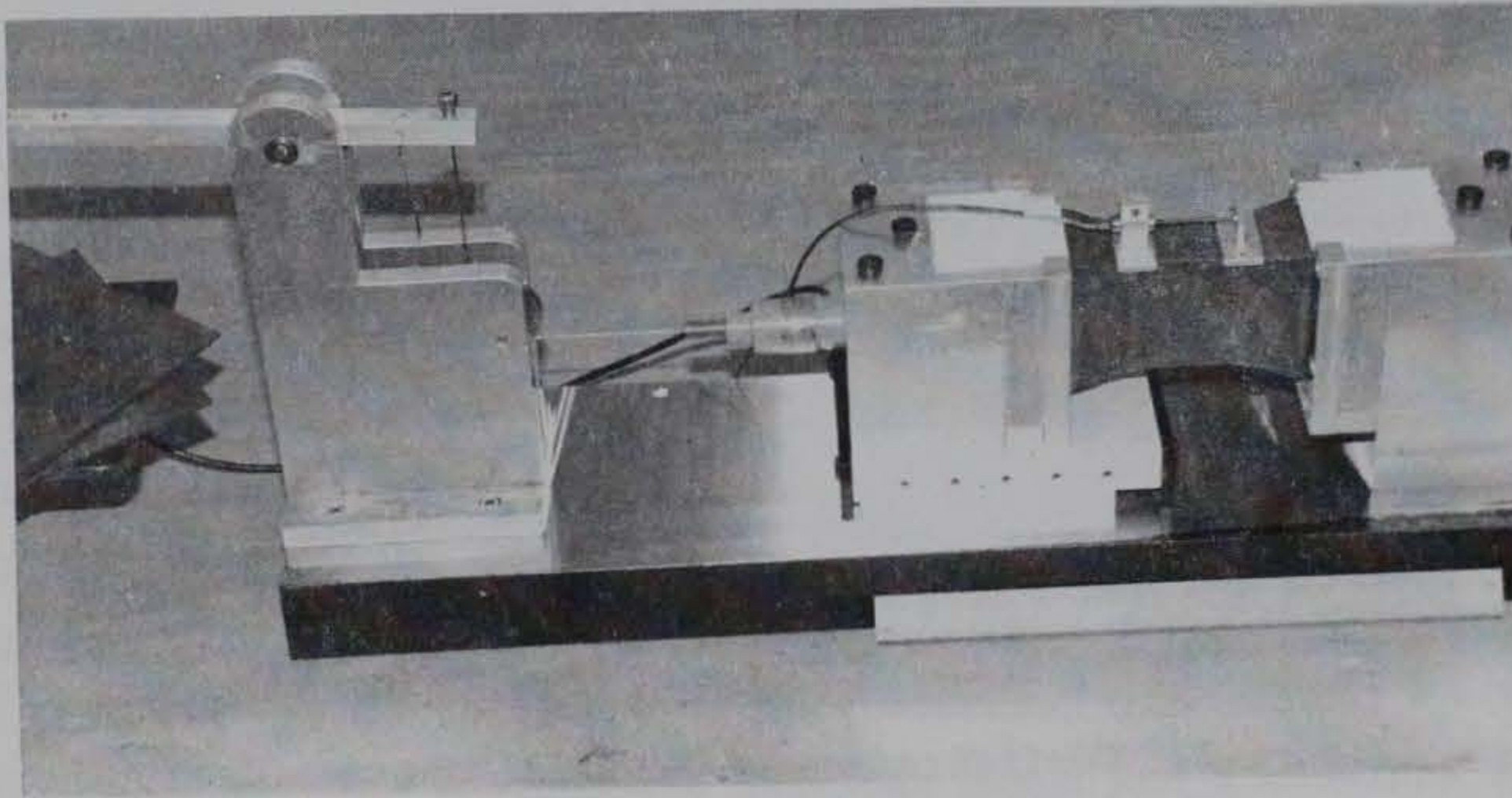


Figure 1. Tensile testing apparatus and deadweight loading system

Sample/Specimen Preparation

13. Specimens tested in this study were first compacted in a brick shape with dimensions 7.6 cm high, 5.1 cm wide, and 22.9 cm long. After compaction, a central section 5.0 cm long was trimmed to dimensions 3.8 cm wide by 6.4 cm high. In addition, tapered notches were trimmed into the specimen

ends to obtain the correct load transfer from the gripping jaws to the specimen (see Figure A7). Details of sample preparation and specimen trimming are presented in Appendix A.

14. Material for a test series was batched at a specified water content and allowed to cure for a minimum of 24 hr. Predetermined equal weights were taken from the batched material and stored in seven watertight containers. From this preweighed material, a sample consisting of seven layers was compacted in a rectangular mold using the Waterways Experiment Station (WES) pneumatic kneading compactor equipped with a square tamping foot with an area of 6.45 cm^2 . The compacted sample was then trimmed to the configuration shown in Figure 2 and allowed to cure in a sealed container for 24 hr before testing. The curing process tended to promote uniform distribution of water throughout the specimen.

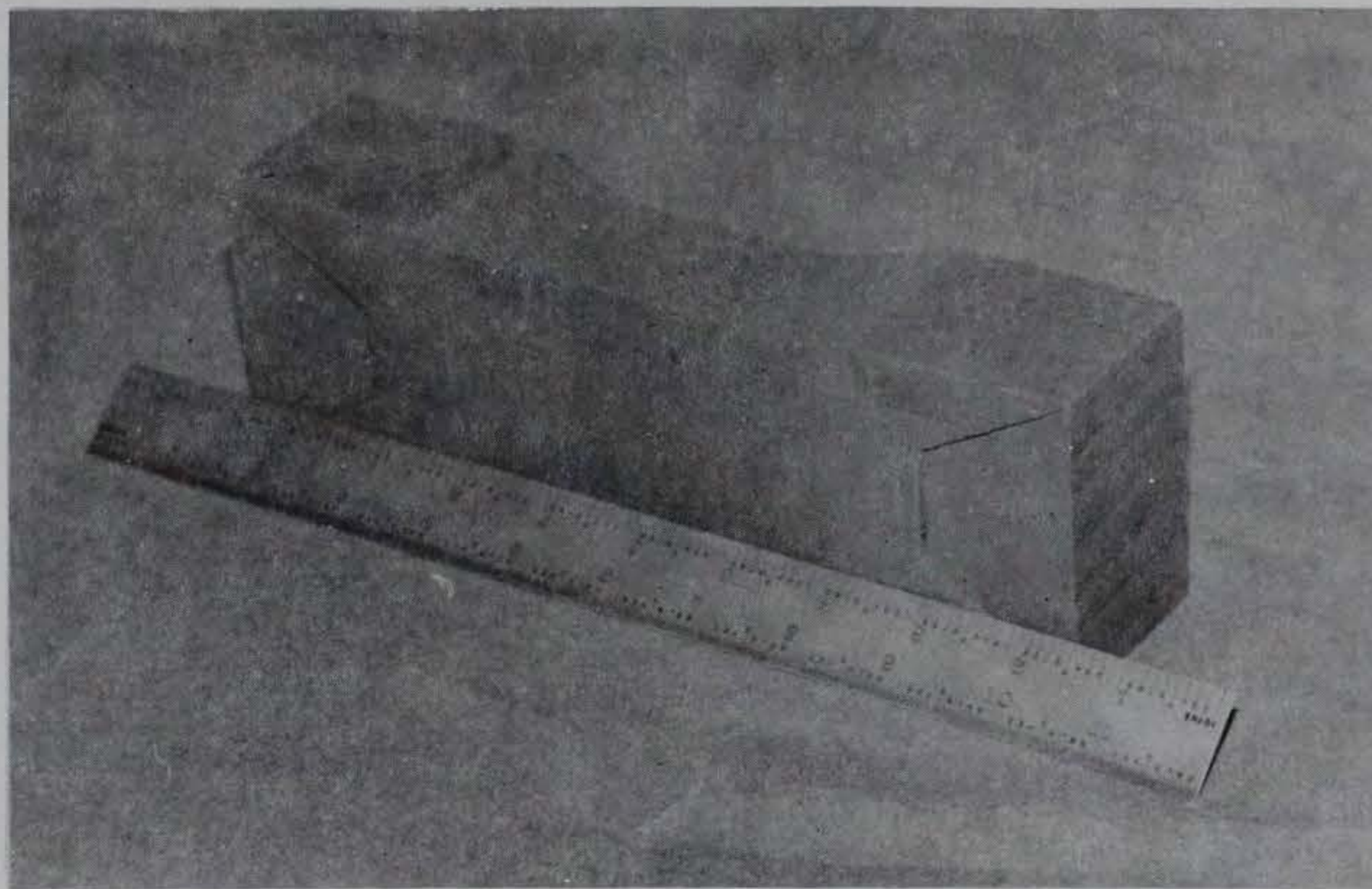


Figure 2. Configuration of tensile specimen upon completion of the trimming procedure

Test Procedure

15. Before placement of the specimen in the grips of the testing device, approximately 5.0 cm of each end was dipped in molten wax (approximately 190°F), which hardens into a thin coating. Each grip was then lined with filter paper, the specimen was placed in the test device, and the grips

were filled with Hydrostone. The filter paper facilitated removal of the Hydrostone and cleaning of the device at completion of the test. The remainder of the specimen (not in the grips) was covered with petroleum jelly. Finally, the LVDT was installed in the specimen's reduced section at a 5.0-cm gage length. After placement of the specimen in the testing device, all electronic equipment was checked for calibration. The specimen was then incrementally loaded (stress-controlled) at 1-min intervals with load and deformation readings being monitored continuously until failure occurred. A somewhat arbitrary loading program of 2.7 kN/m^2 per increment was selected to ensure that all tests would be comparable even though other loading schemes might match field behavior better. Figure 3 shows a typical plot of load versus deformation as monitored during the test. At conclusion of the tensile test, a water content sample was obtained from the fracture zone that was normally located in the central portion of the specimen; the water content was used to determine the amount of water lost during specimen preparation and testing. A detailed test procedure is given in Appendix A.

Commentary on Test Development

16. The brittle behavior of soil in tension magnifies test design problems; errors normally considered as acceptable in Q tests limit the feasibility of the tensile test. These problems include: specimen alignment, twisting of specimen during loading, stress concentrations caused by the gripping method, specimen repeatability and homogeneity, and difficulties associated with small strain measurements. Problems in alignment and twisting were solved through proper equipment design and construction, while stress concentrations were reduced by using appropriate specimen dimensions, shape, and gripping technique. The appropriate specimen shape and dimensions were chosen based partly on general experience with testing materials in tension and partly from trial and error. Uniformity and repeatability of specimens were obtained through controlled batching, compaction, and trimming procedures.

17. The gripping technique was more problematic because it was found that even with the reduction of the central area, the specimen tended to fail within the end-grips. The cause of the premature failure in the end-grips was related to a number of factors that were identified through a developmental

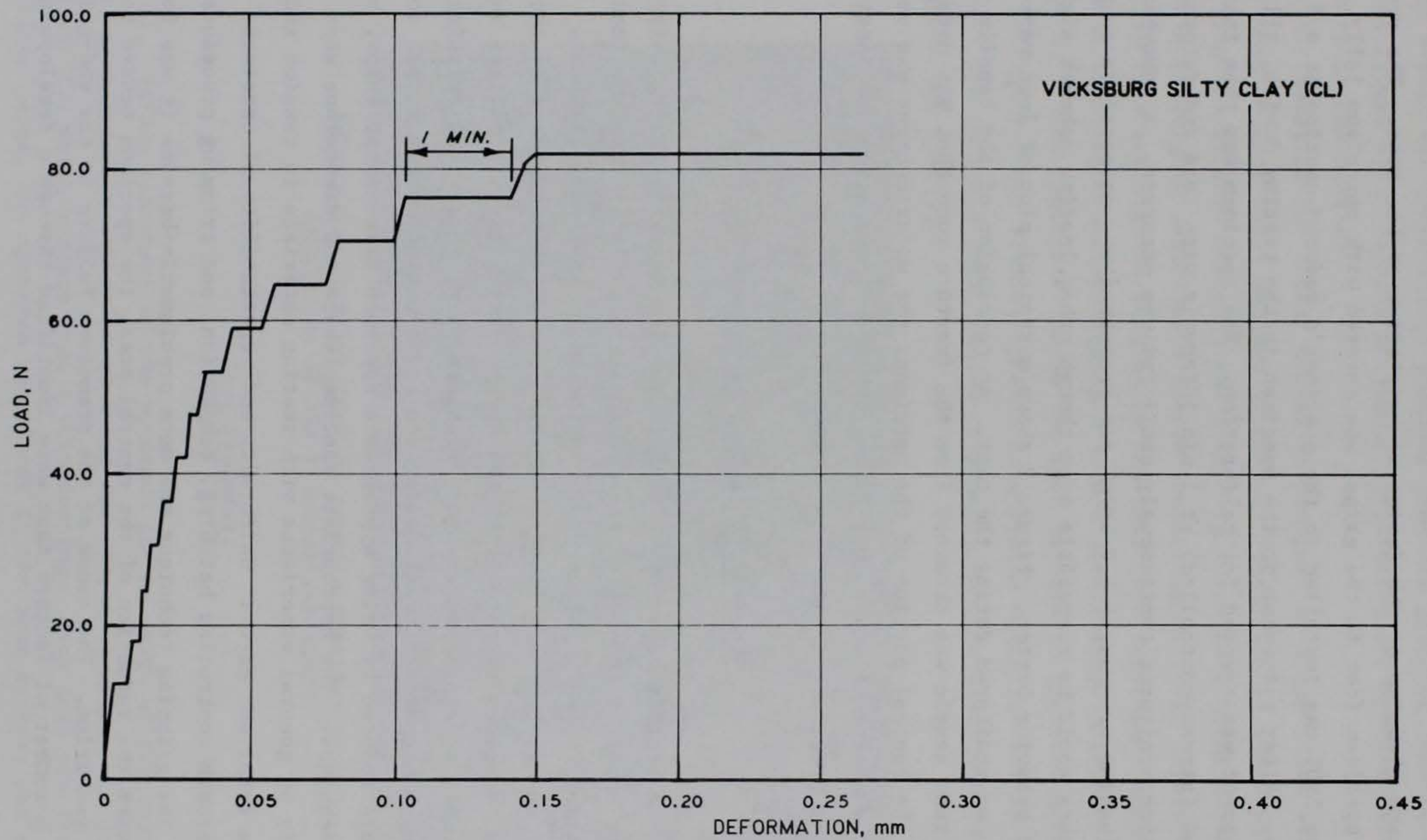


Figure 3. Typical plot of load versus deformation for direct tensile test on Vicksburg silty clay

test program consisting of 33 tests. During this test series, various restraining materials and gripping configurations were used. A chronology of the testing methodology development, consisting of the type of restraining material used, results and analysis of each test, and the associated corrective action taken, is presented in Table 1. From a mechanical standpoint, the optimal gripping technique called for satisfying two conflicting requirements: the load must be applied as a uniform stress to avoid a stress concentration at the edge of the gripping jaw, and the alignment of the load must be maintained precisely. The first requirement implies a flexible load transfer medium, whereas the second requirement implies a rigid medium. Other factors considered in determining the restraining material are its toxicity, workability, availability to most soil laboratories, and ease of preparation and cleanup of the test device. Two materials that satisfied these requirements were wax (e.g. paraffin-microcrystalline mixture) and Hydrostone.

18. Hydrostone and wax were first tried independently as load transfer materials but both were unsuitable. Wax permitted too much movement between the gripping jaws and specimen. As the wax cooled, it shrank nonuniformly away from the specimen ends causing an uneven gripping surface. Upon loading, either the specimen ends completely slipped from the wax or failure occurred in the grips. Hydrostone, a water-based mixture, allowed the specimen ends to have access to free water while it cured, thereby reducing soil strength and causing rupture to occur in the specimen ends instead of the gage length. Also, there was evidence that stress concentrations resulting from the large difference in stiffness between Hydrostone and soil caused failure of the specimen at the edges of the grips. The Hydrostone had the advantage of high strength, rigidity, and simplicity of use, and it was therefore decided to mitigate its disadvantages through improved specimen preparation techniques.

19. The combined use of Hydrostone and wax, in addition to a tapered notch in the specimen ends, gave acceptable results. A thin wax coating was first applied to the specimen ends, isolating them from the free water in the Hydrostone. Hydrostone was then used to encapsulate the specimen ends, resulting in a rigid gripping media. Upon curing, the Hydrostone tended to expand and then clamp the wax to the specimen ends, resulting in the required gripping pressure and alignment. The tapered slots carved in the specimen ends redistributed the gripping stresses with minimal movement during loading and consequently increased the gripping strength.

20. The measured strains were on the order of 1×10^{-4} cm/cm, requiring a precise measuring technique. Various measuring instruments and methods for mounting these instruments were used as described in Table 1. However, a LVDT with a range of ± 1.25 mm press-mounted at a 5.0-cm gage length in the reduced center section of the specimen provided reproducible results with the necessary precision.

21. A problem that always exists when measuring small quantities is that the desired measurement can be easily obscured by phenomena that are otherwise insignificant. For example, evaporation after completion of the test setup caused strain from shrinkage of the specimen (see Figure 4). Evaporation of water from the test specimen while it was being compacted and placed in the test apparatus is inevitable as indicated by the differences in initial and final water contents. This water loss tended to affect both the accuracy of the strain measurements and test reproducibility. In wetter specimens, the shrinkage strains exceeded strains caused by loading, making interpretation of test results impossible. To eliminate the problem, the surface of the specimen that was not encapsulated in Hydrostone was coated with petroleum jelly. The petroleum jelly was viscous enough not to penetrate the specimen's surface and affect its strength. It can be seen in Figure 4 that after application of the petroleum jelly, the shrinkage of the specimen stopped, implying that the specimen's water content was stabilized.

Compression Tests

22. The Q tests were performed on cylindrical specimens trimmed from rectangular-shaped samples compacted in the tensile test mold. A series of three specimens was tested from each rectangular-shaped sample using confining pressures of 50, 145, and 290 kN/m^2 . The specimens were trimmed so that the longitudinal axis was perpendicular to the compaction layers. Thus, the maximum principal stress in the Q test corresponded to the zero stress direction in the tensile test. The specimens were tested under strain control using the Q test procedures presented in EM 1110-2-1906 (Dept. of the Army, Office of the Chief of Engineers 1970). The Q test data can be found in Appendix D.

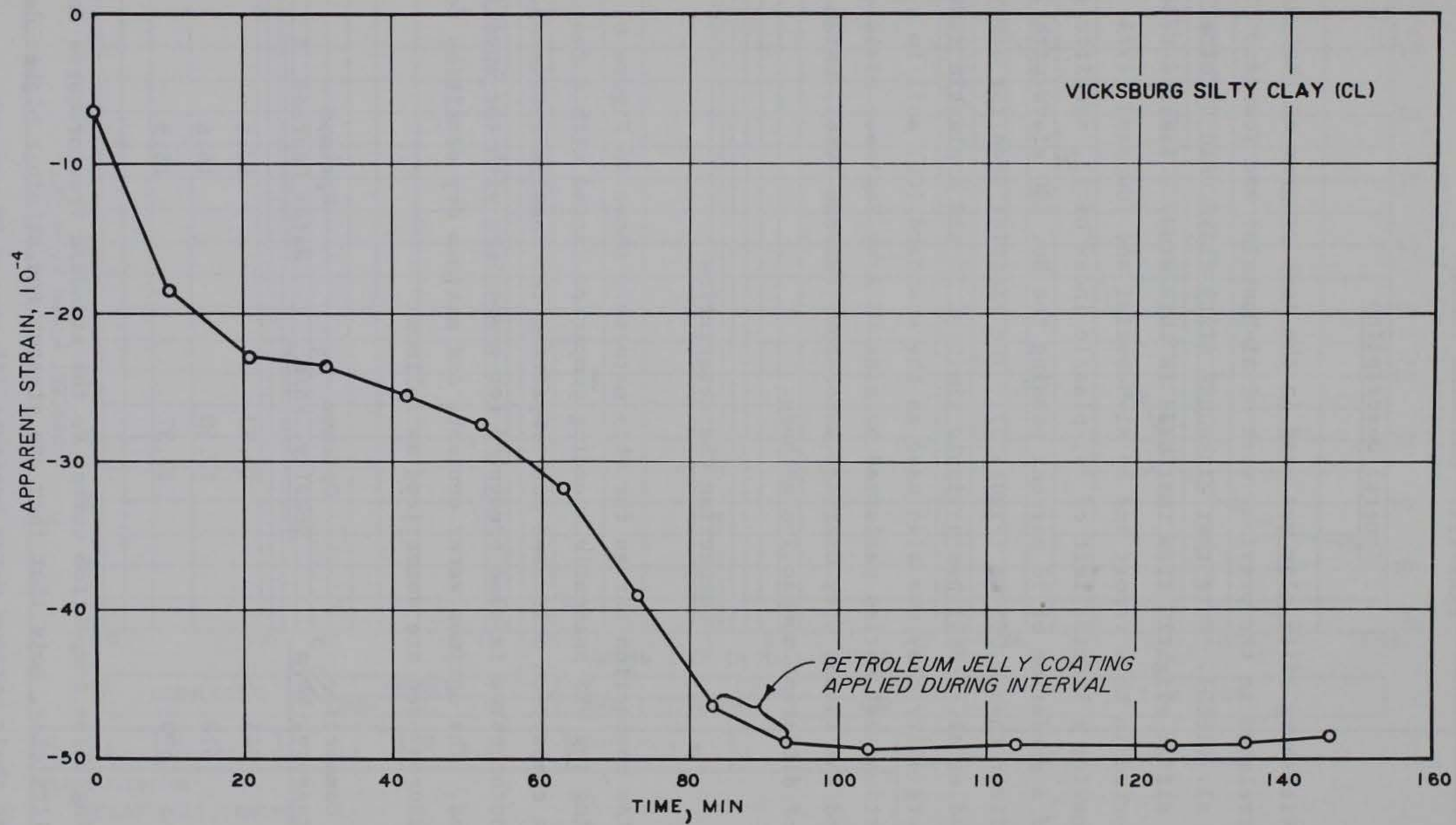


Figure 4. Straining (due to evaporation) in a compacted Vicksburg silty clay specimen during specimen setup

PART III: MATERIAL TESTED

General Description

23. Vicksburg silty clay was used in the test program so that data could be correlated to the previous work of Al-Hussaini and Townsend (1974) and Seed et al. (1960). Note that Vicksburg silty clays used by other researchers differ slightly from that used in this study. Tensile test results reported in this report and by Al-Hussaini and Townsend (1974) are for a material having a liquid limit of 34, plastic index of 13, specific gravity of 2.68, and a gradation of 98 percent passing the No. 200 sieve with 20 percent being finer than 0.005 mm (Figure 5). The material used for compression tests by Seed et al. (1960) had a liquid limit of 35 and a plastic index of 19. Vicksburg silty clay was also used as the standard (CL) soil in a round-robin compaction test series performed by nine US Army Engineer Division laboratories and the Kansas City District laboratory (Strohm 1966), which allowed comparison of different compaction methods.

Compaction Characteristics

24. The compaction curves for this material, shown in Figure 6, were obtained using the WES pneumatic kneading compactor fitted with a foot 2.54 cm square and a compaction mold used for compacting the tensile specimens. A standard Proctor curve is also presented for comparison with the kneading compactor curves. The optimum water contents and maximum dry densities for compaction pressures used are summarized as follows:

<u>Compaction Pressure, kN/m³</u>	<u>Optimum Density, kN/m³</u>	<u>Optimum Water Content, %</u>
345	16.93	17.6
518	17.50	16.6
690	17.37	15.9

When comparing these compaction curves to the standard Proctor curve for Vicksburg silty clay, note that they are steeper and attain a higher degree of saturation at their optimum water contents (85 versus 80 percent,

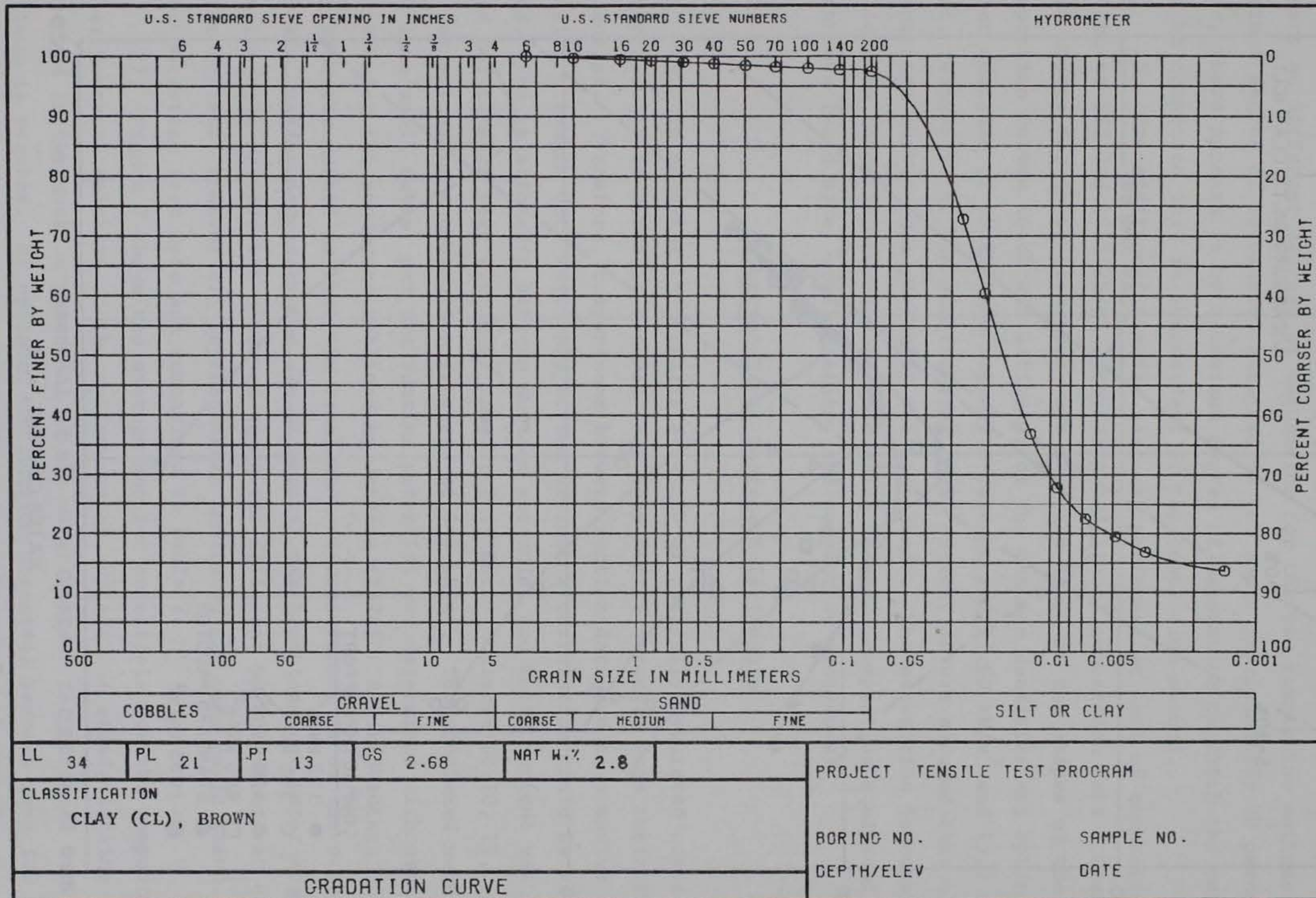


Figure 5. Gradation curve for Vicksburg silty clay

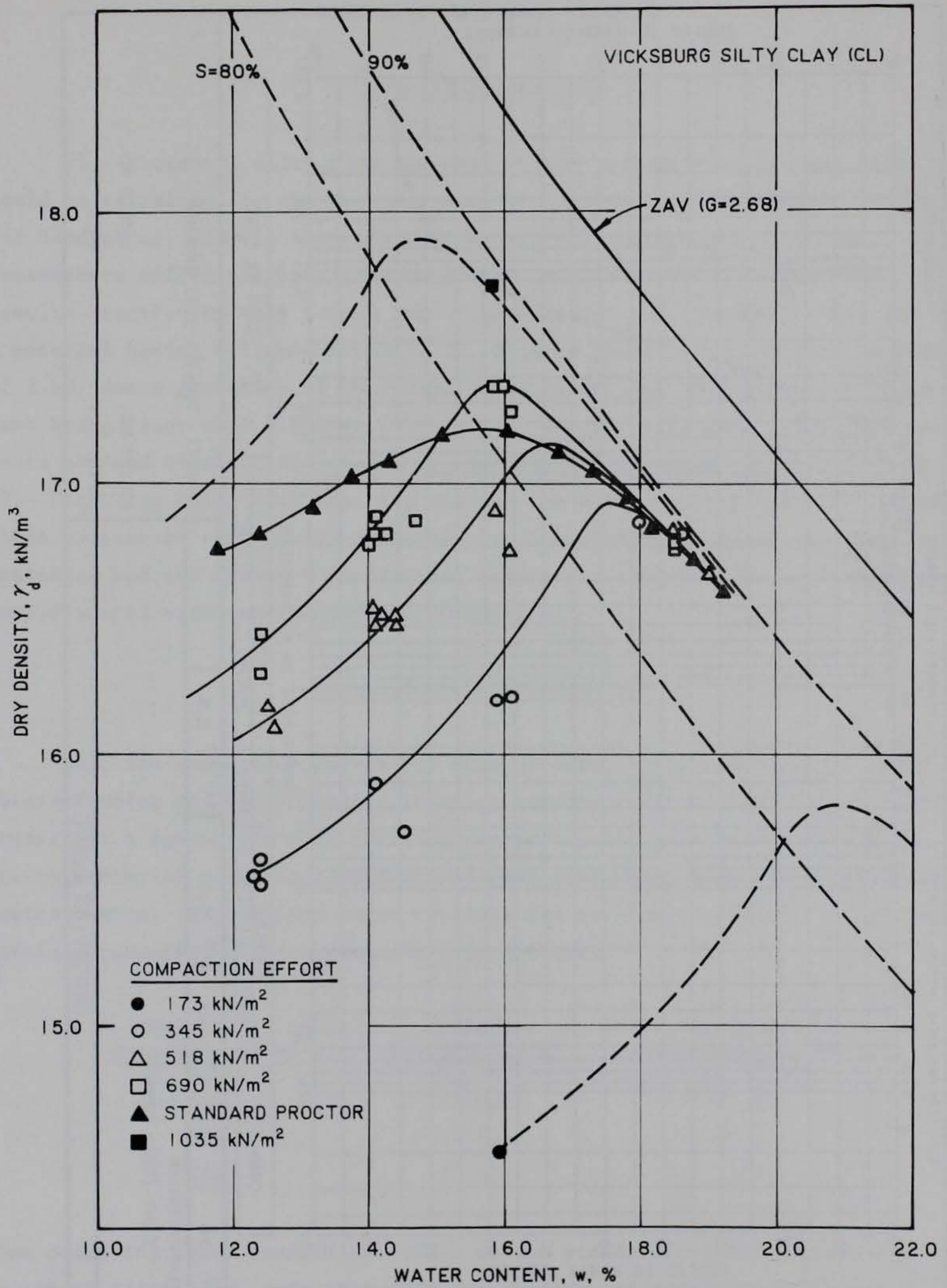


Figure 6. Compaction curves for Vicksburg silty clay

respectively). It is interesting that although the optimum water content occurs at different degrees of saturation for the two compaction methods, the maximum degree of saturation attained is the same, approximately 90 percent. Thus, there appears to be a maximum degree of saturation to which the material can be compacted that is independent of the compaction method.

25. One additional tensile test was performed at each of compaction pressures 173 and 1035 kN/m², providing additional compaction data. Compaction curves for these pressures were sketched based on the shapes of the other compaction curves to obtain estimates of the maximum densities and optimum water contents of 15.82 kN/m³ and 21.8 percent and 17.90 kN/m³ and 15.2 percent, respectively. In constructing these curves, it was assumed that all compaction curves have generally the same shape. The assumption is considered valid when comparing curves obtained using the same compaction equipment and technique (mold size, configuration, and compaction procedure).

Suction-Water Content Relationship

26. In studying the tensile strength of partially saturated compacted materials, it is normally assumed that they derive strength from their suction potential. Therefore, comparisons between suction data and compressive and tensile strength data were made to see if such a correlation could be verified. The relationship between suction potential and water content was developed for tensile test specimens compacted at water contents of 10, 12, 14, and 18 percent using a compaction pressure of 345 kN/m². The specimens were trimmed into small cubes, and the suction potential was determined with psychrometers using the procedure outlined by Johnson (1974). A disadvantage of the psychrometer method is that the resolution of measurement is on the order of 100 kPa, making necessary the use of several psychrometers per water content. Considerable scatter was observed among the different psychrometers at each water content; however all psychrometers indicated the same basic trend. Suction potential test data are summarized in Table 2.

27. Figure 7 shows the average suction potentials for the compacted water contents relative to the optimum water content. A steady decline is observed in the suction potential as the water content is increased until optimum is reached. At optimum, the suction potential becomes very low (see discussion in Appendix C). Sufficient data were not obtained to determine the

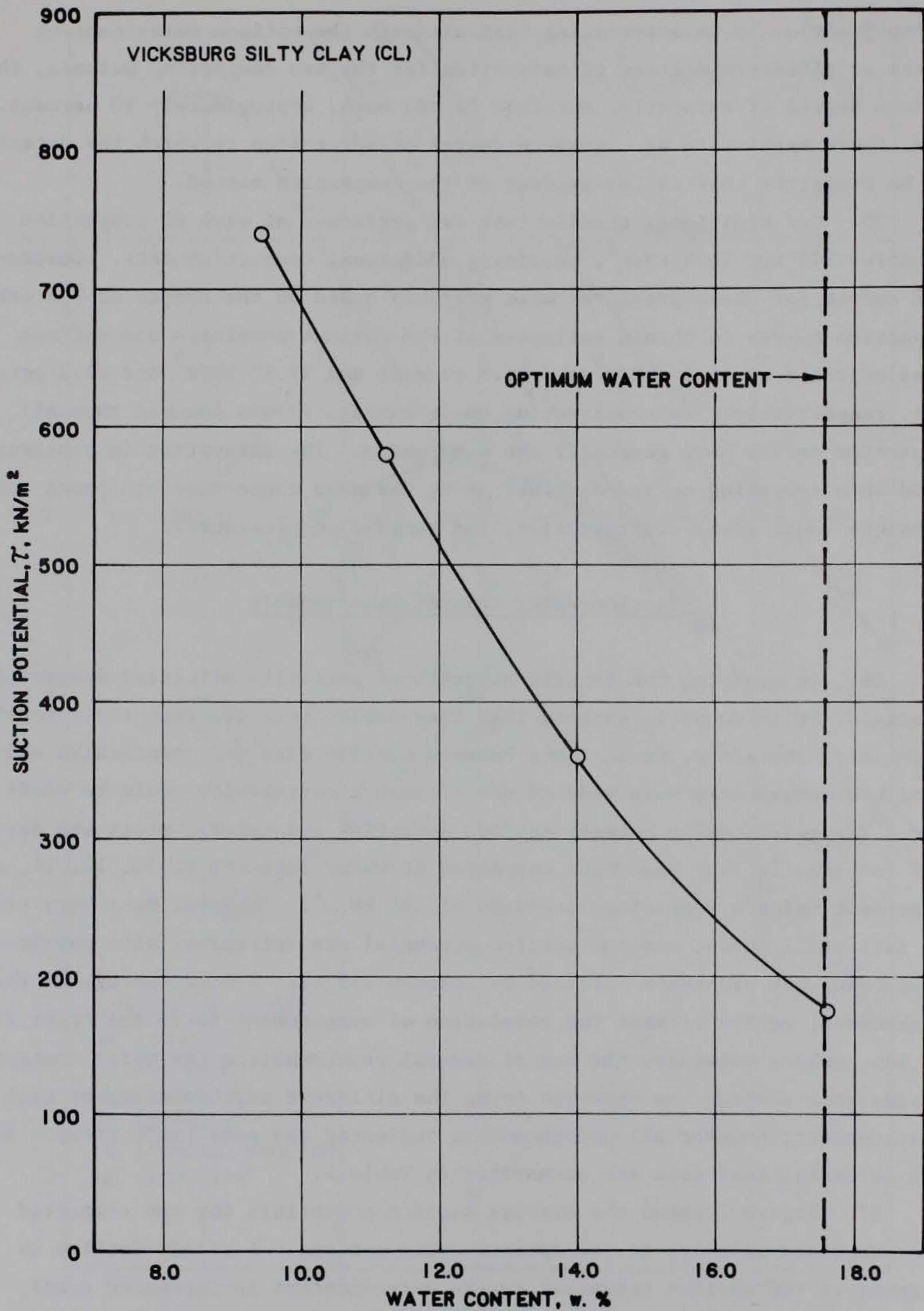


Figure 7. Suction potential versus optimum water content for Vicksburg silty clay (345 kN/m² compaction pressure)

influence of compaction effort on the suction versus water content relationship.

PART IV: TEST RESULTS

Test Program

28. The test data from the main series of direct tensile tests performed on Vicksburg silty clay are presented according to specimen water content in Table 3. The main series was separated into four groups with material in each group being batched at water contents of 12, 14, 16, and 18 percent. Each group contained a minimum of two specimens at each of these compaction pressures—345, 518, and 690 kN/m². In general, the test data shown in Table 3 appear to be consistent and repeatable. However, a noticeable decrease from the initial to the final water content was observed that is attributed to water loss during specimen compaction, trimming, and setup.

Strength Versus Suction

29. Figure 8 shows an increase in tensile strength as the material's suction potential increases, indicating that the tensile strength depends on suction potential. Also shown is a reduction in tensile strength starting at the transition of the water content from dry to wet of the optimum. Thus, the suction-strength relationship consists of two parts: (a) dry of optimum where the strength is nearly constant, and (b) wet of optimum where the strength falls off rapidly. The extrapolation of behavior to zero suction is based on the general relationship between water content and strength observed for specimens at other compaction efforts for which suction measurements were not obtained.

Strength Versus Kneading Pressure

30. Figure 9 shows that the tensile strength increases with compaction pressure until the water content is wet of optimum, where a sharp decrease in tensile strength occurs. The strength loss on the wet side of optimum is often related to "overcompaction" that occurs when the degree of saturation is great enough to permit excess pore pressures to develop. It was also observed that when compacting wet of optimum, the compaction foot tended to push material laterally rather than compress material in a punching manner as for

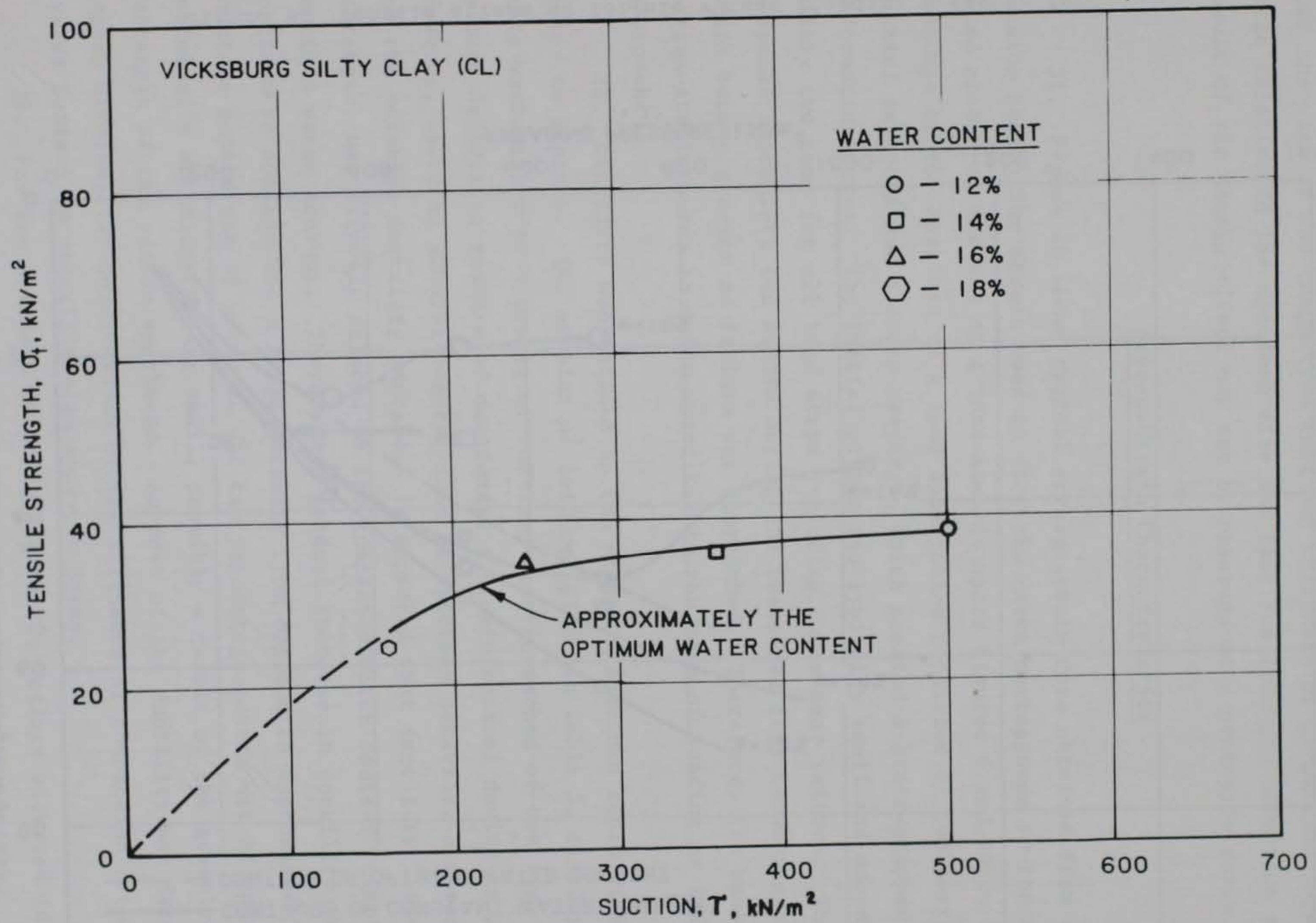


Figure 8. Tensile stress at failure versus suction potential for Vicksburg silty clay contoured with respect to water content

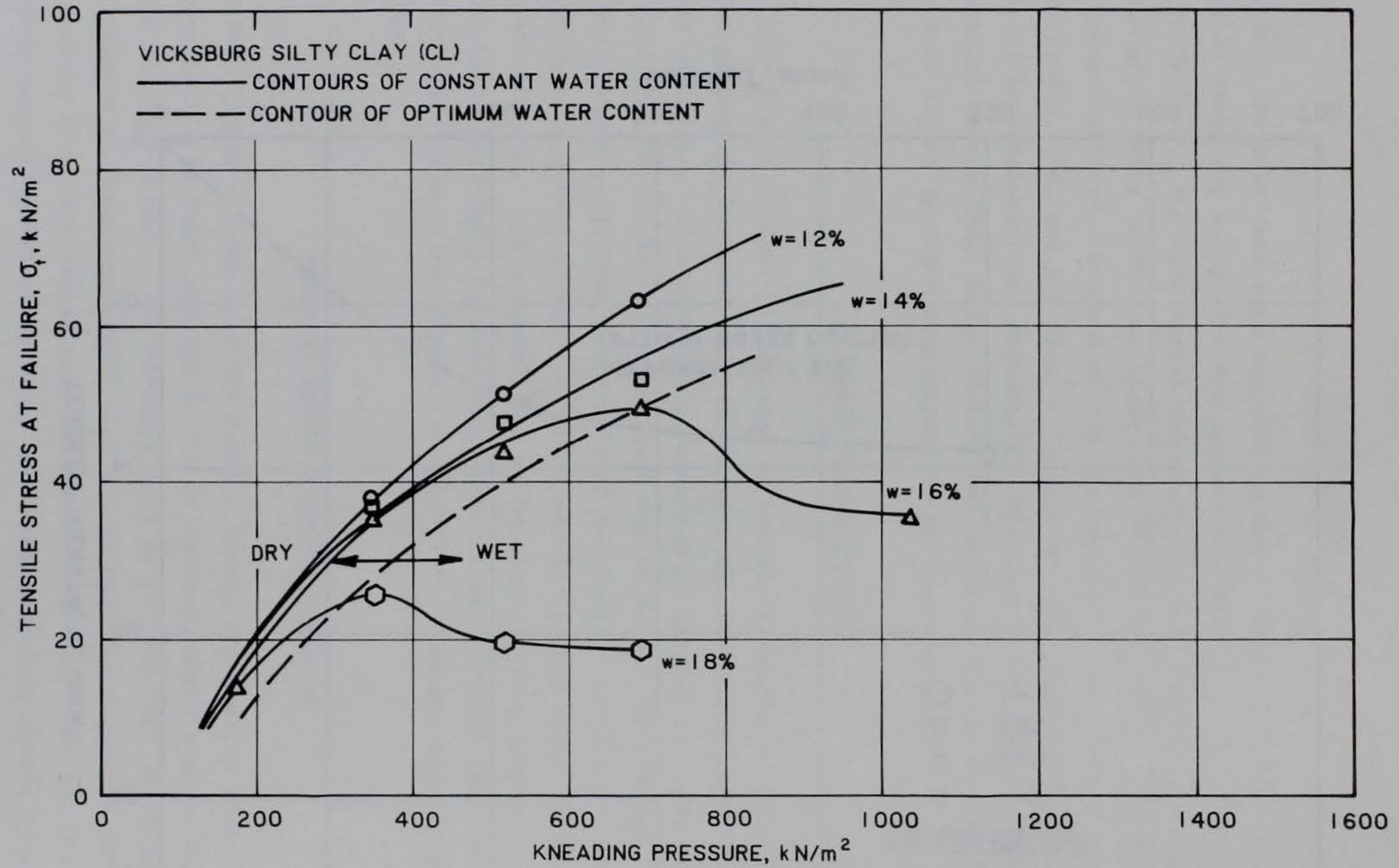


Figure 9. Tensile stress at failure versus kneading pressure for Vicksburg silty clay

the dryer material. The shearing action in the wet material may damage the specimen and make it weaker as the compaction pressure is increased. Note that the size of the compaction foot and thickness of compaction layer are large relative to the specimen size and that the strength reduction as a result of the damage effect may not be observed at a prototype scale.

Stress-Strain Characteristics

31. Figure 10 shows typical stress-strain data obtained from the direct tension test. The strain used to plot the curve corresponds to the accumulated strain at the end of a load step (compare Figures 4 and 10). The response of the specimen to a load application consisted of two parts, an initial response and a creep response, which created a stair-stepped load-deformation curve. The initial strain was typically small and was approximately the same for all load steps including those near failure. The creep response represents the strain during the sustained load between each step, which became greater as failure was approached. Therefore, the measured stress-strain curve is quite sensitive to the rate of loading as failure is approached.

32. Ductility was defined as the strain a specimen could withstand prior to rupture. The strains at failure, given in Table 3, display considerable variability as a result of the load-control method of testing. To obtain a more definitive measure of ductility, a strain control device is preferable. However, based on general observations of specimen behavior, a clear picture of the relative ductility emerged. It appeared that ductility, like tensile strength, was directly related to the compacted water content relative to optimum water content. There was a gradual increase in ductility from dry of optimum to optimum and a large increase from optimum to approximately two percentage points wet of optimum. At two percentage points wet of optimum, the material's ductility became small, possibly a result of the greatly reduced strength of the wetter specimens. As most of the ductility was derived from creep strains, the observations of the influence of compaction pressure and water content on ductility also apply to creep.

33. For the specimen shown in Figure 10, failure occurred in the tapered portion of the specimen between the grip and gage length. However, the stress-strain curve, which is indicative of conditions within the gage

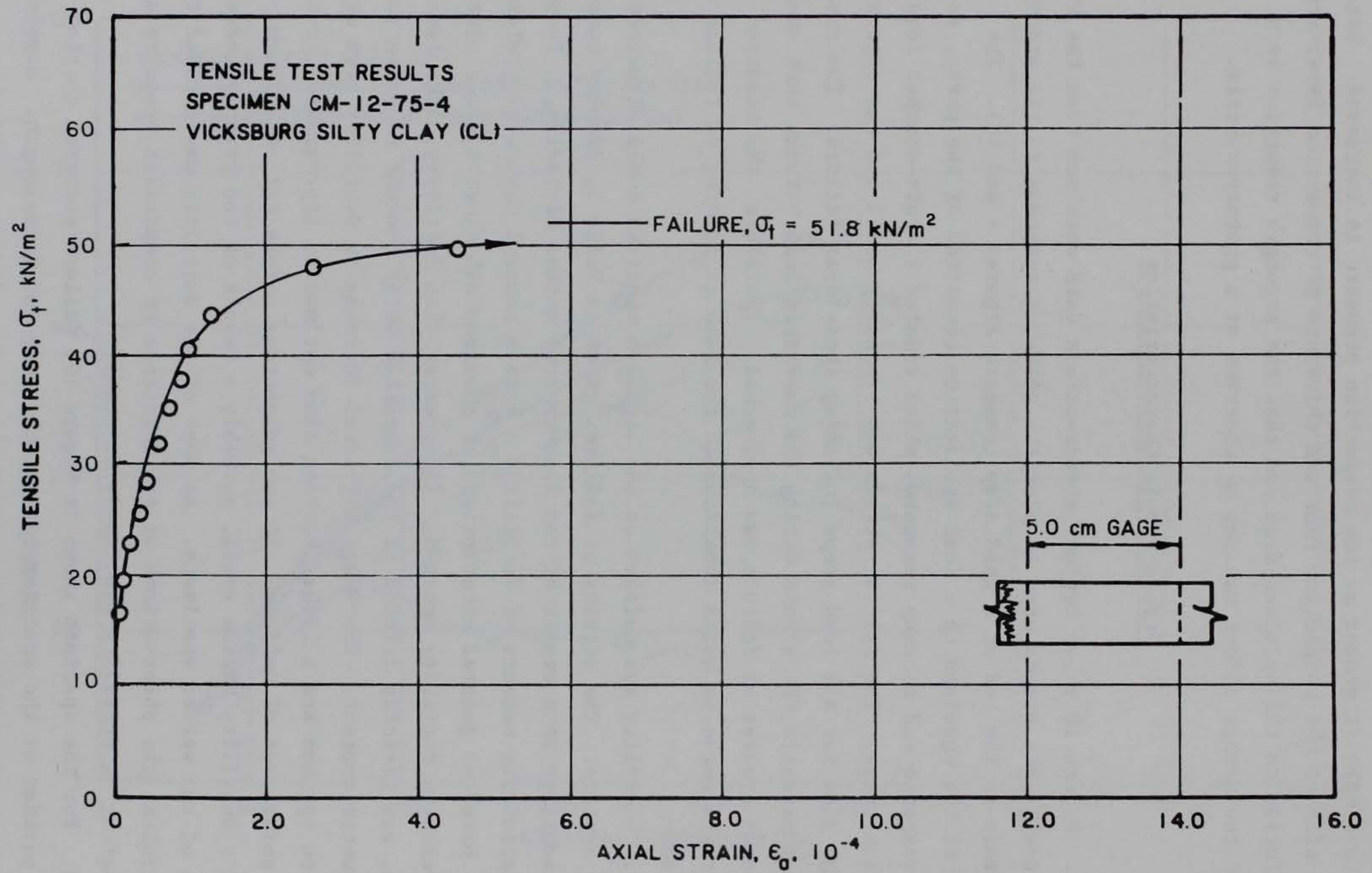


Figure 10. Typical stress-strain curve for direct tensile test on Vicksburg silty clay

length, shows the entire specimen to be in a state of failure. This condition implies that strains are relatively uniform within the specimen up to the point of rupture. It should be noted that of the 36 specimens tested, 28 failed in the gage length (see figures in Appendix B). However, the failure plane in all specimens occurred as a planar fracture running perpendicular to the specimen's longitudinal axis.

Triaxial Compression Test Data

34. The Q test data presented in Table 4 combined with the tensile test data permitted construction of a complete failure envelope for uniaxial loading; these data are summarized in Figure 11. The straight-line strength envelopes shown on the figure are for the purpose of extrapolating compressive strength to the q axis; all comparisons between compressive and tensile strengths are based on these extrapolated values. The compressive strengths correlated with tensile strengths in that specimens having the greater compressive strengths also had the greater tensile strengths. All the Q test specimens compacted dry of optimum displayed approximately the same $\tan \phi_u$, indicating that these specimens all behaved as partially saturated. The ϕ_u of 27 deg is lower than the 33 deg measured in drained tests on Vicksburg silty clay (Peters 1982), which suggests that a moderate pore pressure response was created even in the dryer specimens.

35. The Q test data, supplemented by the test results of Seed et al. (1960), were used to construct Figure 12. It is seen that the relationship between strength, water content, and compaction pressure is identical in form to that for tensile strength. Note that the failure envelopes for the Q test results are nearly parallel (see Figure 11), indicating that differences in strength are the result of differences in the cohesion intercept. Therefore, the factors influencing the cohesion parameter appear to be the same as those influencing tensile strength.

36. To ensure that data from this study and from Seed et al. were comparable, a plot of dry density versus kneading pressure was constructed (see Figure 13). Data at both the optimum water content and optimum ± 2.0 percent indicate that the compaction characteristics of materials used in the two studies are comparable.

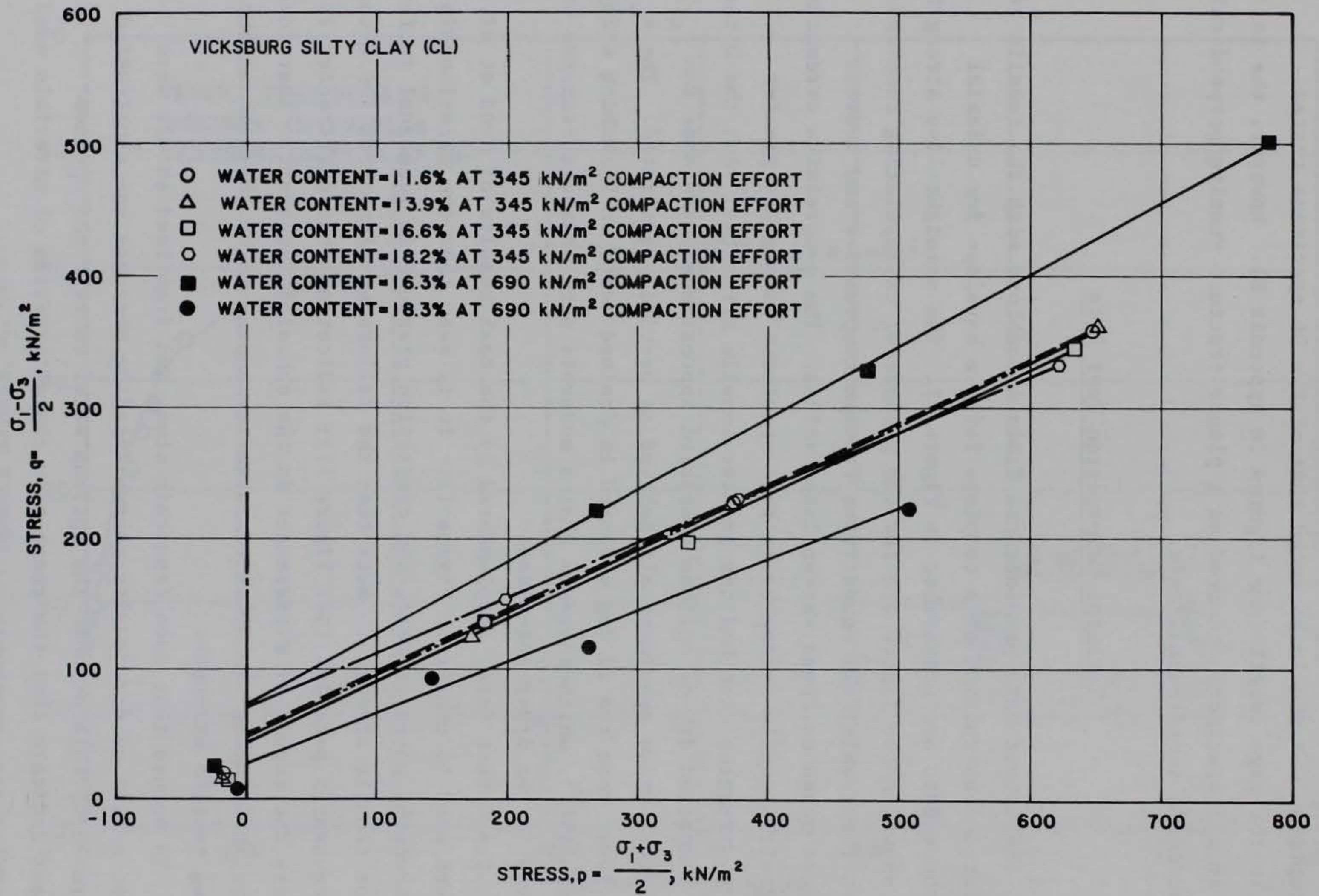


Figure 11. Strength data for tension and compression tests on Vicksburg silty clay

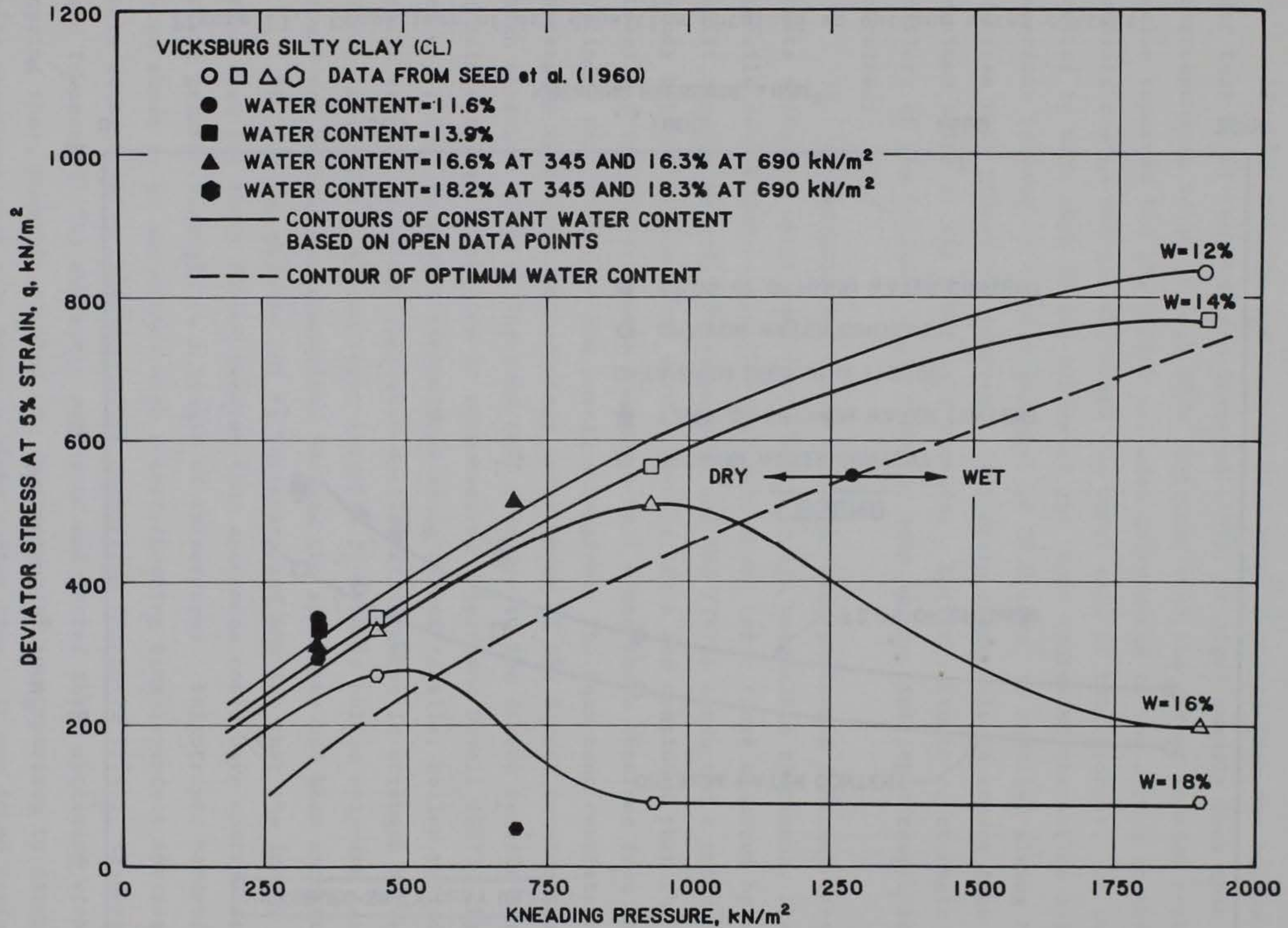


Figure 12. Compressive strength at 5 percent strain versus kneading pressure for Vicksburg silty clay contoured with respect to water content

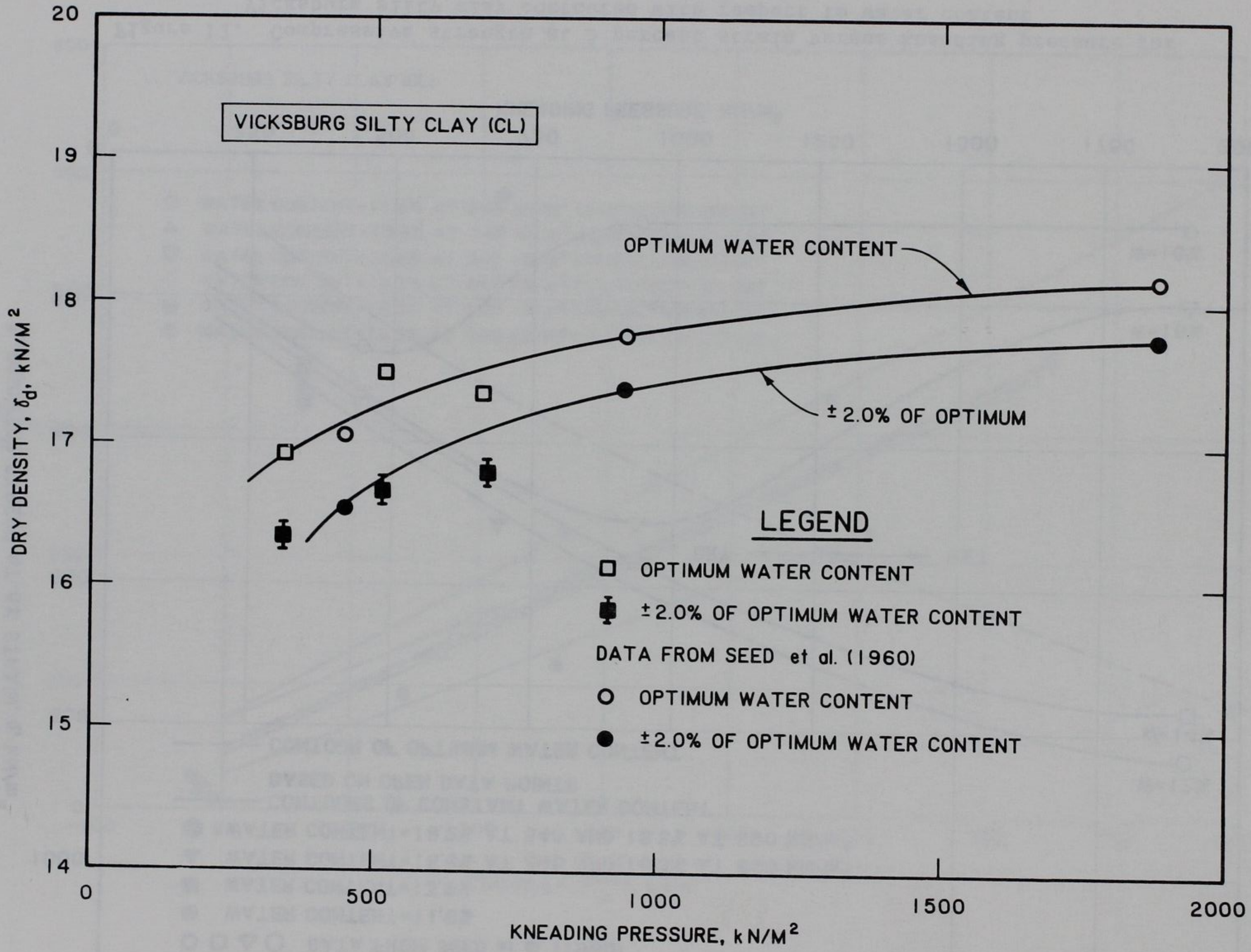


Figure 13. Comparison of dry densities obtained at optimum water content versus kneading pressure

Comparisons to Published Data

37. The tensile strength of 20.4 kN/m^2 reported from the hollow cylinder test by Al-Hussaini and Townsend (1974) is significantly less than the corresponding value of 34.9 kN/m^2 obtained with the direct tension test. The value reported for the hollow cylinder corresponds to the stress at the intermediate radius between the inner and outer wall of the cylinder. It is interesting to note that if the stress at the inner radius of the hollow cylinder specimen is used, a tensile strength of 28.8 kN/m^2 is obtained giving the two devices more comparable results. It appears reasonable to expect that the maximum value at the inner wall provides a better estimate of strength because failure of the cylinder would occur as soon as the limiting strength is obtained.

38. Al-Hussaini and Townsend (1974) also performed indirect tensile tests using the split tensile method. In all comparable specimens, the direct tensile device gave strengths that were about twice those measured by the split tensile method. Satyanarayana and Rao (1972) conducted a comparative study between indirect and direct tensile tests and concluded that the direct tensile test gave strengths one and a half times those obtained from the split cylinder test that gave the lowest strengths. The beam test consistently gave strengths that were approximately twice those of the direct tension test. The high strength found in the beam test relative to the direct tensile test is consistent with experience in rock testing (Obert and Duvall 1967). Bai et al. (1982) presented comparisons among direct tensile, hollow cylinder, and split tensile tests and indicated smaller differences in strength between the direct and split cylinder tests (results from their hollow cylinder tests could not be used for comparison because the specimens had been saturated).

39. It was pointed out by Satyanarayana and Rao that the longer curing time used for their direct tension test specimens could have contributed to their greater strength as a result of thixotropy. Thixotropic hardening has been shown to be associated with a corresponding time-dependent increase in pore water tension (suction) after compaction (Mitchell 1976). Al-Hussaini and Townsend (1974) evidently compacted and tested their specimens without curing them, possibly causing the lower strength in comparison to direct tensile specimens that were given a 24-hr curing time. It was found during the preliminary phases of test development in this study that specimens tested

without being cured gave erratic results, indicating that results are sensitive to the time interval between specimen preparation and testing. The curing time was necessary to achieve repeatability.

PART V: DISCUSSION OF RESULTS

Implications to Strength Theories

40. The observed trends in tensile test data that were outlined in previous sections agree well with published literature and point to a consistent picture of the mechanisms governing the tensile strength of compacted soils. These data also present a clear picture of how the tensile strength should be modeled for purposes of analysis. Consider these observations:

- a. In every case failure occurred as a planar fracture running perpendicular to the specimen axis.
- b. Tensile strength fell below the Mohr-Coulomb envelope as defined from the Q test. The ratio of tensile to compressive strength ranged from 0.2 to 0.4.

It is quite common to account for the failure behavior of soil in tension by defining a tensile "cutoff" to the failure envelope on the tension side of the effective stress origin. Also, it is common to treat the strength component due to suction by defining an equivalent effective stress axis:

$$\sigma' = (\sigma - u_a) + \chi(u_a - u_w) \quad (1)$$

where

σ = total stress

σ' = effective stress

u_a = pore air pressure

u_w = pore water pressure

χ = factor that depends on the degree of saturation
(e.g. Bishop et al. 1960)

The two observations cited at the beginning of this section are used below to show that, in general, tensile strength should not be defined in terms of effective stress and that the use of an equivalent effective stress is inadequate even for compressive strength.

41. First, the use of Equation 1 in conjunction with the Mohr-Coulomb failure law is inconsistent with the observed tensile fracture. Consider that the use of a χ factor in a definition of effective stress implies that the effective stress strength envelope is simply shifted to the tensile side by the amount $\chi(u_a - u_w)$. Therefore, failure of a partially saturated soil in

tension should be similar to failure of a saturated soil in an undrained extension test in that failure should occur as either necking or by formation of shear planes. From the first observation, failure was never observed to be of the shearing type, and the only case where ductile failure modes in tension tests were reported in the literature (Thorne et al. 1980) involved natural clayey soils that were most likely saturated and thus behaved as undrained extension tests. In general, the use of Equation 1 will lead to an incorrect prediction of ductile shear failure in the tensile region.

42. The second observation leads to the conclusion that the strength of the compacted soil is modeled well by a Griffith-type theory, which predicts that different failure modes occur in tension and compression. Several researchers have in fact proposed application of the modified Griffith theory to compacted soil (Bishop and Garga 1969; Shen 1982) with some success. To apply the theory to partially saturated (noncemented) soils, the question of effective stress must be addressed because the tensile strength becomes negligible when the material is saturated. Thus, the tensile strength is derived from capillary tension that evidently makes suction an important variable.

43. Incidentally, another inconsistency appears when applying the effective stress concept to partially saturated soils in compression. Suppose several saturated, overconsolidated specimens are to be tested in drained triaxial compression. If the specimens are consolidated at low confining pressures and then sheared, they will tend to be dilative and fail in a brittle fashion. In contrast, specimens consolidated to a sufficiently high stress to return the specimens to a normally consolidated state will be contractive and appear ductile. Specimens consolidated to intermediate stress levels will correspondingly display failure mechanisms ranging from dilative-brittle to contractive-ductile. Now, if a specimen is desaturated by drying or by introducing air pressure u_a , Equation 1 indicates that it should become more ductile because the extra effective stress due to suction brings the specimen closer to being normally consolidated. Experience indicates that if desaturation influences behavior at all, the tendency is toward becoming more brittle upon drying. It is again seen that the strength derived from suction is not simply due to an increase in intergranular stress but also must be due to the strength of the water surface tension acting as cementation.

Correlation Between Effective Stress and Suction

44. The difficulty with applying the effective stress concept to partially saturated soils is that the relationship between mechanical behavior and suction is more complex than implied by Equation 1. Olsen and Langfelder (1965) found that the negative pore pressure in a compacted soil depends strongly on water content but not on degree of saturation. If strength is derived directly from soil suction, there should be a direct correspondence between water content and strength. For example, the compaction curve, which could be viewed as an indicator of resistance to compaction (density) versus water content, clearly indicates that degree of saturation plays a greater role than would be indicated by a relationship based on suction alone. Therefore, the contribution of suction to shear strength involves a mechanism more complicated than simply adding a component to the effective confining pressure.

45. Fredlund (1979) applied the state variable concept to obtain the shear strength law:

$$\tau = c' + (\sigma - u_a)\tan \phi' + (u_a - u_w)\tan \phi'' \quad (2)$$

where

τ = shear stress at failure

c' = effective stress cohesion intercept

ϕ' = angle of internal friction related to normal stresses

ϕ'' = angle of internal friction related to matrix suction

Equation 2 can be criticized in the same fashion as Equation 1. In fact, if χ is taken to be constant, then the above equation reduces to the Bishop theory with $\tan \phi'' = \chi \tan \phi'$. However, the essence of Fredlund's relationship does not rest in the Mohr-Coulomb form of Equation 2, but rather in the fact that the contribution of suction is independent of the other stress quantities (Fredlund and Morgenstern 1977). That is, rather than incorporating suction into an equivalent effective stress, it should be treated as an independent state variable, whereby the failure law would take the form:

$$\tau = c' + f_1(\sigma - u_a) + f_2(u_a - u_w) \quad (3)$$

where f_1 and f_2 are functions to be determined experimentally. Equation 1 is, of course, a particular case of Equation 3. An alternative failure law that is consistent with the state variable approach is described in the following paragraphs. The proposed relationship is equivalent to Equation 2 for compressive stress states and also predicts the correct failure mechanism in tension.

46. Using the Griffith theory for fracture and the modification by Brace (1960), three distinct failure criteria based on stress state can be identified. Consider a specimen subjected to the stresses σ_t and σ_c (shown in Figure 14), where stresses are negative in tension. From Griffith theory, criteria 1 and 2 follow:

$$1. \text{ For } \quad -\sigma_t > -\sigma_c \text{ and } (3\sigma_t + \sigma_c) < 0: \\ \sigma_t = -T_o \quad (4a)$$

$$2. \text{ For } \quad -\sigma_t > -\sigma_c \text{ and } (3\sigma_t + \sigma_c) > 0: \\ (\sigma_t - \sigma_c)^2 = 8T_o(\sigma_t + \sigma_c) \quad (4b)$$

where T_o is the positive tensile strength parameter. From the Brace modification to Griffith theory, criterion 3 follows:

$$3. \text{ For } \quad \sigma_t < \sigma_c \text{ and } \sigma_t \geq 0, \sigma_c \geq 0: \\ -\mu(\sigma_c - \sigma_t) + (\sigma_c - \sigma_t)\sqrt{1 + \mu^2} = 4T_o \quad (4c)$$

where $\mu = \tan \phi$ and ϕ is the friction angle between the crack faces.

47. The stress states corresponding to each criterion are shown in Figure 14 along with the failure mechanism that should be observed for each case. Failure in the direct tensile test is controlled by criterion 1, whereas failure in the Q test is controlled by criterion 3. The boundary between criteria 2 and 3 corresponds to the unconfined compression test. The stress conditions corresponding to criterion 2 involve both compression and tension and were not produced by any of the tests performed in this study.

48. Equation 4c is clearly equivalent in form to the Mohr-Coulomb criteria, wherein the cohesion intercept is proportional to the tensile strength parameter. Therefore, a correspondence can be made between the tensile

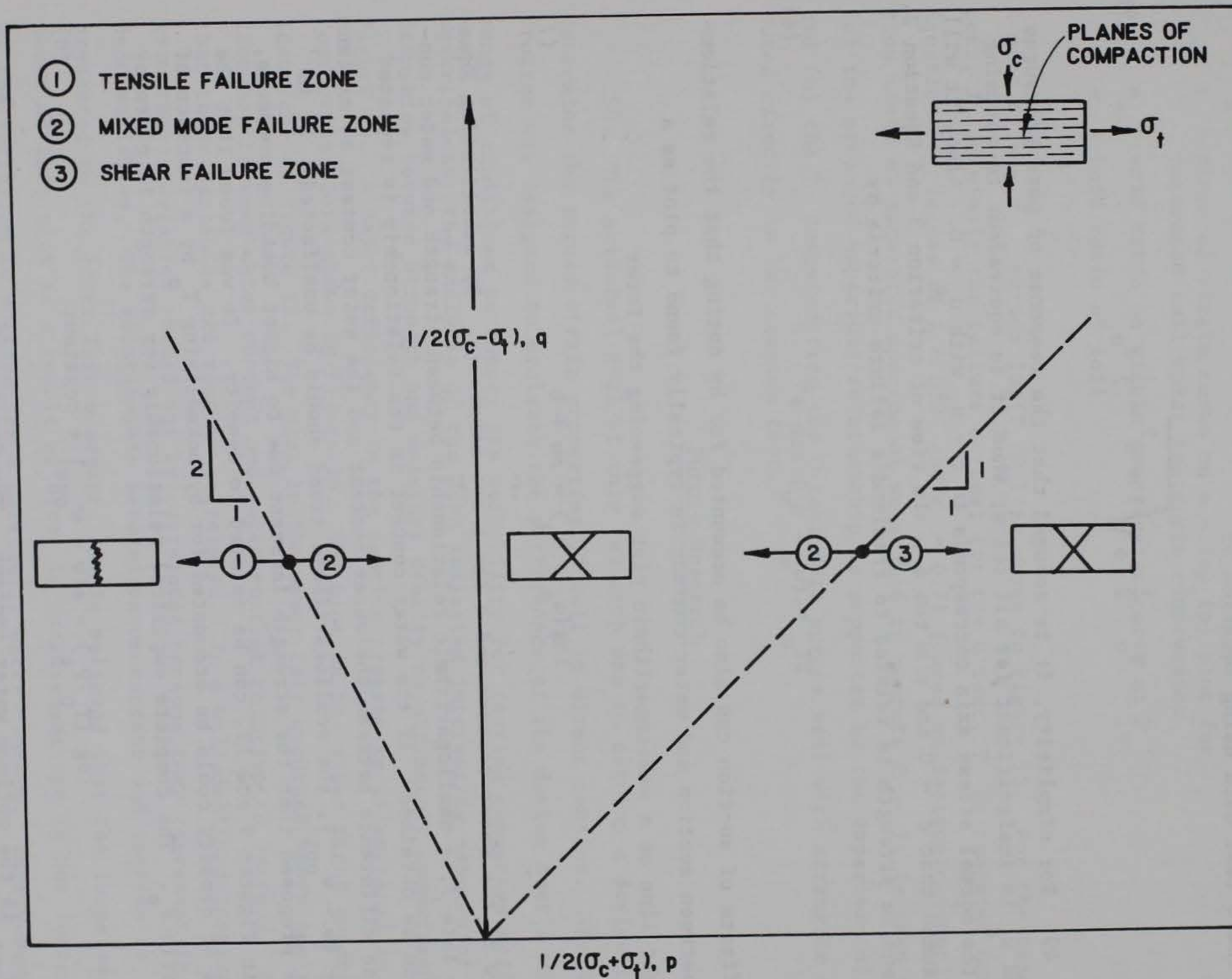


Figure 14. Failure zones dictated by the Griffith-Brace theory and failure mechanism associated with each zone

strength measured in the direct tensile test and the cohesion intercept of the failure envelope of the Q tests. If the value of the cohesion intercept is denoted as a_o in q-p coordinates and c_o in τ - σ coordinates, T_o can be computed from the Q test data using Equation 5:

$$T_o = \frac{1}{2} a_o \sqrt{1 + \mu^2} = \frac{1}{2} c_o \quad (5)$$

49. For simplicity, it is assumed that the response of pore pressures u_w and u_a is insignificant for all tests; thus it is equivalent to assuming that the normal stress axis corresponds to $\sigma - u_a$ with $u_a = 0$. Also, it will be assumed that $c' = 0$ and $\mu \approx \tan \phi_u$. In view of criterion 3 and Equation 2, the tensile strength is related to Fredlund's failure criteria by

$$2T_o = (u_a - u_w) \tan \phi'' \quad (6)$$

The effects of suction can also be accounted for by noting that the relationship between suction and water content is typically found to plot as a straight line on a semilogarithmic plot suggesting the form:

$$\log(u_a - u_w) = aw + b \quad (7)$$

where w is the water content and a and b are constants. By substituting Equation 6 into 7, a semilogarithmic relationship between strength and water content can be obtained. If the water content in the relationship is replaced with the difference between the water content and the water content at maximum density ($w - w_{opt}$), the semilogarithmic trend should be unaffected. It is further proposed that the strength increase due to higher kneading pressure, shown in Figures 9 and 12, can be related to density. It was found that the effects of density could be accounted for by normalizing T_o by a function of void ratio P_e . The complete empirical relationship for strength is given by

$$\log (T_o/P_e) = a(w - w_{opt}) + \text{constant} \quad (8)$$

where w_{opt} is the optimum water content. The function P_e is given by

$$P_e = P_a \exp [(e_a - e)/\lambda] \quad (9)$$

where

P_a = atmospheric pressure

λ = slope of virgin curve on $e - \log_e(p)$ plot for saturated soil under isotropic compression

e_a = void ratio on virgin compression curve at P_a

e = void ratio of soil

A plot of $w - w_{opt}$ versus $\log(T_o/P_e)$ is shown in Figure 15. For the tension test, T_o is simply the failure stress; for the Q test, T_o is computed from Equation 5. Values of $\lambda = 0.07$ and $e_a = 0.71$ (based on isotropic consolidation tests on saturated specimens) were used to compute P_e . It is seen that (a) the proposed empirical relationship is supported by the experimental data, and (b) the T_o computed from the Q test data agrees well with strengths measured directly in the tension test.

Future Research

50. The principal goal of this research was to develop a device to determine the stress-strain properties of soil in direct tension. The test program was designed to evaluate the performance of the device over a wide range of conditions to ensure its suitability for testing compacted soils. Nevertheless, the analysis of the data indicated interesting aspects of relationships between strength and moisture density as ultimately summarized in Figure 15. A major deficiency in the testing program is illustrated in the four cross plots shown in Figure 16. The plot in the upper right quadrant is identical to Figure 15. The plot in the upper left quadrant shows the relationship between water content and water content relative to optimum. Note that these variables are roughly correlated. In a well-designed testing program these variables should not be correlated because they represent independent variables. The relationship between water content and suction is presented in the lower left quadrant. It is believed that the large scatter shown in this plot is a result of error in measurement and is not indicative of the variation in suction for a particular water content. Improvements in testing technique are needed to better verify this relationship. The plot in

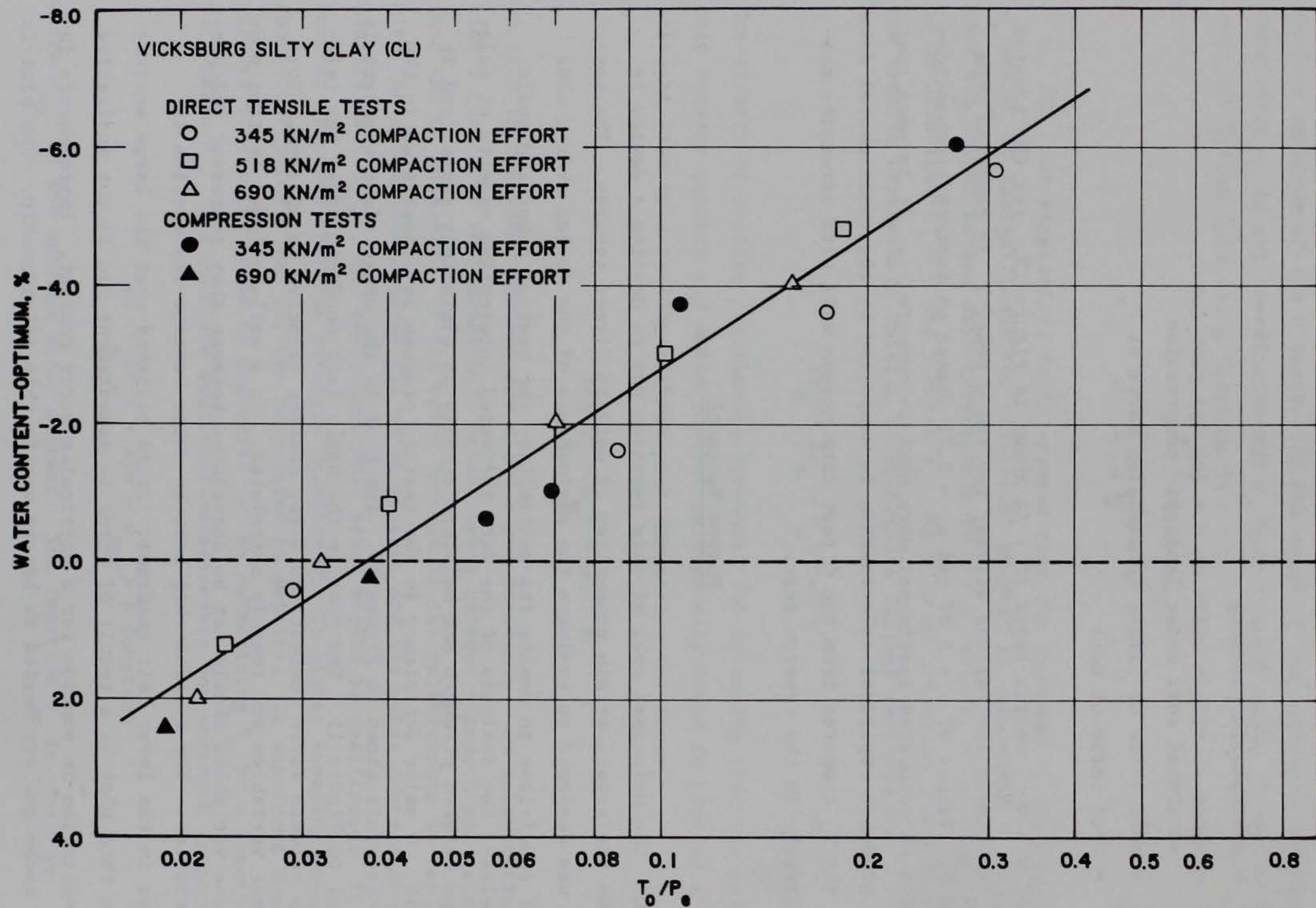


Figure 15. Plot of normalized tension versus water content using strength based on the Griffith-Brace theory for Vicksburg silty clay

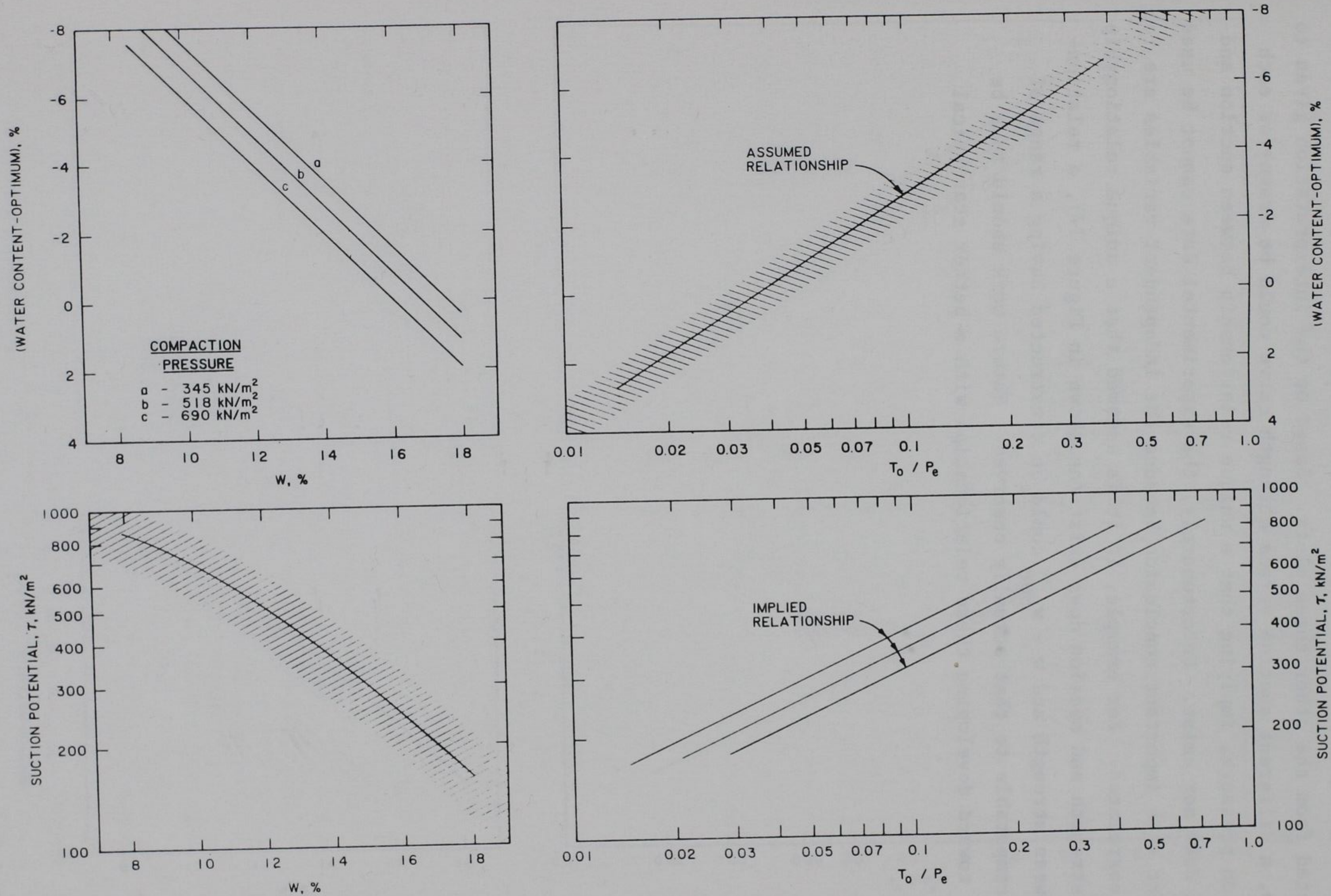


Figure 16. Relationship between strength, suction, and water content assuming correlation between strength and water content-optimum (shaded area shows measured data scatter)

the lower right quadrant is the implied suction versus strength relationship constructed from the other three plots. Based on the interpretation given to the data, a different suction versus strength curve could be drawn for each compaction pressure, implying that a unique relationship between suction and strength does not exist. Unfortunately, the experimental data cannot be used to support this important conclusion because the independent variables are too closely correlated. For example, if it is assumed that a unique relationship between strength and suction does exist (as shown in Figure 17), a relationship between strength and $w - w_{opt}$ could be constructed having a range of scatter comparable to that actually observed. Future work should thus be oriented toward developing these relationships with a better statistical basis.

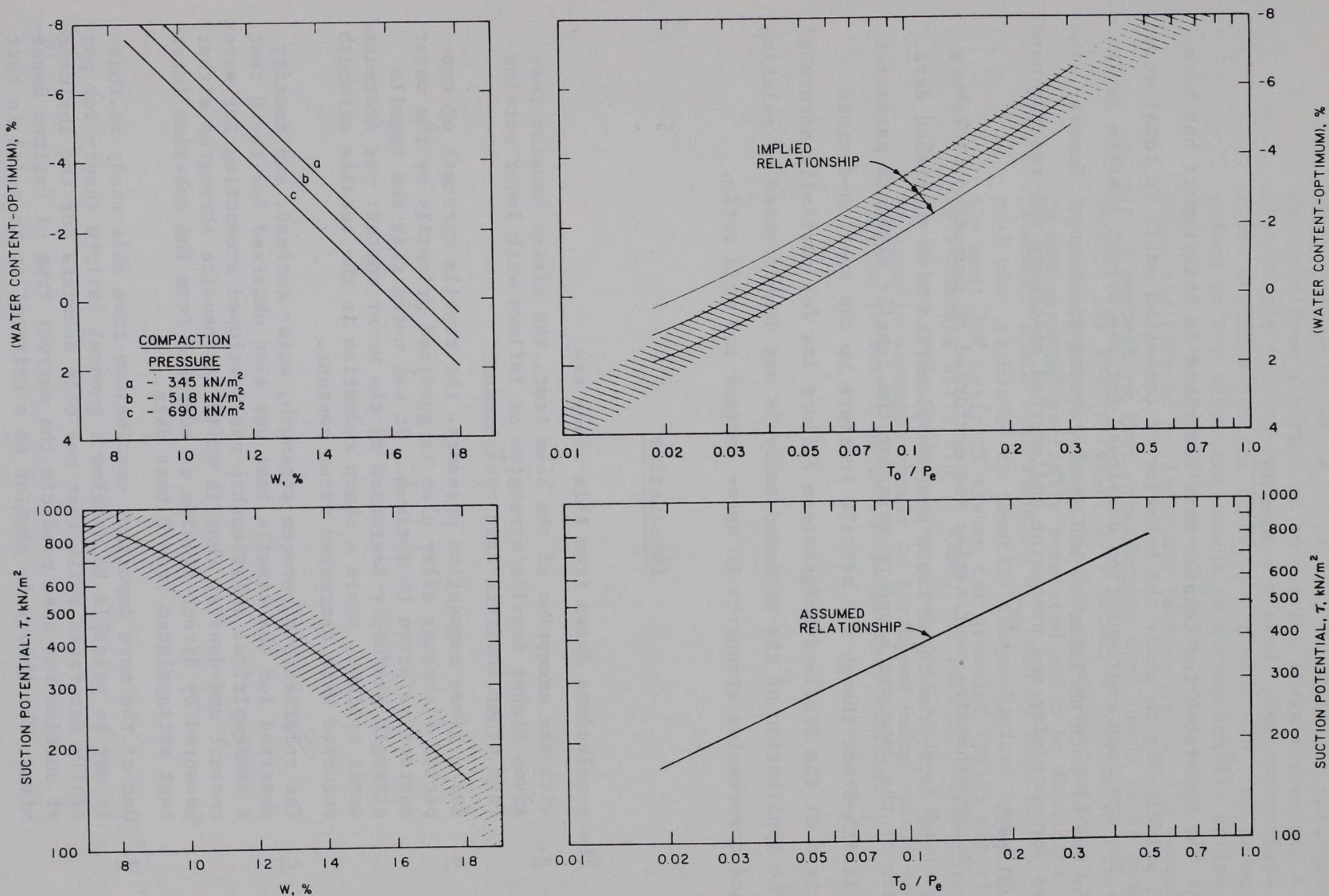


Figure 17. Relationship between strength, suction, and water content assuming correlation between strength and suction (shaded area shows measured data scatter)

PART VI: SUMMARY AND CONCLUSIONS

Summary

51. The apparatus and tension test described in this report has been developed principally to study the behavior of compacted soils in total stress tension. The specimen configuration developed for the direct tensile device allows the use of both undisturbed and reconstituted specimens. However, the techniques for obtaining and preparing undisturbed specimens for testing need to be developed.

52. A comprehensive test series was performed on compacted Vicksburg silty clay; the data from these tests were supplemented with published data. An analysis of the data was based on relating the tensile strength parameter of the Griffith-Brace theory for brittle fracture to the suction-derived cohesion term of the Fredlund-Morgenstern failure law for partially saturated soils. The application of the proposed analysis was demonstrated by relating tensile and compressive strengths to water content and void ratio.

Conclusions

53. The conclusions drawn from this study are:

- a. With the exception of the beam test, the direct tension test gives higher tensile strengths at failure with lower strains than other indirect test apparatuses.
- b. For a given compaction pressure, the tensile strength of compacted Vicksburg silty clay is governed primarily by the water content relative to optimum. It was noted that the tensile strength gradually decreased as the water content was increased until optimum, where a sharp reduction in the tensile strength occurred with increased water content.
- c. The relationship between strength, water content, and density observed for the tensile test was also observed for the Q test. A semiempirical relationship was developed accounting for water content and density that is valid for tensile strengths either measured by direct tension or computed from the cohesion intercept extrapolated from Q test data.
- d. One of the more important conclusions from this study is that it may be possible to develop a general failure theory for partially saturated soils that not only accounts for the influence of suction but also predicts the correct type of failure mechanism. The theory is similar to a critical state model in that

it is based on a state surface containing both void ratio and water content as state variable. The "line of optimums" obtained from a series of compaction tests represents a projection of the surface onto the e-w axes. The appropriate stress state variable for the theory would be $\sigma - u_a$, which would reduce to the effective stress as conventionally defined, when degree of saturation increases to the point where the air phase takes the form of occluded air bubbles and $u_a - u_w$ equals zero.

- e. It is emphasized that considerable work needs to be done to develop the theory fully; more detailed testing of other soil types is required. In particular, an investigation is needed on noncompacted partially saturated soils to determine if a reference state equivalent to w_{opt} can be identified. Conceptual work is needed to identify the mechanical basis of using the modified Griffith theory for granular (silt) materials such as Vicksburg silty clay. Also, the role of excess pore pressures and their influence on μ requires study. Future studies on tensile strength should be performed using strain-controlled loading to better define behavior near failure.

REFERENCES

- Ajaz, A. 1980. "Time-Dependent Behaviour of Compacted Clays in Tension and Compression," Geotechnique, Vol 30, No. 1, pp 67-76.
- Ajaz, A., and Parry, R. H. G. 1974. "An Unconfined Direct Tension Test for Compacted Clays," Journal of Testing and Evaluation, American Society of Testing and Materials, Vol 2, No. 3, pp 163-172.
- _____. 1975. "Stress-Strain Behaviour of Two Compacted Clays in Tension and Compaction," Geotechnique, Vol 25, No. 3, pp 495-512.
- _____. 1976. "Bending Test for Compacted Clays," Journal of the Geotechnical Engineering Division, American Society of Civil Engineers, Vol 102, GT9, pp 929-943.
- Al-Hussaini, M. M., and Townsend, F. C. 1973. "Tensile Testing of Soils, A Literature Review," Miscellaneous Paper S-73-24, US Army Engineer Waterways Experiment Station, CE, Vicksburg, Miss.
- _____. 1974. "Investigation of Tensile Testing of Compacted Soils," Miscellaneous Paper S-74-10, US Army Engineer Waterways Experiment Station, CE, Vicksburg, Miss.
- Andrei, M. S. 1961. "Written Contributions (in French)," Proceedings of the Fifth International Conference on Soil Mechanics and Foundation Engineering, Vol 3, pp 116-117.
- Bai, S., Shen, X., and Su, B. 1982. "Devices for Measuring the Tensile Strength of Soils (in Chinese)," Collected Research Papers, Water Conservancy and Hydroelectric Power Research Institute, Vol 8, pp 55-62 (Translated by Tse-Shan Hsu).
- Bishop, A. W., Alpan, I., Blight, G. E., and Donald, I. B. 1960. "Factors Controlling the Strength of Partly Saturated Cohesive Soils," Research Conference on Shear Strength of Cohesive Soils, American Society of Civil Engineers, University of Colorado, Boulder, Colo., pp 503-532.
- Bishop, A. W., and Garga, V. K. 1969. "Drained Tension Tests on London Clay," Geotechnique, Vol 19, No. 2, pp 309-313.
- Brace, W. F. 1960. "An Extension of the Griffith Theory of Fracture to Rock," Journal of Geophysical Research, Vol 65, pp 3477.
- Conlon, R. J. 1966. "Landslide on the Toulouste River, Quebec," Canadian Geotechnical Journal, Vol 11, No. 3, pp 113-144.
- Department of the Army, Office of the Chief of Engineers. 1970. "Laboratory Soils Testing," Engineering Manual 1110-2-1906, Washington, DC.
- Fang, H. Y., and Hirst, T. J. 1973. "A Method For Determining the Strength Parameters of Soils," Highway Research Record No. 463, Highway Research Board, pp 45-50.
- Fredlund, D. G. 1979. "Appropriate Concepts and Technology for Unsaturated Soils," Second Canadian Geotechnical Colloquium, Canadian Geotechnical Journal, Vol 16, No. 1, pp 121-139.

Fredlund, D. G., and Morgenstern, N. R. 1977. "Stress State Variables for Unsaturated Soils," Journal of the Geotechnical Engineering Division, American Society of Civil Engineers, Vol 103, No. GT5, pp 447-466.

Haefeli, R. 1950. "Investigations and Measurements of the Shear Strengths of Saturated Cohesive Soils," Proceedings of the Conference on the Measurement of the Shear Strength of Soils in Relation to Practice, Session 4, pp 186-208.

Hasegawa, H., and Ikeuti, M. 1964. "On the Tensile Strength of Disturbed Soil," Symposium on Rheology and Soil Mechanics, Edited by Kravtdrenco, J. and Sirieys, P. M., Springer, Berlin, pp 405-412.

Hudson, W. R., and Kennedy, T. W. 1968. "An Indirect Tensile Test for Stabilized Materials," Research Report 98-1, Center For Highway Research, The University of Texas at Austin, Austin, Texas.

Johnson, L. D. 1974. "Psychrometric Measurement of Total Suction in a Tri-axial Compression Test," Miscellaneous Paper S-74-19, US Army Engineer Waterways Experiment Station, CE, Vicksburg, Miss.

Krishnayya, A. V. G., and Eisenstein, Z. 1974. "Brazilian Tensile Test for Soils," Canadian Geotechnical Journal, Vol 11, No. 4, pp 632-642.

Krishnayya, A. V. G., Eisenstein, Z., and Morgenstern, N. R. 1974. "Behavior of Compacted Soil in Tension," Journal of the Geotechnical Engineering Division, American Society of Civil Engineers, Vol 100, GT9, pp 1051-1061.

Lee, I. K., ed. 1968. "Strength and Deformation of Soil and Rock," Soil Mechanics Selected Topics, Elsevier, New York, pp 268-283.

Leonards, G. A., and Narain, J. 1963. "Flexibility of Clay and Cracking of Dams," Journal of the Soil Mechanics and Foundations Division, American Society of Civil Engineers, Vol 89, No. SM2, pp 47-98.

Lushnikov, V. V., Vulis, P. D., and Litvinov, B. M. 1973. "Relationship of the Moduli of Deformation in Soil Composition and Tension," Soil Mechanics and Foundation Engineering, Vol 10, No. 6, pp 403-405 (Translated by Consultants' Bureau, New York).

Mitchell, J. K. 1976. "Soil Structure and Its Stability," Fundamentals of Soil Behavior, Wiley, New York, pp 210-212.

Moore, R. K. 1975. Discussion of "Behavior of Compacted Soil in Tension," Journal of the Geotechnical Engineering Division, American Society of Civil Engineers, Vol 101, No. GT9, pp 985-987.

Narain, J., and Rawat, P. C. 1970. "Tensile Strength of Compacted Soils," Journal of the Soil Mechanics and Foundations Division, American Society of Civil Engineers, Vol 96, No. SM6, pp 2185-2190.

Obert, L., and Duvall, W. I. 1967. "Mechanical Properties and Behavior of Rock," Rock Mechanics and the Design of Structures in Rock, Wiley, New York, pp 301-317.

Olsen, R. E., and Langfelder, L. J. 1965. "Pore Pressures in Unsaturated Soils," Journal of the Soil Mechanics and Foundations Division, American Society of Civil Engineers, Vol. 91, No. SM4, pp 127-150.

Parry, R. H. G., and Nadarajah, V. 1974. "Anisotropy in a Natural Soft Clay Silt," Engineering Geology, Vol 8, No. 3, pp 287-309.

- Peters, J. F. 1982. "Constitutive Theory for Stress-Strain Behavior of Frictional Materials," Ph. D. dissertation submitted to the graduate college, University of Illinois at Chicago, Chicago.
- Ramanathan, B. and Raman, V. 1974. "Split Tensile Strength of Cohesive Soils," Soils and Foundations, The Japanese Society of Soil Mechanics and Foundation Engineering, Vol 14, No. 1, pp 71-76.
- Satyanarayana, B., and Rao, K. S. 1972. "Measurement of Tensile Strength of Compacted Soil," Geotechnical Engineering, Vol 3, No. 1, pp 61-66.
- Seed, H. B., Mitchell, J. K., and Chan, C. K. 1960. "The Strength of Compacted Cohesive Soils," Research Conference on Shear Strength of Cohesive Soils, American Society of Civil Engineers, University of Colorado, Boulder, Colo., pp 877-964.
- Shen, X. 1982. "The Tensile Behaviors of Compacted Cohesive Soils (in Chinese)," Collected Research Papers, Water Conservancy and Hydroelectric Power Research Institute, Vol 8, pp 63-73 (Translated by Tse-Shan Hsu).
- Strohm, W. E. Jr. 1966. "Preliminary Analysis of Results of Division Laboratory Tests on Standard Soil Samples," Miscellaneous Paper No. 3-813, US Army Engineer Waterways Experiment Station, CE, Vicksburg, Miss.
- Thorne, C. R., Tovey, N. K., and Bryant, R. 1980. "Recording Unconfined Tension Tester," Journal of the Geotechnical Engineering Division, American Society of Civil Engineers, Vol. 106, No. GT11, pp 269-1273.
- Townsend, D. L., Sangrey, D. A., and Walker, L. K. 1969. "The Brittle Behaviour of Naturally Cemented Soils," Proceedings of the Seventh International Conference on Soil Mechanics and Foundation Engineering, Vol 1, Session 4, pp 411-417, Mexico.
- Tschebotarioff, G. P., Ward, E. R., and DePhilippe A. A. 1953. "The Tensile Strength of Disturbed and Recompactd Soils," Proceedings of the Third International Conference on Soil Mechanics and Foundation Engineering, Vol 1, Sessions 1-4, pp 207-210, Switzerland.
- Uchida, I., and Matsumoto, R. 1961. "On the Test of the Modulus of Rupture of Soil Sample," Soil and Foundation, The Japanese Society of Soil Mechanics and Foundation Engineering, Vol 2, No. 1, pp 51-55.

Table 1
Chronology of Developmental Test Program

Test Grouping	Gripping and Deformation Measuring Method	Results	Analysis of Test Results	Corrective Action Taken
CM-14-50-1T	- Hot wax - LVDT (see note 1)	Specimen ends slipped from grips	Gripping area insufficient	Gripping area enlarged by addition of spacers to grips
CM-14-50-2T	"	Specimen broke in reduced section	-----	None
CM-14-50-3T	"	Specimen broke in grips	Specimen ends have insufficient strength	Wire reinforcement compacted into specimen ends in layers 3 and 5 (6 wires per layer)
CM-14-50-4T	"	Specimen slipped from grips	Wire reinforcement too complicated	Changed to Hydrostone as a gripping media
CM-14-50-5T	- Hydrostone - LVDT (see note 1)	Specimen broke in grips	Specimen ends have insufficient strength	Used lime on specimen ends to increase this strength, also realigned apparatus
CM-14-50-6T	"	Specimen broke in grips	Lime inadequate and too messy	Try rubber membrane around specimen ends to isolate specimen ends from water in hydrostone
CM-14-50-7T	"	Specimen broke in grips	Possible alignment problem	Realigned apparatus, used rubber membrane around specimen ends
CM-14-50-8T	"	Specimen slipped from grips	Not enough gripping strength and center section too strong	Reduced top of center section (2.75" x 1.5"), eliminated rubber membrane
CM-14-50-9T	"	Specimen broke in grips	Specimen nonsymmetric	Reduced top and bottom of center section (2.5" x 1.5")
CM-12-50-10T	"	Specimen broke in grips	Water in Hydrostone weakening specimen ends	Kept reduced center section (2.5" x 1.5"), reverted back to wax as a gripping media, also carved notches in specimen ends to improve gripping
CM-12-50-11T	- Hot wax - LDVT (see note 1)	Specimen broke at edge of grip	Gripping of wax uneven	None
CM-12-75-12T	- Hot wax - LVDT	Mixed	Various analyses	Tried different notch configuration and various methods of attaching LVDT to specimen
CM-16-50-13T	"	"	"	"
CM-12-50-14T	"	"	"	"
CM-12-50-15T	"	"	"	"
CM-12-50-16T	"	"	"	"
CM-12-50-17T	"	"	"	"
CM-12-75-18T	"	"	"	"
CM-12-75-19T	"	"	"	"
CM-16-50-20T	"	"	Try noncontact measuring system	Try proximity probes to measure deformations
CM-16-50-21T	- Hot wax with notched ends (see note 2) - Proximity probes	Specimen broke in grips	Deformation measurements results poor	None
CM-16-50-22T	"	Specimen broke in reduced section	"	None
CM-16-50-23T	- Hot wax with notched ends (see note 2) - Proximity probes	Specimen broke in reduced section	Good strength but deformation measurements results poor	None
CM-12-50-24T	"	Specimen broke in reduced section, but poor deformation response	Proximity probes inadequate (mounting system poor)	Change back to LVDT with current mounting method (see note 3)
CM-12-50-25T	- Hot wax with notched ends (see note 2) - LVDT (see note 3)	Specimen slipped from grips	Wax shrinking away from ends	Change wax mixture to minimize wax shrinkage (50/50 microcrystalline to paraffin mixture)
CM-12-50-26T	"	"	Less shrinkage but wax too hot	Try cooler wax temperature 120°F
CM-12-75-27T	"	Specimen broke in grips	Not uniform gripping of wax	Increase wax temperature to 130°F
CM-12-75-28T	"	Specimen slipped from grips	"	Increase wax temperature to 140°F
CM-12-75-29T	"	"	"	Try combination of wax and Hydrostone as restraining media
CM-12-75-30T	- Notched ends dipped in hot wax, restrained with Hydrostone (see note 2) - LVDT (see note 3)	Specimen broke in center section	Results encouraging	None
CM-12-75-31T	"	"	Hydrostone sticking to grips and hard to clean apparatus after test	Line grips with filter paper to prevent sticking
CM-12-75-32T	"	"	"	None
CM-12-75-33T	"	"	Use this technique in main test series	None

Note 1: Two small holes drilled in specimen at gage length, holes filled with Hydrostone, and LVDT mounting bracket embedded in Hydrostone.
 Note 2: A triangular-shaped tapered notch is carved into both sides of each end of the specimen. This configuration was found to distribute the restraining stress best of all configurations tried.
 Note 3: LVDT mounting bracket prongs press fit against specimen sides in the reduced center section at a 5.0-cm gage length.

Table 2
Suction Potential Test Data (345 kN/m² Compaction Pressure)

<u>Test No.</u>	<u>w percent</u>	<u>e</u>	<u>S percent</u>	<u>t °C</u>	<u>E μv</u>	<u>τ kN/m²</u>
CM-10-50-1a	8.84	0.752	31.8	22.5	6.0	1571.2
CM-10-50-1b	9.32	0.735	34.2	22.5	3.3	864.2
CM-10-50-1d	9.35	0.752	33.5	22.5	3.5	916.5
CM-10-50-1f	9.20	0.764	32.4	22.5	2.1	549.9
CM-10-50-1g	9.37	0.734	34.5	22.5	1.6	419.0
CM-10-50-1h	9.25	0.752	33.2	22.5	1.5	392.8
CM-10-50-1i	9.37	0.739	35.0	22.5	2.0	523.7
CM-12-50-2a	11.83	0.776	41.1	21.8	2.3	614.7
CM-12-50-2b	11.39	0.780	39.4	21.8	2.3	614.7
CM-12-50-2d	13.00	0.795	44.1	21.8	1.8	481.1
CM-12-50-2f	11.23	0.822	36.9	21.8	2.2	588.0
CM-12-50-2g	11.01	0.808	36.8	21.8	2.0	534.6
CM-12-50-2h	11.06	0.790	37.8	21.8	1.6	427.6
CM-12-50-2i	10.78	0.793	36.7	21.8	3.2	855.3
CM-14-50-3a	14.30	0.707	54.6	21.7	1.1	294.9
CM-14-50-3b	14.10	0.704	54.0	21.7	1.0	268.1
CM-14-50-3d	14.30	0.687	56.2	21.7	1.5	402.1
CM-14-50-3f	14.12	0.682	55.9	21.7	1.4	375.3
CM-14-50-3g	14.08	0.692	54.9	21.7	1.4	375.3
CM-14-50-3h	14.44	0.675	57.8	21.7	0.6	160.8
CM-14-50-3i	14.08	0.683	55.6	21.7	1.3	348.5
CM-18-50-4a	17.50	0.625	75.6	22.2	0.7	184.9
CM-18-50-4b	17.69	0.627	76.2	22.2	0.6	158.5
CM-18-50-4d	17.64	0.610	78.1	22.2	1.0	264.2
CM-18-50-4f	17.88	0.630	76.7	22.2	0.7	184.9
CM-18-50-4g	17.72	0.628	76.2	22.2	0.6	158.5
CM-18-50-4h	17.72	0.603	79.3	22.2	0.6	158.5
CM-18-50-4i	17.59	0.603	78.7	22.2	0.7	184.9

Note: The definitions of the headings are: w = water content, e = void ratio, S = degree of saturation, t = temperature, E = psychrometer output, and τ = suction potential.

Table 3

Direct Tension Test Data at Failure

Test No.	w_i percent	w_f percent	K_p kN/m ²	γ_d kN/m ³	ϵ_{tf} percent	σ_{tf} kN/m ²
CM-12- 50- 1	12.3	12.2	345.0	15.55	0.035	37.3
CM-12- 50- 2	12.4	11.6	345.0	15.61	0.040	37.3
CM-12- 50- 3	12.4	11.9	345.0	15.52	0.073	40.0
CM-12- 75- 4	12.5	12.0	517.5	16.18	0.056	51.8
CM-12- 75- 5	12.6	11.9	517.5	16.10	0.050	51.1
CM-12-100- 6	12.4	--	690.0	16.31	0.065	64.2
CM-12-100- 7	12.4	11.8	690.0	16.45	0.020	62.1
CM-14- 50- 8	14.1	13.7	345.0	15.90	0.068	37.3
CM-14- 50- 9	14.5	13.9	345.0	15.72	0.054	35.2
CM-14- 75-10	14.1	13.5	517.5	16.53	0.035	43.5
CM-14- 75-11	14.1	13.4	517.5	16.48	0.030	49.7
CM-14- 75-12	14.4	13.0	517.5	16.49	0.010	61.4
CM-14- 75-14	14.4	13.4	517.5	16.51	0.020	49.0
CM-14- 75-16	14.2	13.4	517.5	16.51	0.023	53.1
CM-14- 75-33	14.3	13.8	517.5	16.32	0.023	38.6
CM-14- 75-34	14.1	13.9	517.5	16.37	0.095	38.6
CM-14-100-13	14.2	13.5	690.0	16.82	0.062	53.1
CM-14-100-15	14.1	13.4	690.0	16.89	--	49.7
CM-14-100-17	14.1	13.5	690.0	16.82	0.045	53.1
CM-14-100-18	14.0	13.4	690.0	16.78	0.118	60.7
CM-14-100-32	14.7	13.9	690.0	16.87	--	53.2
CM-16- 25-35	16.1	15.9	172.5	14.53	0.021	13.8
CM-16- 50-19	15.9	15.6	345.0	16.20	0.128	34.5
CM-16- 50-20	16.1	15.5	345.0	16.21	0.096	35.2
CM-16- 75-21	16.1	15.5	517.5	16.75	0.044	38.6
CM-16- 75-22	15.9	15.6	517.5	16.90	0.098	43.5
CM-16-100-23	16.1	15.6	690.0	17.26	0.103	49.7
CM-16-100-24	15.9	15.2	690.0	17.36	0.175	53.8
CM-16-100-25	16.0	15.3	690.0	17.36	--	45.5
CM-16-150-36	16.2	15.8	1035.0	17.74	--	35.2
CM-18 -50-26	18.0	17.2	345.0	16.86	--	23.5
CM-18 -50-27	18.6	17.4	345.0	16.82	0.070	27.6
CM-18- 75-28	18.5	17.7	517.5	16.82	--	20.0
CM-18- 75-29	19.0	18.0	517.5	16.68	0.140	19.3
CM-18-100-30	18.5	17.6	690.0	16.79	--	19.3
CM-18-100-31	18.5	18.1	690.0	16.78	0.060	17.3

Note: The definitions of the headings are: w_i = initial water content, w_f = final water content, K_p = compaction pressure, γ_d = dry density, ϵ_{tf} = strain at failure, and σ_{tf} = stress at failure.

Table 4

Triaxial Compression Test Data at Failure

Test No.	w percent	K_p kN/m^2	γ_d kN/m^3	ϵ_{1f} percent	$\frac{\sigma_{1f} - \sigma_{3f}}{2}$	$\frac{\sigma_{1f} + \sigma_{3f}}{2}$
					kN/m^2	kN/m^2
CM-12- 50- 1C	11.7	345.0	15.32	5.0	133.9	182.2
CM-12- 50- 2C	11.6	345.0	15.43	10.0	225.9	370.8
CM-12- 50- 3C	11.6	345.0	15.41	15.0	359.3	649.1
CM-14- 50- 4C	14.0	345.0	15.80	6.0	124.8	173.1
CM-14- 50- 5C	13.9	345.0	16.04	10.0	225.9	370.8
CM-14- 50- 6C	13.8	345.0	16.02	15.0	360.7	650.5
CM-16- 50- 7C	16.6	345.0	16.24	6.0	135.9	184.2
CM-16- 50- 8C	16.6	345.0	16.07	20.0	194.6	339.5
CM-16- 50- 9C	16.6	345.0	16.34	20.0	345.0	634.8
CM-16-100-10C	16.3	690.0	17.42	5.0	220.1	268.4
CM-16-100-11C	16.3	690.0	17.39	8.0	329.1	474.0
CM-16-100-12C	16.3	690.0	17.69	10.0	500.9	790.7
CM-18- 50-13C	18.2	345.0	16.71	9.5	151.1	199.4
CM-18- 50-14C	18.2	345.0	16.67	15.0	229.8	374.7
CM-18- 50-15C	18.3	345.0	16.76	15.0	331.2	621.0
CM-18-100-16C	18.5	690.0	16.07	15.0	92.5	140.8
CM-18-100-17C	18.3	690.0	16.34	15.0	115.9	260.8
CM-18-100-18C	18.3	690.0	15.94	15.0	220.1	509.9

Notes: The definitions of the headings are: w = water content, K_p = compaction pressure, γ_d = dry density, ϵ_{1f} = axial strain at failure, σ_{1f} = axial stress at failure, and σ_{3f} = confining stress at failure. The dry densities were based on weights of compression test specimens and are generally less accurate than those reported in Table 2.

APPENDIX A: TENSILE TEST PROCEDURE

Introduction

1. The direct tensile test is intended for the determination of the strength of compacted soils when subjected to a state of uniaxial tension. The test is designed to develop a uniform state of tensile stress that permits a direct computation of tensile strength from the total load applied. In contrast, indirect methods of determining tensile strength, such as beam and split cylinder (Brazilian) tests, require a computation of the stress state within the specimen at failure, which in turn requires an assumption of the soil properties. Generally, stresses are computed assuming the soil to be elastic up to failure. Another important feature of the direct method is the accuracy of strain measurements. Similar to stress determinations, strains are determined directly from the measured displacement within a specified gage length. The direct tensile test provides additional data on the cohesive strength of soils at low or negative normal stresses and thus supplements unconfined compression tests and Q tests. The test is principally useful for evaluating the strength of partially saturated compacted soils or possible chemically treated compacted soils (i.e. pavement subgrades). The strength determined from the test is always stated in terms of total stress; effective stress at failure cannot be determined because no measurements are made of pore water or pore air pressures.

Apparatus

2. The apparatus should consist of the following:
- a. The tensile loader consists of two gripping jaws, rigid base, slide table, load cell, and loading mechanism. One gripping jaw is rigidly attached to the base, while the second gripping jaw is attached to the slide table. The slide table provides for precise alignment of the pulling force along the long axis of the specimen. It is designed to maintain its alignment to within 0.0025 mm over its full travel, and frictional forces within the slide table are not to exceed 0.04 N. The load cell is mounted to the jaw that is attached to the slide table to ensure that the load measured is the actual load applied to the specimen. The attachment between the load cell and loading mechanism is flexible to avoid applying moments to the load cell. The load cell has a full range capacity of 0.45 kN with a

resolution of 0.22 N. The loading mechanism may consist of (1) a dead load pulley system, (2) a pneumatic loading system, or (3) a displacement controlled mechanism based on either a mechanical or hydraulic system. The rigidity of the loading system should be sufficient so that the maximum deflection on any part of the apparatus does not exceed 0.025 mm at the failure load. A loading system based on deadweight loading is shown in Figure A1.

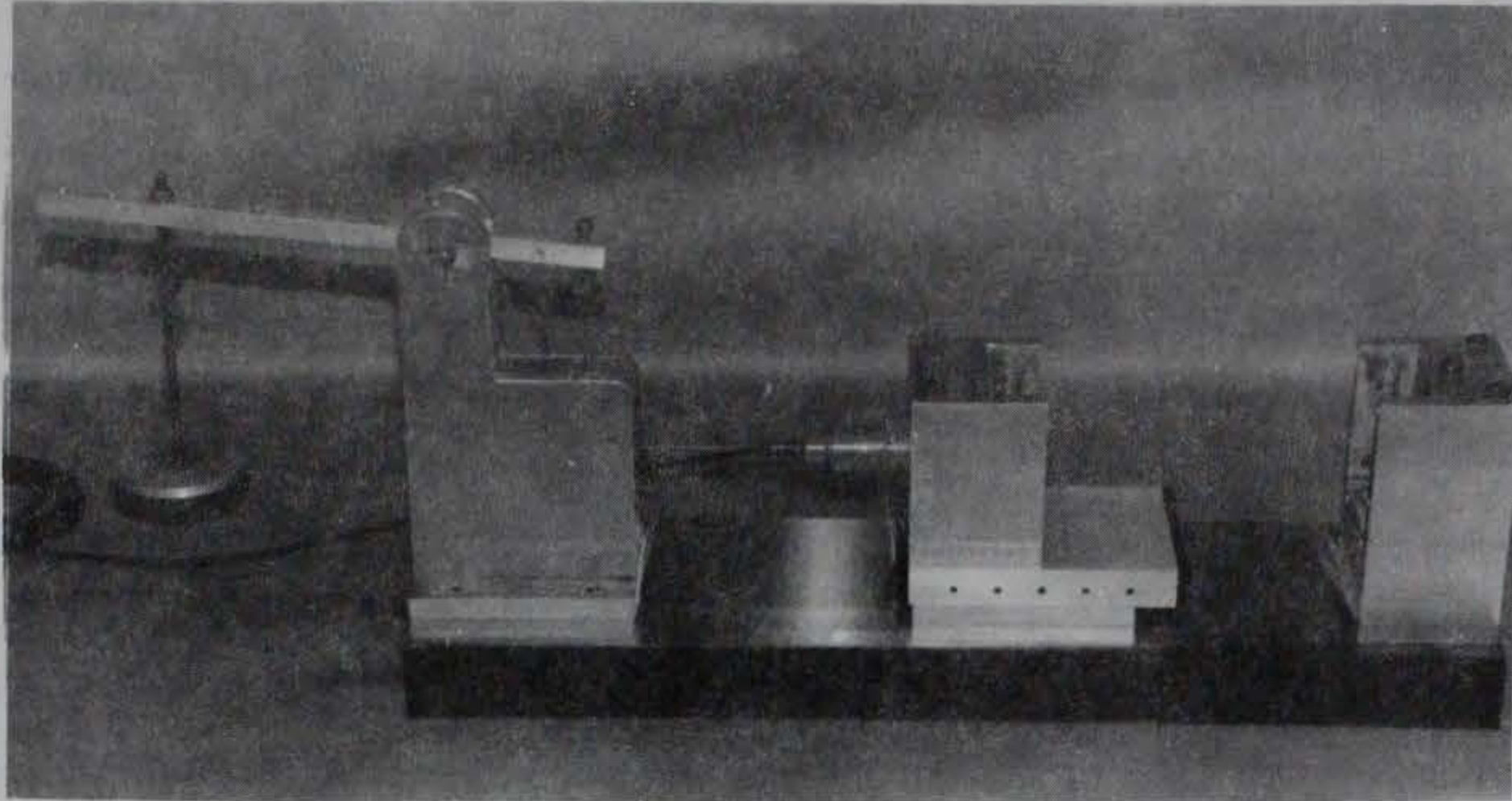
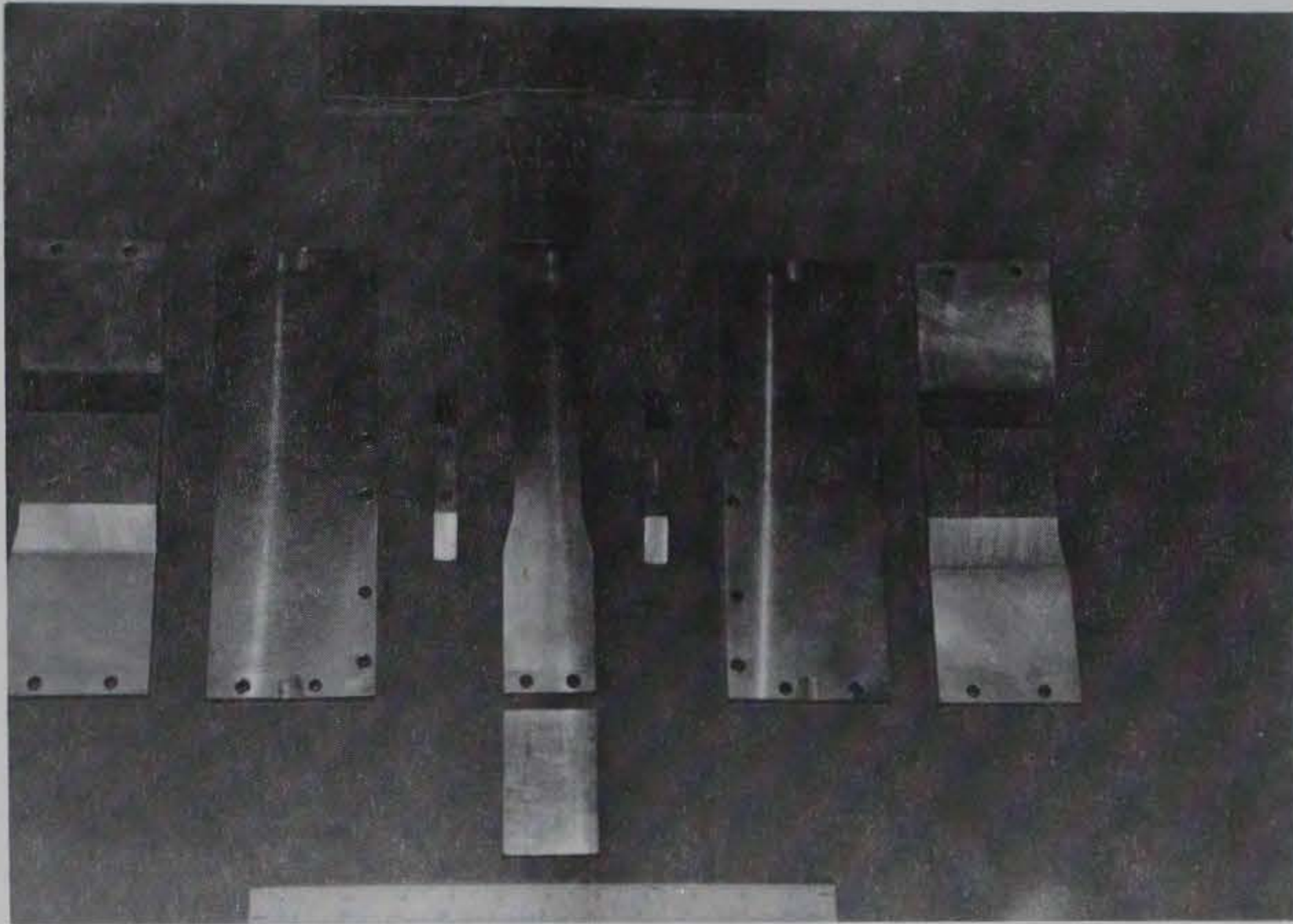


Figure A1. Tensile testing apparatus and deadweight loading system

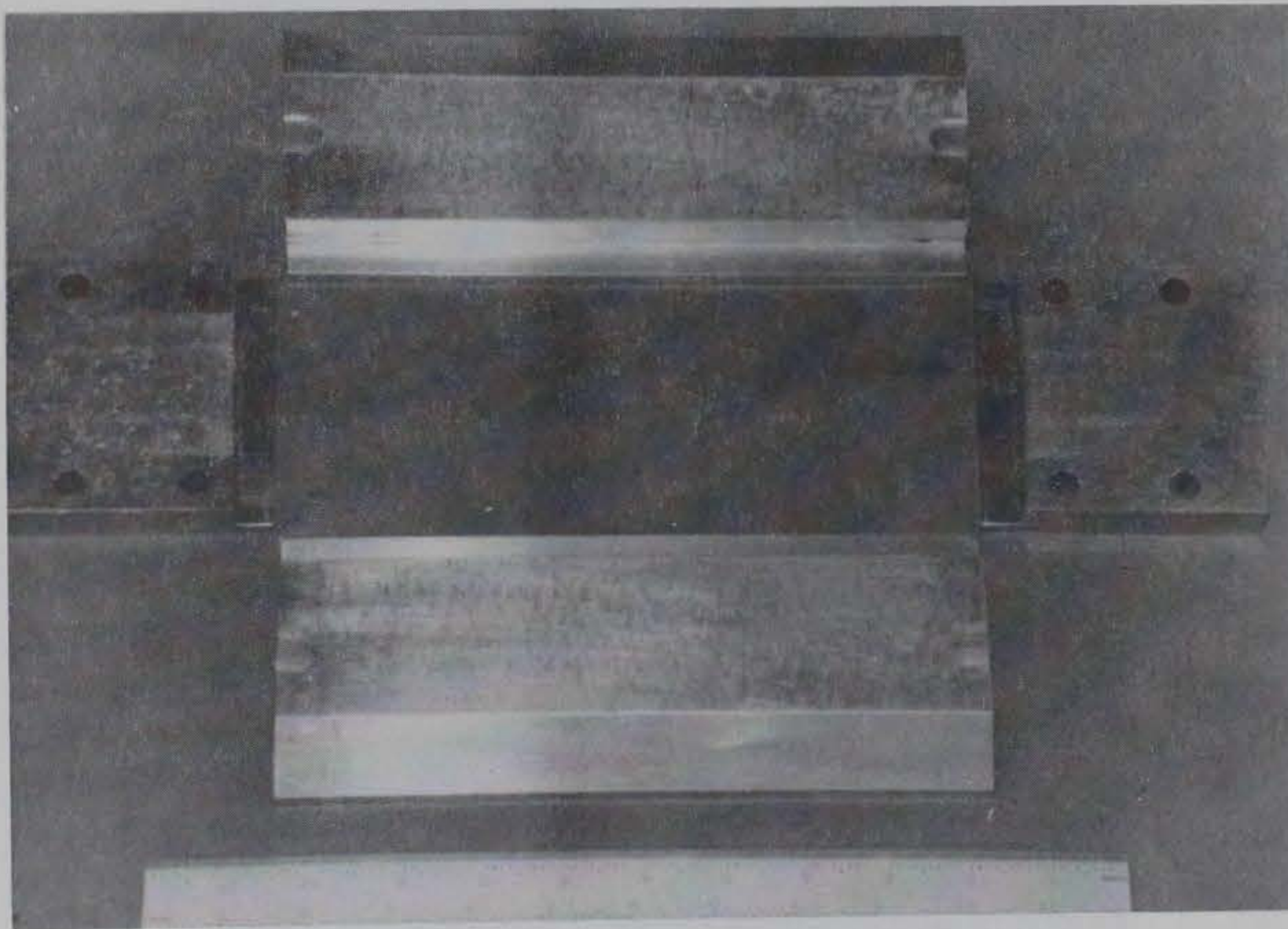
- b. Sample compaction mold consists of compaction mold sides, collar, backplates, and trimming guides. The parts of the compaction mold are presented in Figure A2 and the partially assembled compaction mold in Figure A3.
- c. Compaction tools consists of a compactor capable of delivering up to 1.04-MN/m^2 compaction pressure, a pointed tool for scarifying surface of soil between compaction lifts, and a trimming knife (see Figure A4).
- d. Displacement is measured by a LVDT (shown on a mounting bracket in Figure A5) with a resolution of 0.0025 mm over a gage length of 5.0 cm.
- e. Data are recorded by an electronic recorder capable of graphically displaying a continuous record of displacement and load. If creep rates are to be determined, the recorder must be capable of providing a time record of displacement and load.

Sample/Specimen Preparation

3. Preparation of the specimen consists of batching, compacting, trimming, and curing:



a.



b.

Figure A2. Parts included: (a) the compaction mold with trimming guides, and (b) the compaction collar

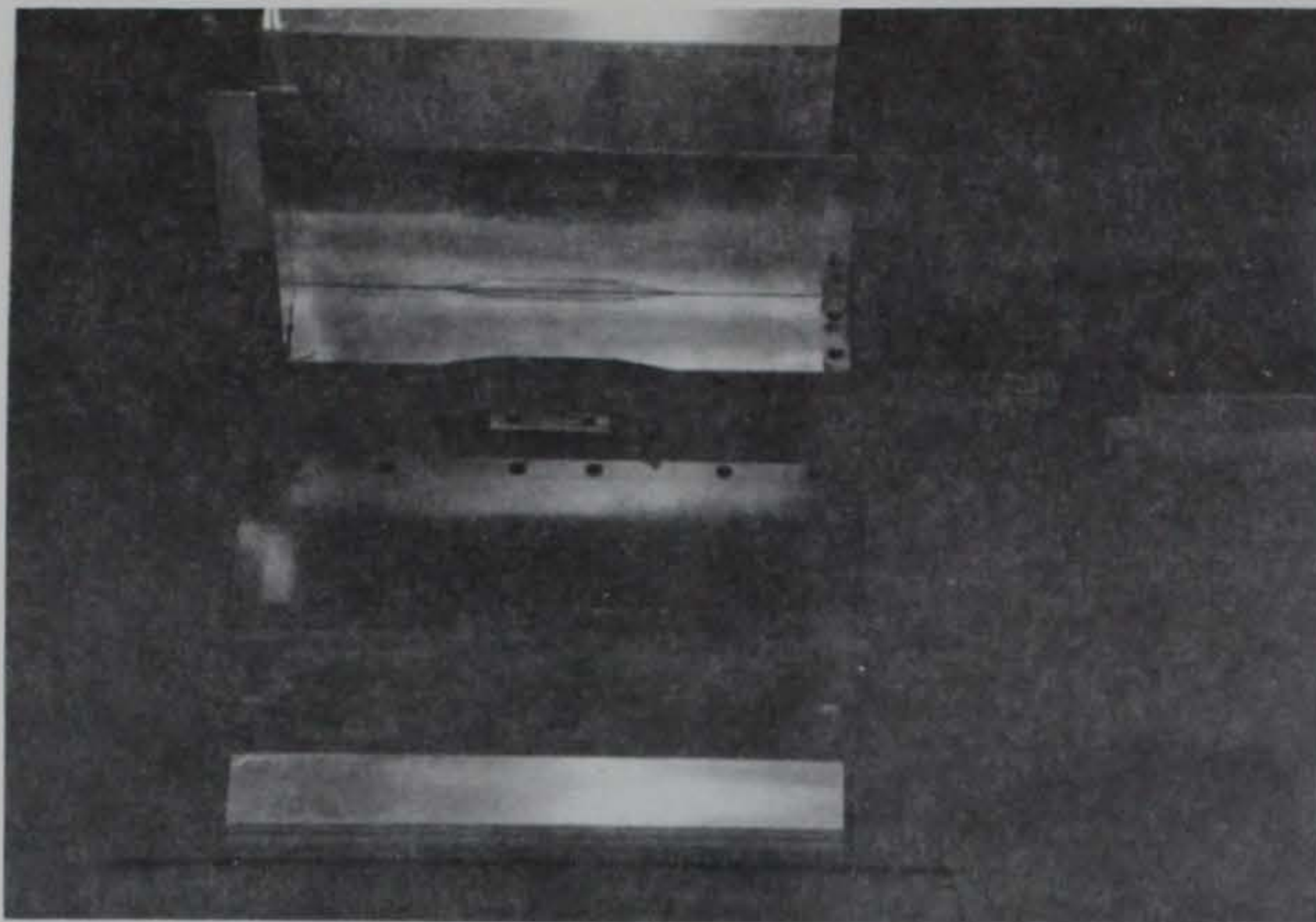


Figure A3. Partially assembled compaction mold and collar

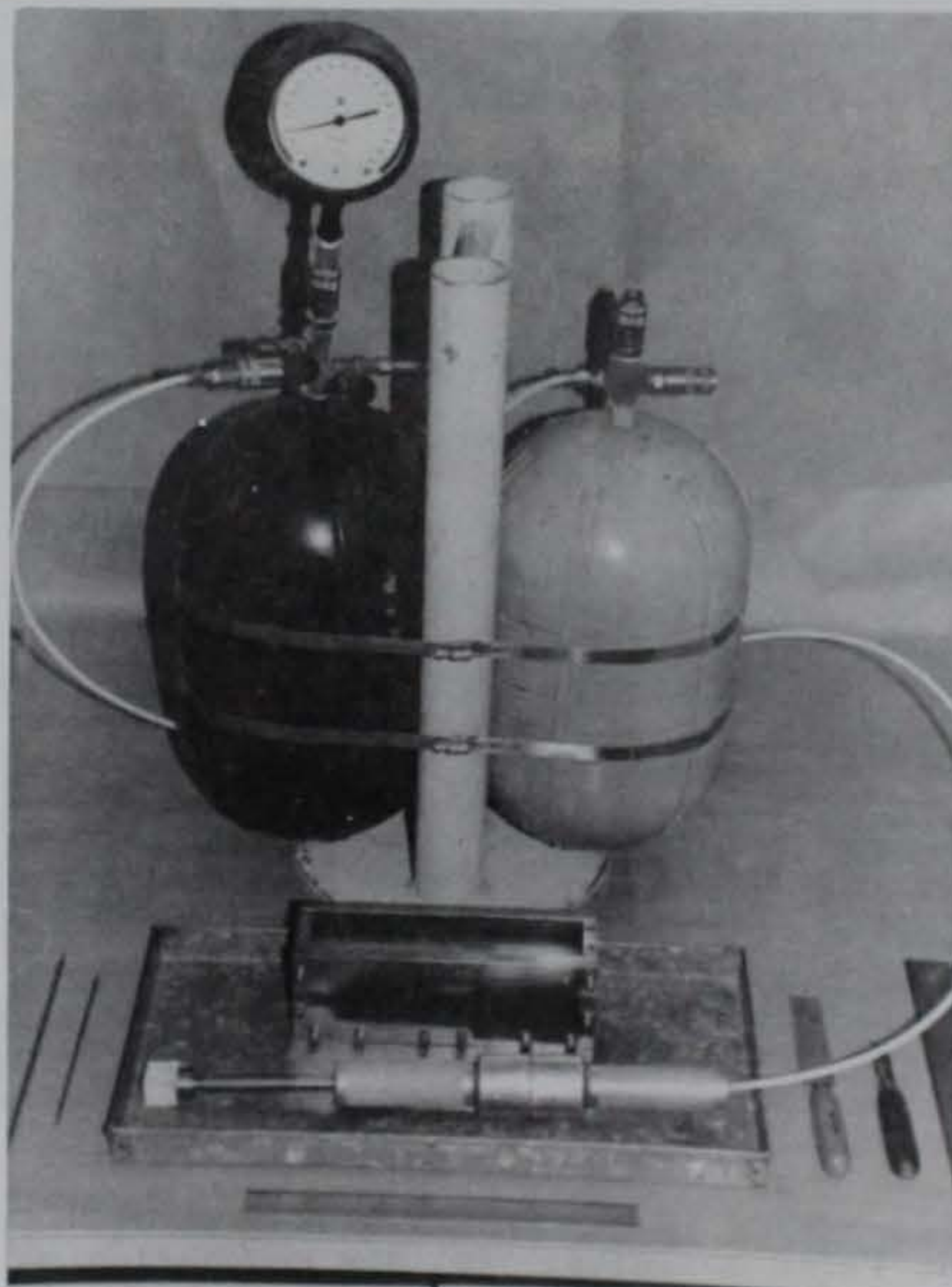


Figure A4. The pneumatic compactor, scarifying tools,
and trimming knives

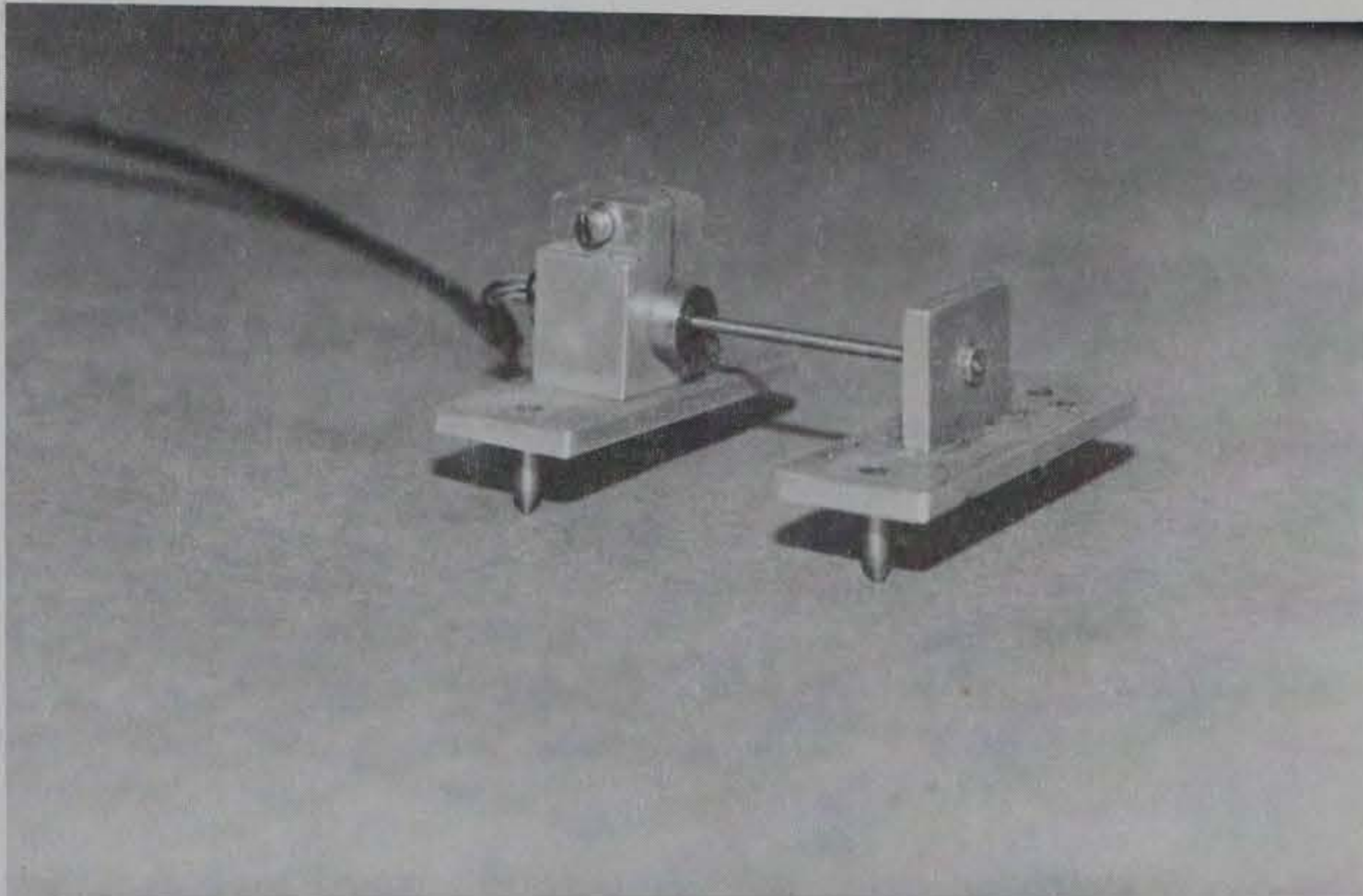


Figure A5. The LVDT and its mounting bracket used with the tensile apparatus

- a. Batching consists of mixing air-dried soil with water to achieve the desired water content. The weight of additional water required is given by

$$W_w = W_T \frac{(w_c - w_i)}{(1 + w_i)} \quad (A1)$$

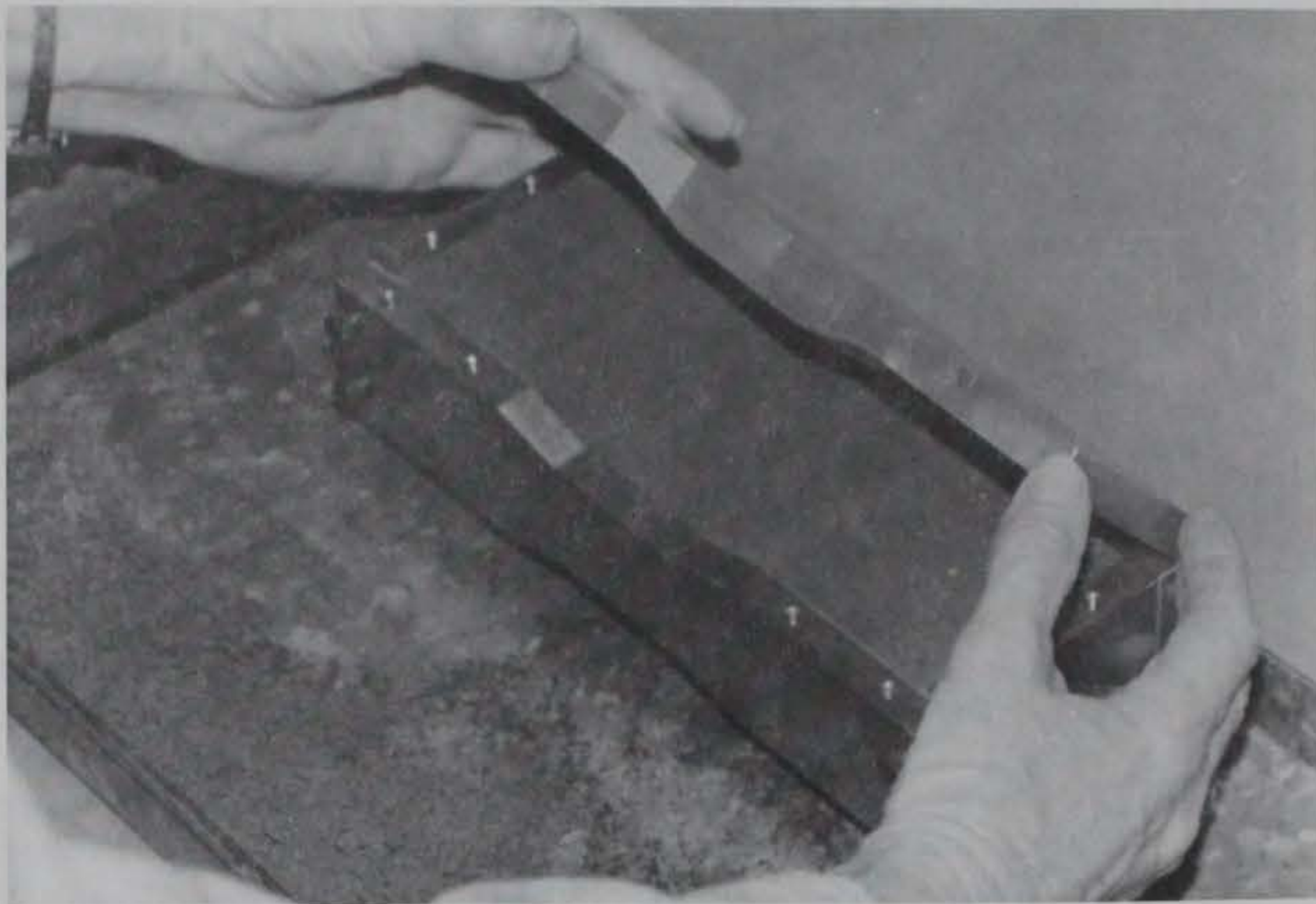
where

- W_w = weight of additional water
 W_T = initial total weight of soil
 w_c = the desired water content
 w_i = the water content of the air-dried soil

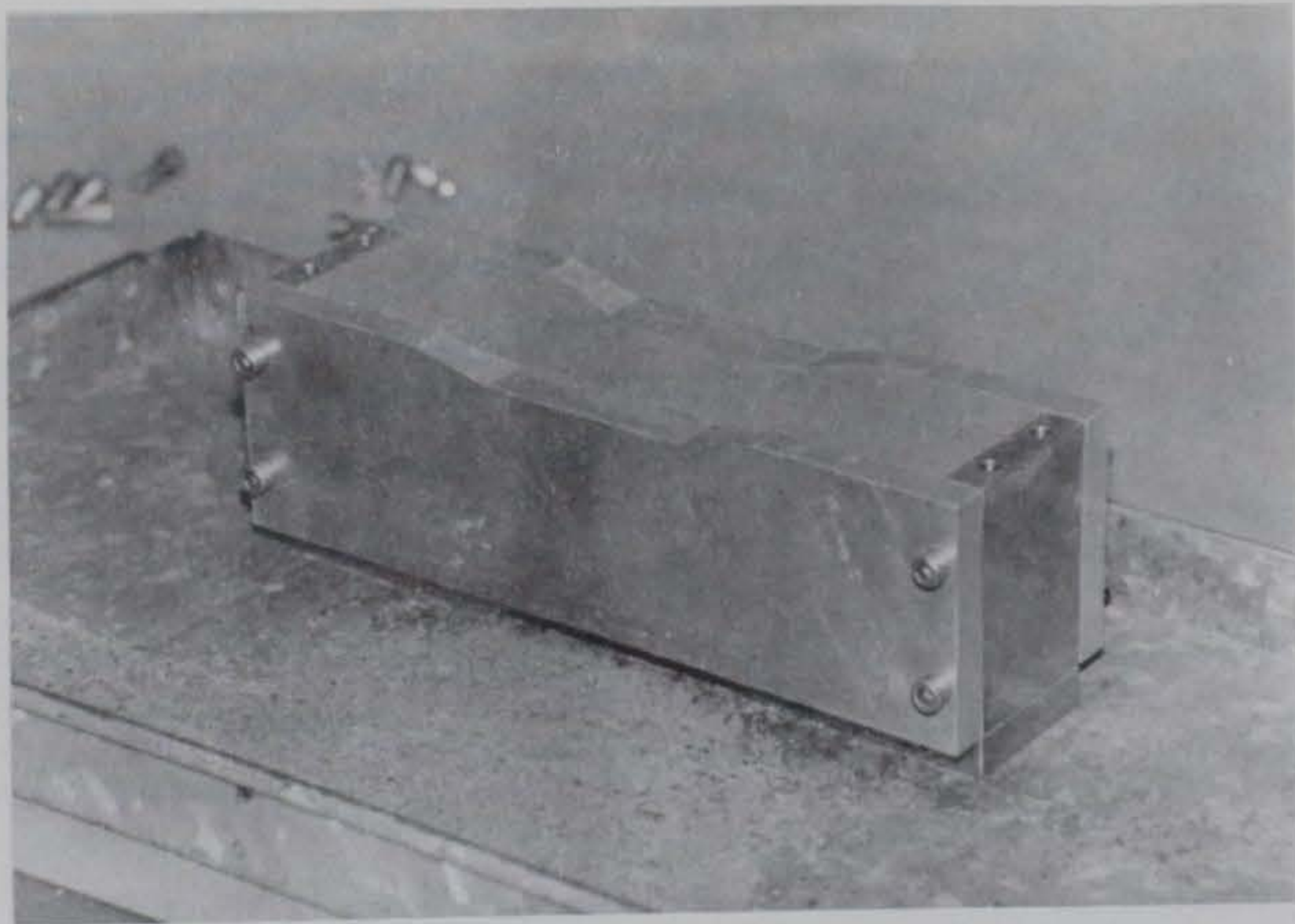
Approximately 18.5 kg of soil is needed for a series of ten tests. The batched material should be stored in a sealed container overnight to promote uniformity of water distribution.

- b. Compaction consists of the following steps:
- (1) Spray inside of the mold with a commercially available aerosol cooking grease (such as "PAM" or "MAZOLA") to keep soil from adhering to the mold during compaction.

- (2) Assemble the mold. The nonstick spray may be applied after mold assembly, if desired. Weigh the assembled mold (without collar attached).
 - (3) For each layer, weigh the required amount of soil and place it in its own plastic bag. The weight of soil for each layer should be determined by trial compaction tests such that the compacted thickness of a layer is 12 mm. The final layer when compacted will give approximately 8 mm of excess soil that is trimmed off the top of the mold when the compaction collar is removed. The water content of the batched material should be determined for each specimen.
 - (4) Spread material for one layer in the mold to a level surface. Press material into a firm but not compacted layer using the foot of the pneumatic compactor.
 - (5) Compact the layer with the WES pneumatic compaction device in 3 passes using 20 tamps per pass. Carefully ensure that compaction pressure is applied evenly by keeping the tamper vertical while applying thrust. Also, avoid over tamping, which occurs when the tamper bottoms out at the end of the thrust.
 - (6) Scarify the surface of compacted layer to a depth of about 6 mm.
 - (7) Repeat steps (4), (5), and (6) for second layer.
 - (8) Put collar on mold and repeat steps (4), (5), and (6) for the remaining five layers.
- c. Trimming is done using a sharpened straightedge. The trimming mold is designed to avoid cracking or otherwise weakening of the specimen during trimming. Care must be taken when removing mold parts to avoid damage to the compacted specimen. It is recommended that suction between soil and mold surface be broken by sliding mold pieces parallel to the specimen surface before pulling mold apart. Trimming should be done according to the following sequence:
- (1) Carefully remove collar and trim top surface level with mold. Patch any spalled areas with trimmings so that an accurate density can be determined.
 - (2) Weigh the mold and compacted soil for determination of density.
 - (3) Attach top trimming guide. Remove one side and associated bottom spacer.
 - (4) Carefully trim specimen to conform to trimming guides.
 - (5) Attach replacement side of mold to support trimmed surface during trimming of opposite side and thus lessen the tendency to crack the specimen by bending (see Figure A6a).
 - (6) Repeat steps (3), (4), and (5) on other side of specimen. Make sure that when second replacement side is attached



a.



b.

Figure A6. Two steps of the trimming procedure shown are: (a) the trimmed reduced section of the specimen ready to receive its mating trimming guide, and (b) the trimmed reduced top section of the specimen

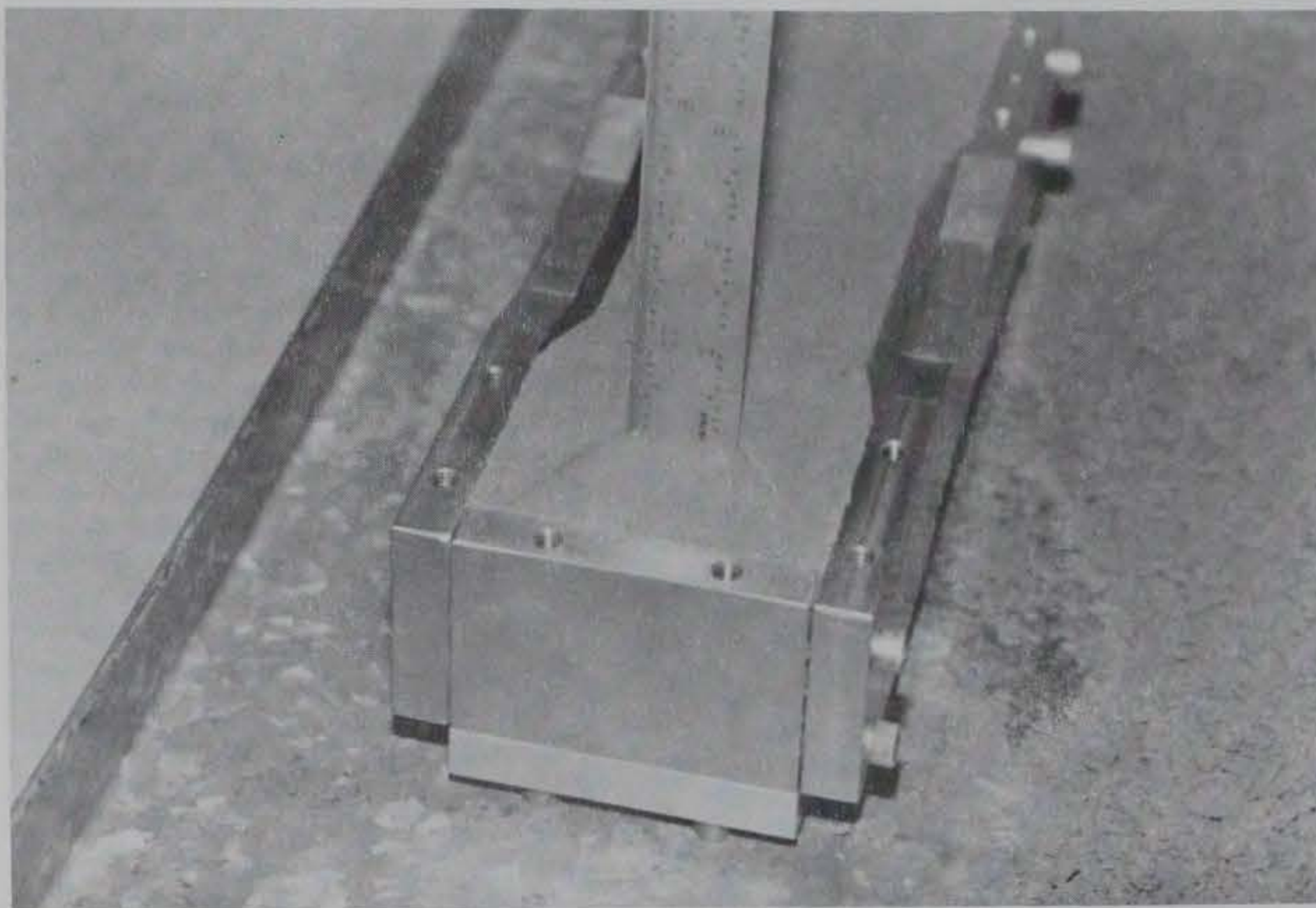
that the notched edge of each side points in the same direction (see Figure 6b).

- (7) Remove top trimming guide.
- (8) Carefully trim specimen (Figure 6b).
- (9) Replace top trimming guide.
- (10) Remove, rotate, and replace sides. The notched edges should now be on the bottom.
- (11) Remove bottom trimming guide and carefully trim specimen.
- (12) Replace bottom trimming guide.
- (13) Remove one of the replacement sides and carefully trim notches in specimen ends (see Figure A7). Replace side.
- (14) Repeat step (13) for opposite side of specimen.
- (15) Carefully remove trimmed specimen from mold and store in a sealed container for an appropriate curing time; typically, the minimum curing time required to achieve repeatable results for Vicksburg silty clay is 24 hr. Trial tests may be needed to establish the appropriate curing time for a particular soil. The storage location and/or container should maintain a high-humidity condition to avoid specimen drying while curing.

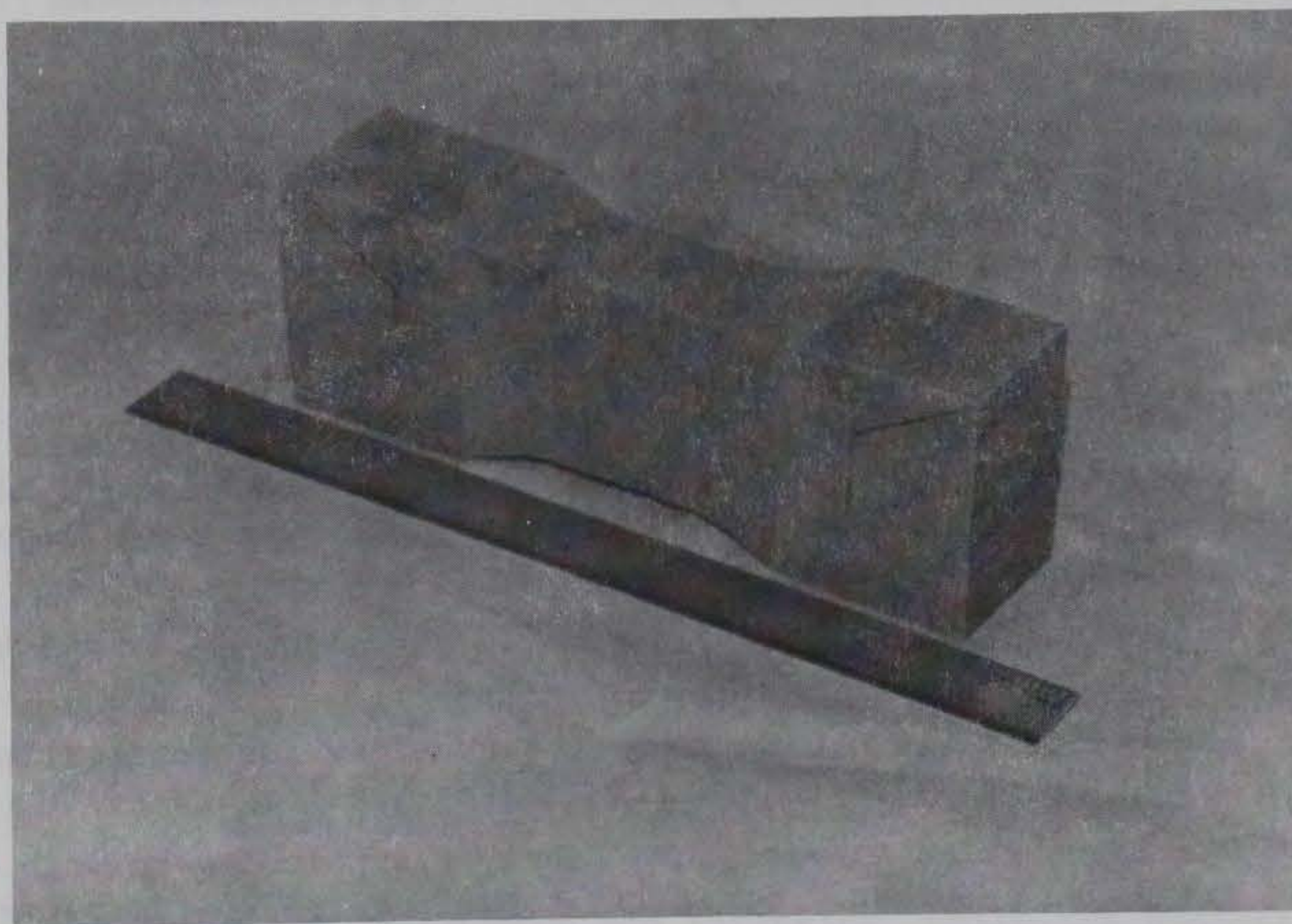
Apparatus Preparation

4. The apparatus is prepared to ensure correct alignment of the specimen in grips and to reduce after-test cleanup. The loader should be prepared as follows:

- a. Coat grips of device with petroleum jelly. The coating helps keep Hydrostone from sticking to the grips.
- b. Line bottom and jaws of grips with filter paper to provide additional protection and facilitate the removal of Hydrostone during disassembly of apparatus at end of test.
- c. Assemble grips on two sides of each grip block. The grips should not be tightened until all pieces are in place to avoid binding and cracking the specimen. All parts of the grips should be coated with a thick layer of petroleum jelly to keep Hydrostone from leaking.
- d. Take the load off slide table by placing support under loading platform (if dead load system is used).



a.



b.

Figure A7. Final trimming steps involve: (a) addition of notches in the end of the specimen, and (b) the completed specimen after removal from the mold

Specimen Setup

5. Specimen setup includes preparation of the specimen for placement in the device and for alignment in the grips as follows:

- a. Dip specimen ends in molten wax to cover ends 3.0 mm past the notch to prevent bleeding of water from the Hydrostone into the soil (Figure A8). To ensure a tight grip, the wax should cling tightly to the soil surface (it will not stick to the soil). If the wax appears to pull away from the soil after cooling, remove it and recoat the ends.

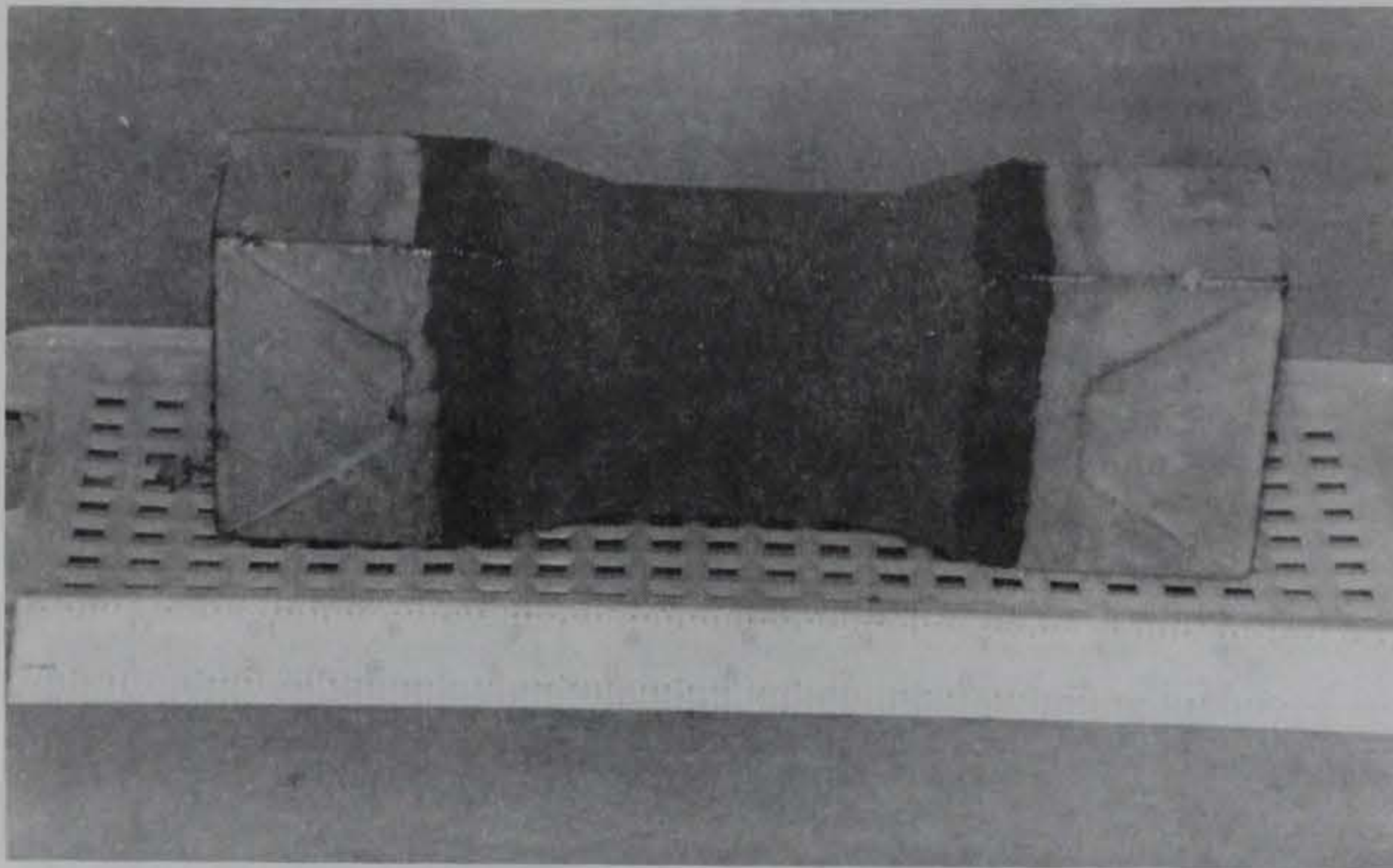


Figure A8. Wax-coated ends of specimen with a coating of petroleum jelly from edge of wax to the start of the reduced section

- b. Insert specimen in grip blocks. Make sure that wax does not extend into the removable portion of the grip to avoid binding when the grip is tightened. Remove any excess wax. Keep the specimen centered in grips.
- c. Coat the remaining grip pieces with petroleum jelly and attach, but do not tighten to the grip block.
- d. Lock slide table 6.0 mm from stop to allow for contraction or expansion of Hydrostone during curing (see Figure A9).
- e. Check the grips to make sure there is no binding between the grips and specimen. Carefully tighten grips to the block. Adjacent screws should not be tightened in sequence; rather tightening should alternate between opposite sides of grip to ensure an even application of pressure on the specimen. Note that the purpose of the grips is not to hold the specimen mechanically, for the specimen is being held by the Hydrostone. The grips are intended to align the specimen and restrain the

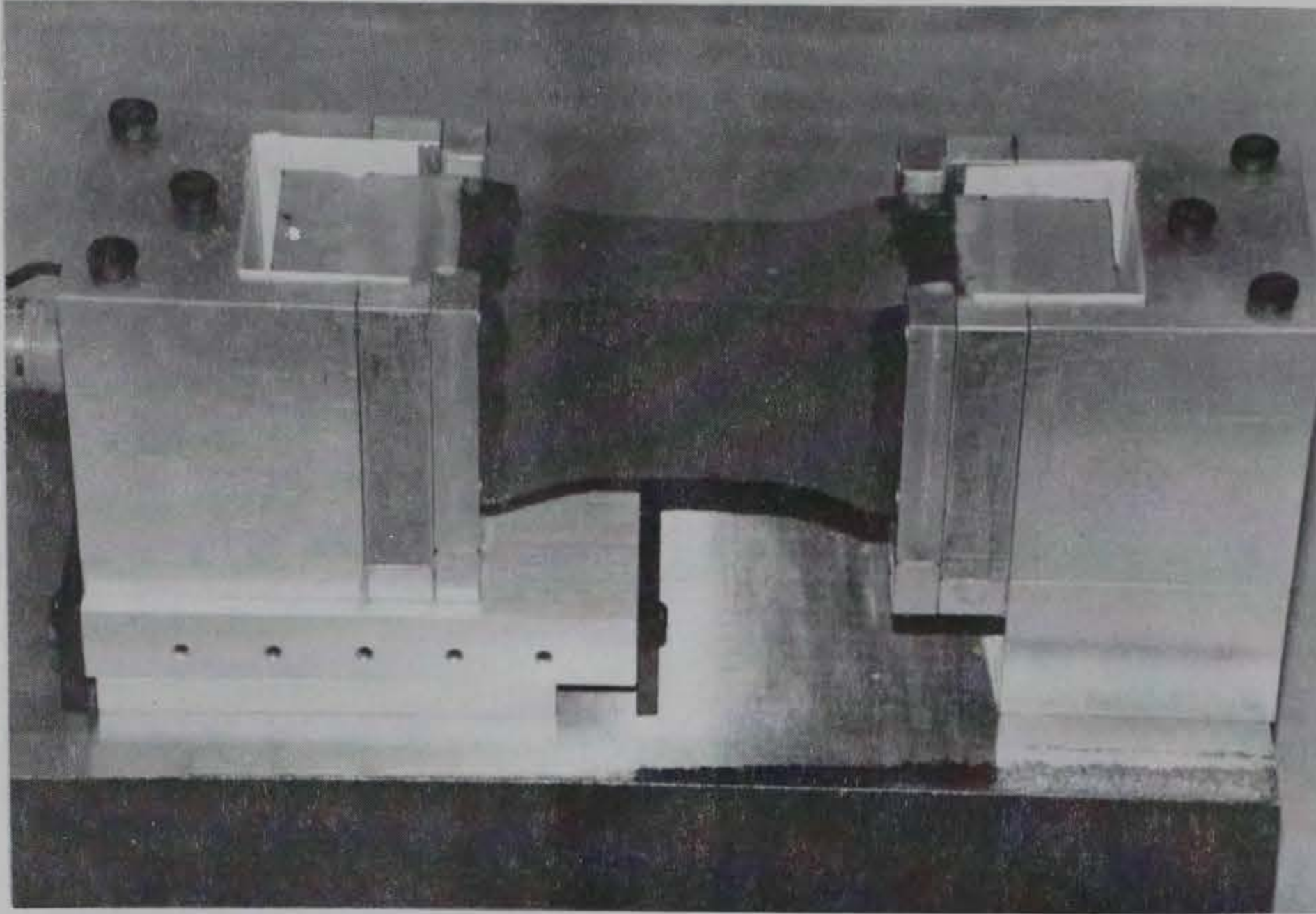


Figure A9. Specimen in grips before pouring of the Hydrostone with with slide table locked approximately 6.0 mm from slide table stop.

cured Hydrostone. Tightening the grips on the specimen may cause cracking.

- f. Hydrostone is used to hold the specimen in the grips. Dry Hydrostone is mixed with water and poured into the annular space between the grip block and soil. Curing of the Hydrostone to its final rocklike consistency takes about one hour. The following steps should be used to mix and place the Hydrostone:
- (1) Mix enough water and Hydrostone to fill both jaws to about 6.0 mm above the specimen. The consistency of the Hydrostone should be similar to a thick slurry that will just flow.
 - (2) Fill one grip half full, then fill the remaining grip completely. Return to the first jaw and complete filling. Do not fill one grip unless the other grip is half filled. When full, the hydrostatic pressure of the Hydrostone in a grip is sufficient to push the specimen out of the grip.
 - (3) After the Hydrostone is in place, remove locking screw from slide table.
 - (4) Coat exposed surfaces of the specimen with petroleum jelly to reduce drying and shrinking, while the Hydrostone is curing.
- g. The LVDT is attached at a 5.0-cm gage length in the reduced section of the specimen as shown in Figure A10 using the following procedure:

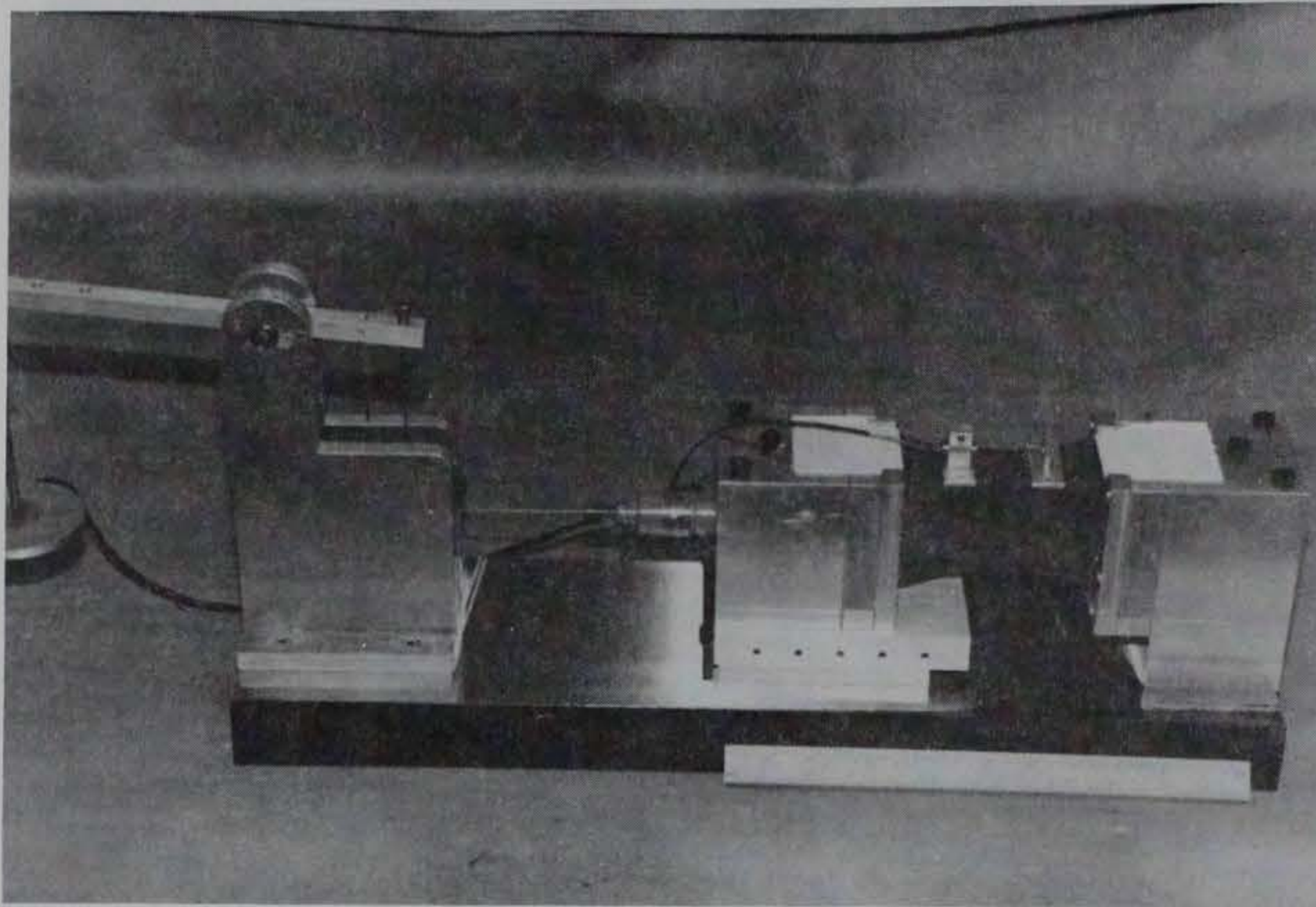


Figure A10. LVDT installed on specimen with slide table unlocked and ready for loading of specimen (weight of loading arm and platform normally used as the initial loading weight)

- (1) Measure and mark a 5.0-cm gage length within the reduced area of the specimen.
 - (2) Make four starter grooves at the points where the strain gage pins are to be inserted into the specimen.
 - (3) Carefully attach the LVDT to specimen by slowly pushing the pins into the starter grooves. The pins should be inserted with a single uniform push to avoid enlarging the starter grooves.
 - (4) Once the LVDT is attached, adjust the LVDT (move either the LVDT core or body) to zero the output. The load cell is also zeroed at this time.
- h. Loading of the specimen by the dead load method is accomplished using the following steps:
- (1) Take initial readings of the LVDT and load cell.
 - (2) Apply first load by removing support from under the loading platform. At this point, the only load on the specimen should be the weight of the platform.
 - (3) After one minute (or other specified loading interval dictated by testing program), take readings of the LVDT and load cell. Note that the readings are supplemental to the chart recorder.

- (4) Add weights to the loading platform at specified time intervals (dictated by testing program) until rupture of the specimen. Readings must be taken on the LVDT and load cell prior to placement of each load.
- (5) After the test is complete, prepare a complete description of the specimen, including location and orientations of the failure surfaces. A photograph of the specimen is preferred. A soil sample should be taken from the gage length area of the specimen for water content determination. With the test now complete, all soil pieces, Hydrostone, and petroleum jelly must be cleaned from the apparatus.

Data Presentation

6. Data to be presented should include:
 - a. A stress-strain curve consisting of a plot of the load/specimen area versus the LVDT reading/gage length where the strain values are based on LVDT reading just prior to placing each load.
 - b. A compaction curve based on combining the dry density versus water content data from several tests. If the tensile tests have been performed at the same water content and density, it will not be possible to construct a complete compaction curve from the data. A special series of specimens must be compacted to provide data for the curve. All tests of a series should be compacted using the same compaction pressure and test mold. Alternatively, the data may be superimposed on a compaction curve obtained by a standard laboratory or field method if available.
 - c. The data sheet(s) containing soil description, water content, density data, and test readings of the load cell and LVDT.

APPENDIX B: TENSILE TEST RESULTS

1. The figures contained herein are individual stress-strain curves for each tensile test. Each test is indicated by a test designation grouping consisting of two letters followed by three sets of numbers: material type, water content (percent), compaction pressure (psi), and test number. For example, the grouping CM-14-75-10 can be separated into its individual parts as follows:

CM - material type (medium plasticity clay)

14 - water content in per cent

75 - compaction pressure in psi

10 - test number

2. Figures that contain strain data not indicative of specimen behavior are indicated by an asterisk. These test data are included in this appendix for test series completeness and not to imply actual material behavior. However, even though the strain data for these specimens may be in error, the strength at failure presented in these figures is considered to be reasonably accurate.

B2

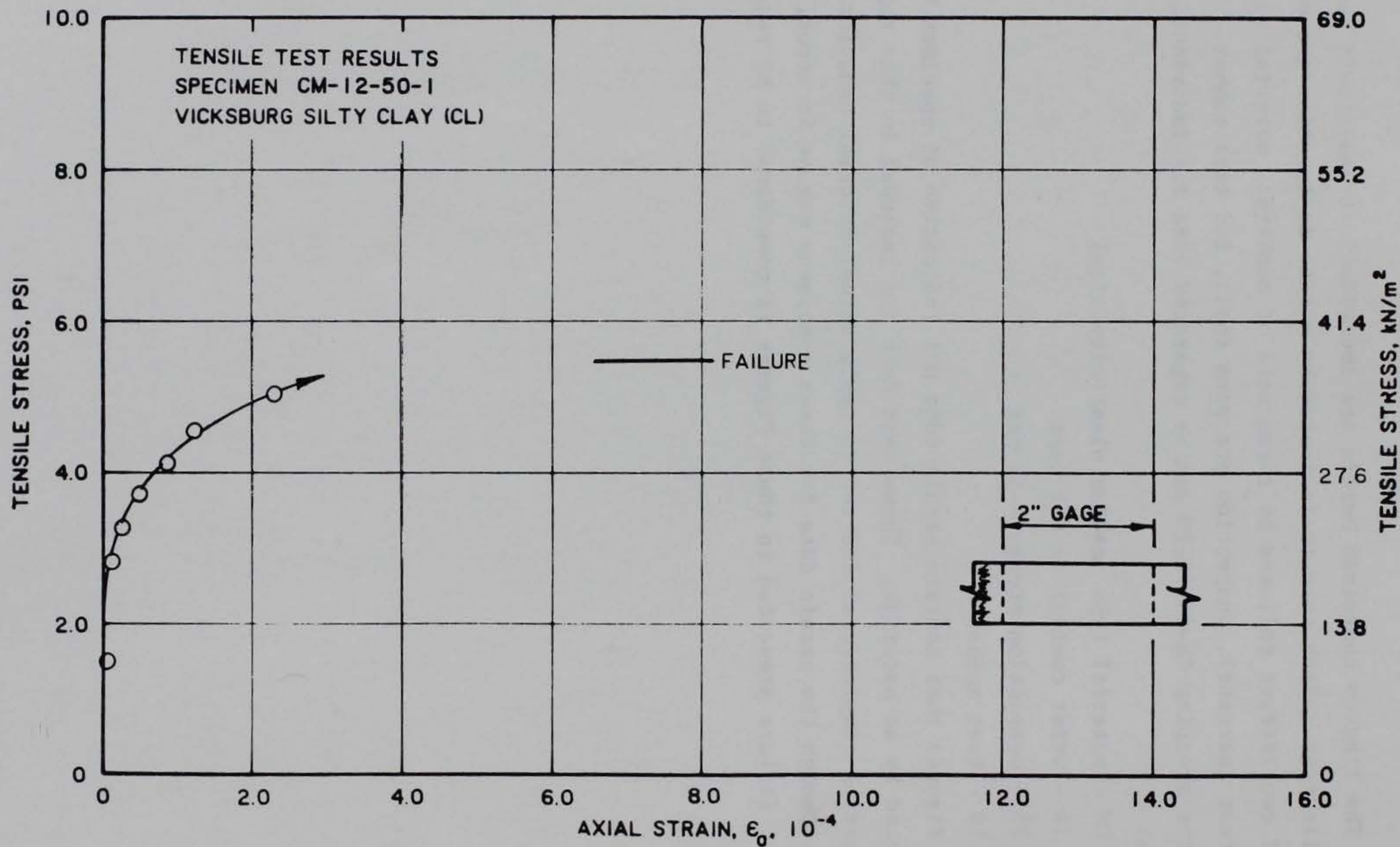


Figure B1. Stress-strain curve for tensile test CM-12-50-1

B3

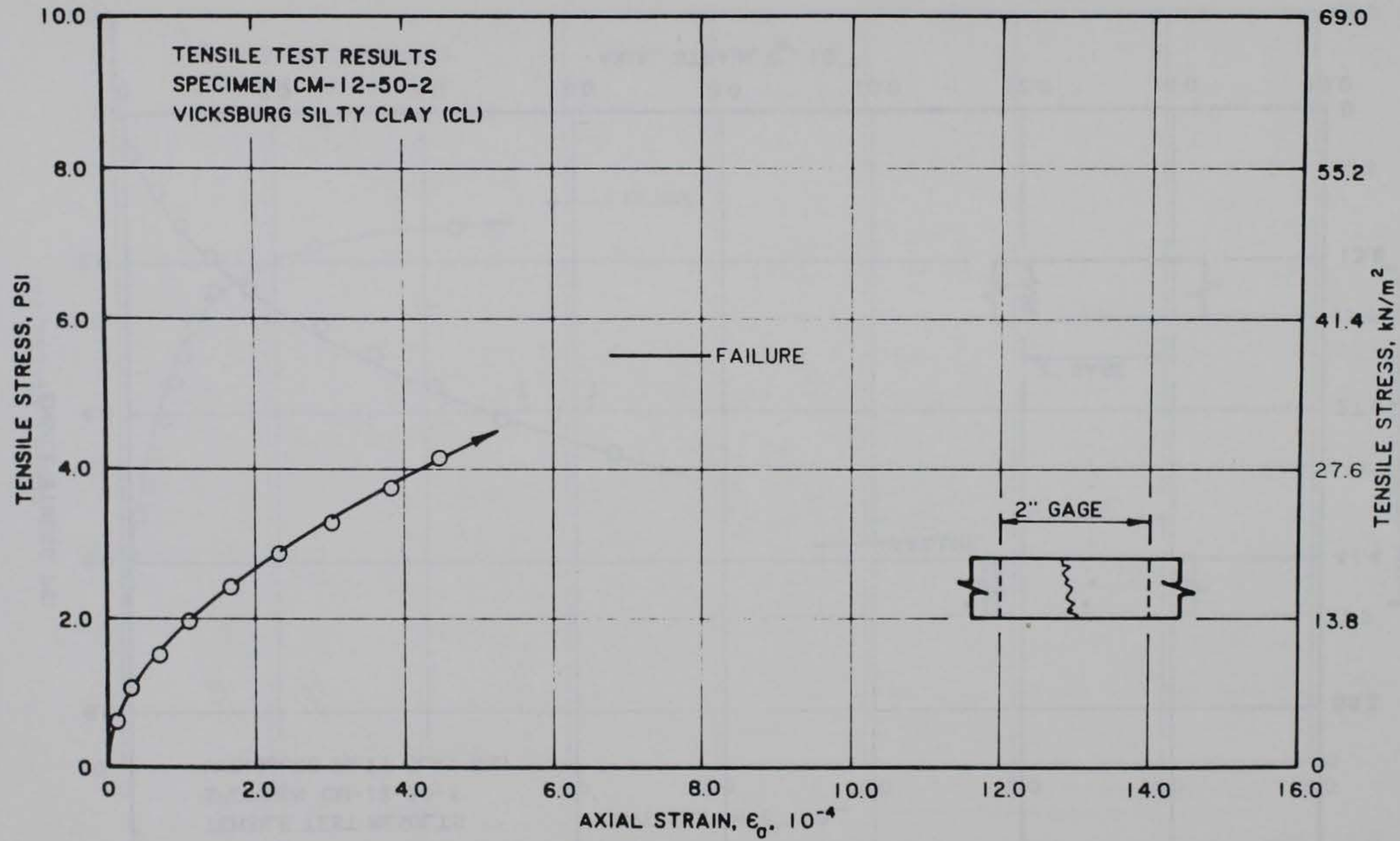


Figure B2. Stress-strain curve for tensile test CM-12-50-2

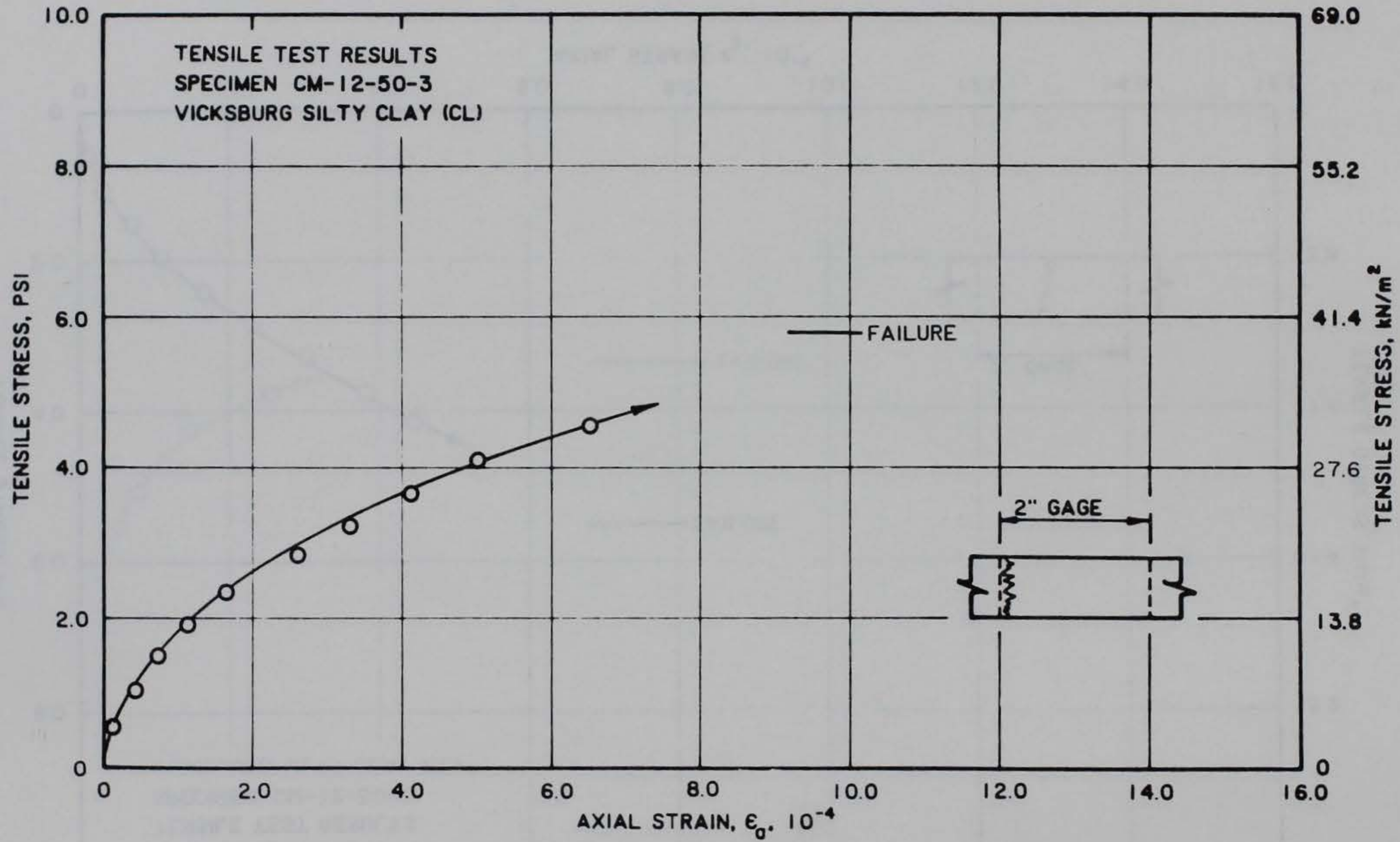


Figure B3. Stress-strain curve for tensile test CM-12-50-3

B5

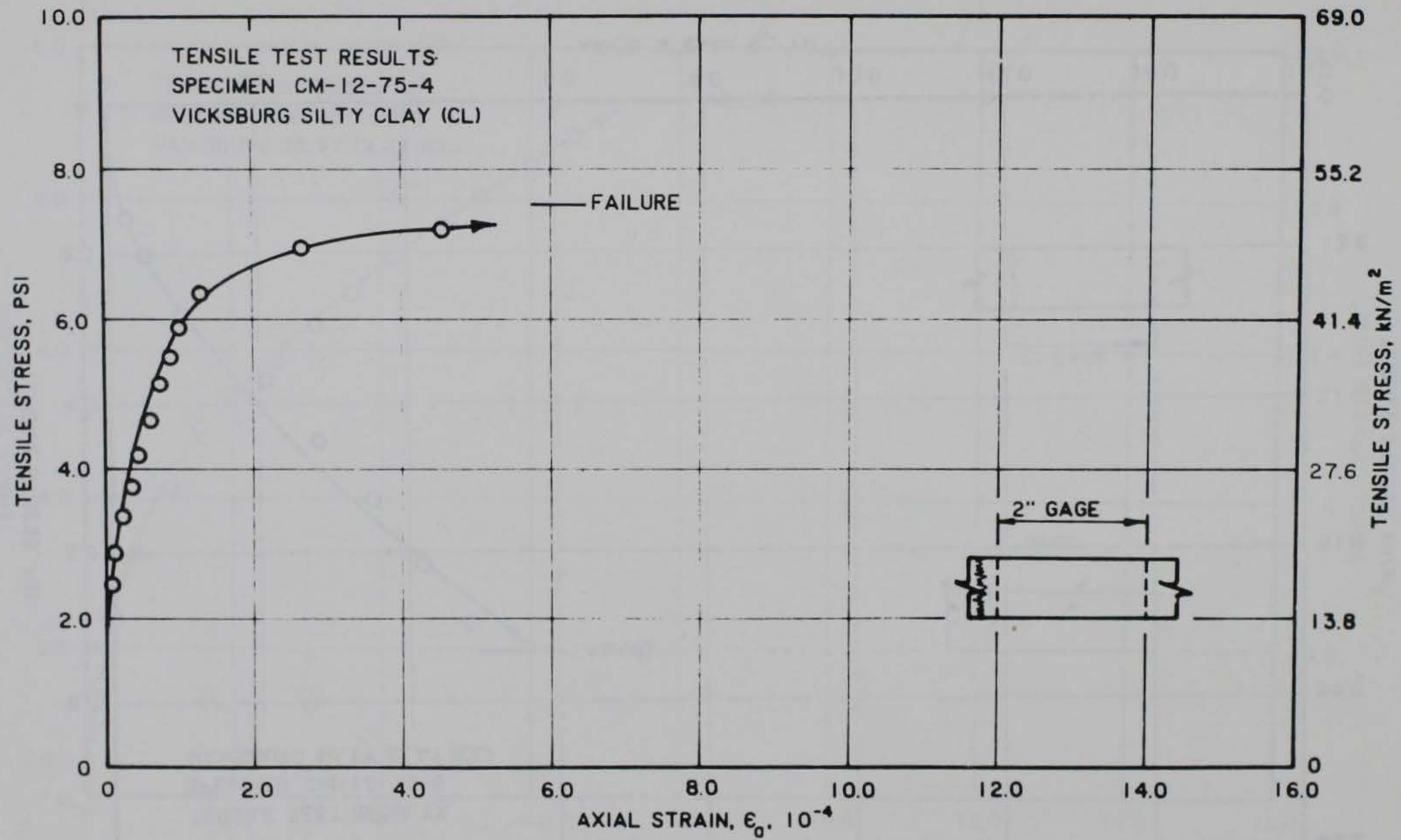


Figure B4. Stress-strain curve for tensile test CM-12-75-4

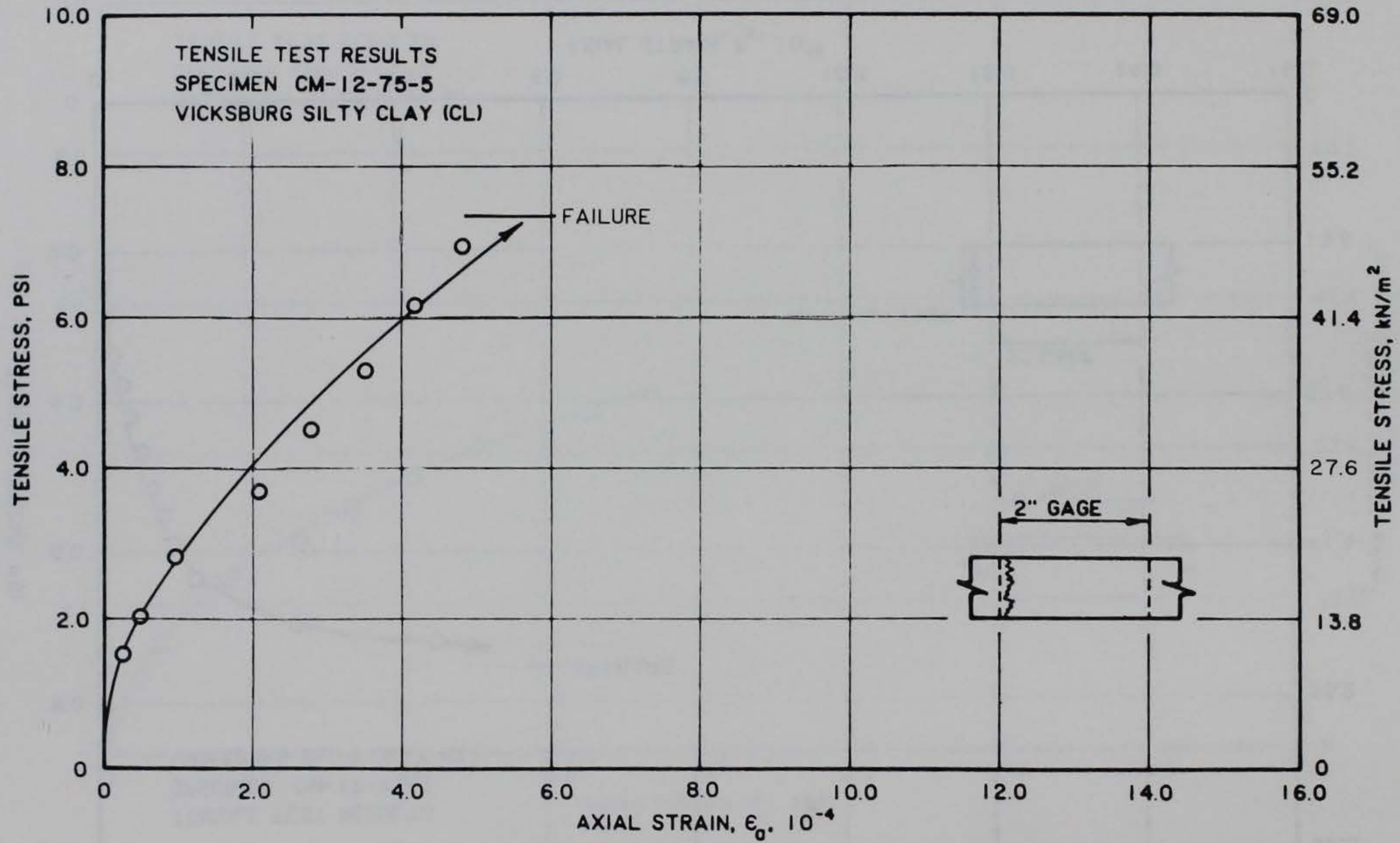


Figure B5. Stress-strain curve for tensile test CM-12-75-5

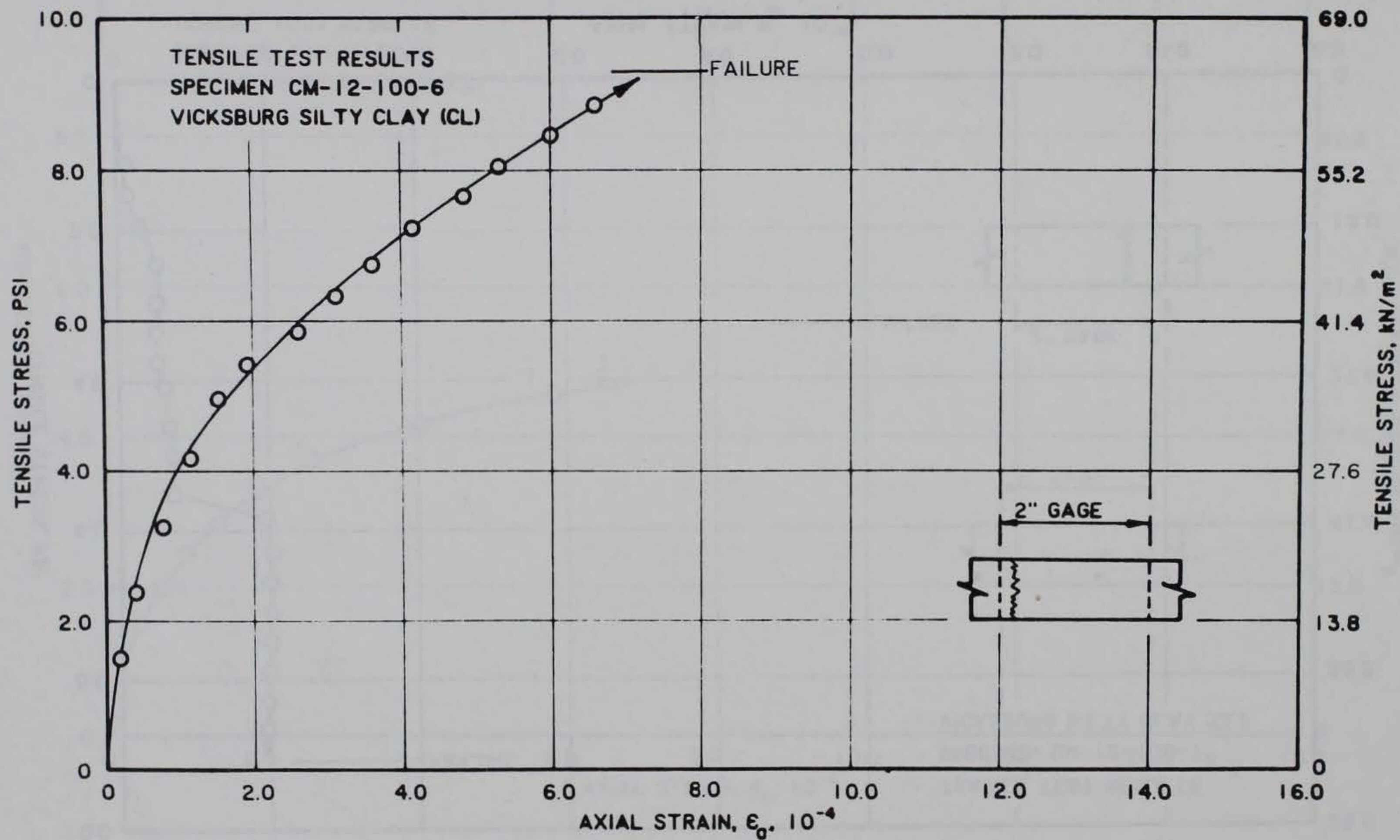


Figure B6. Stress-strain curve for tensile test CM-12-100-6

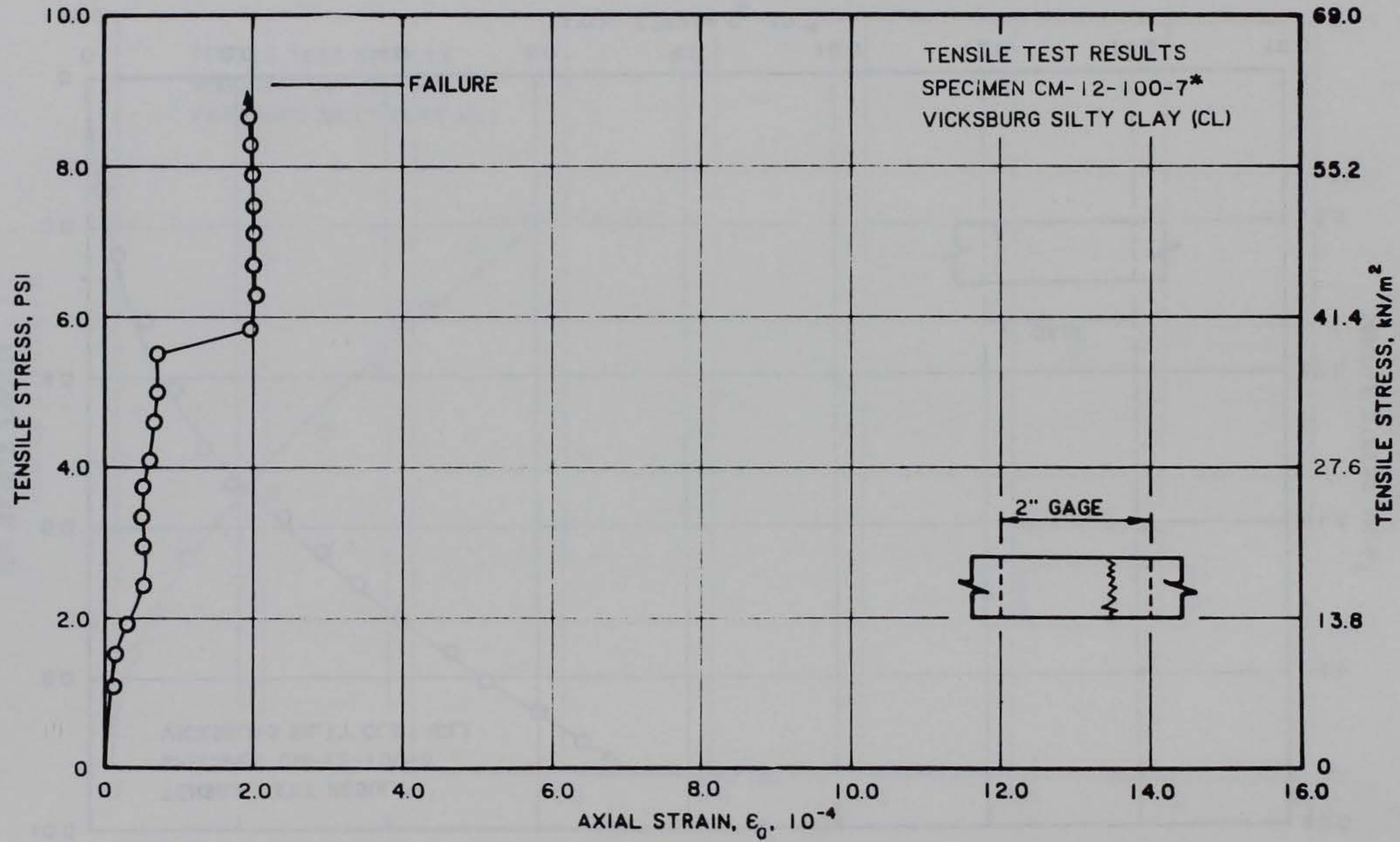


Figure B7. Stress-strain curve for tensile test CM-12-100-7*

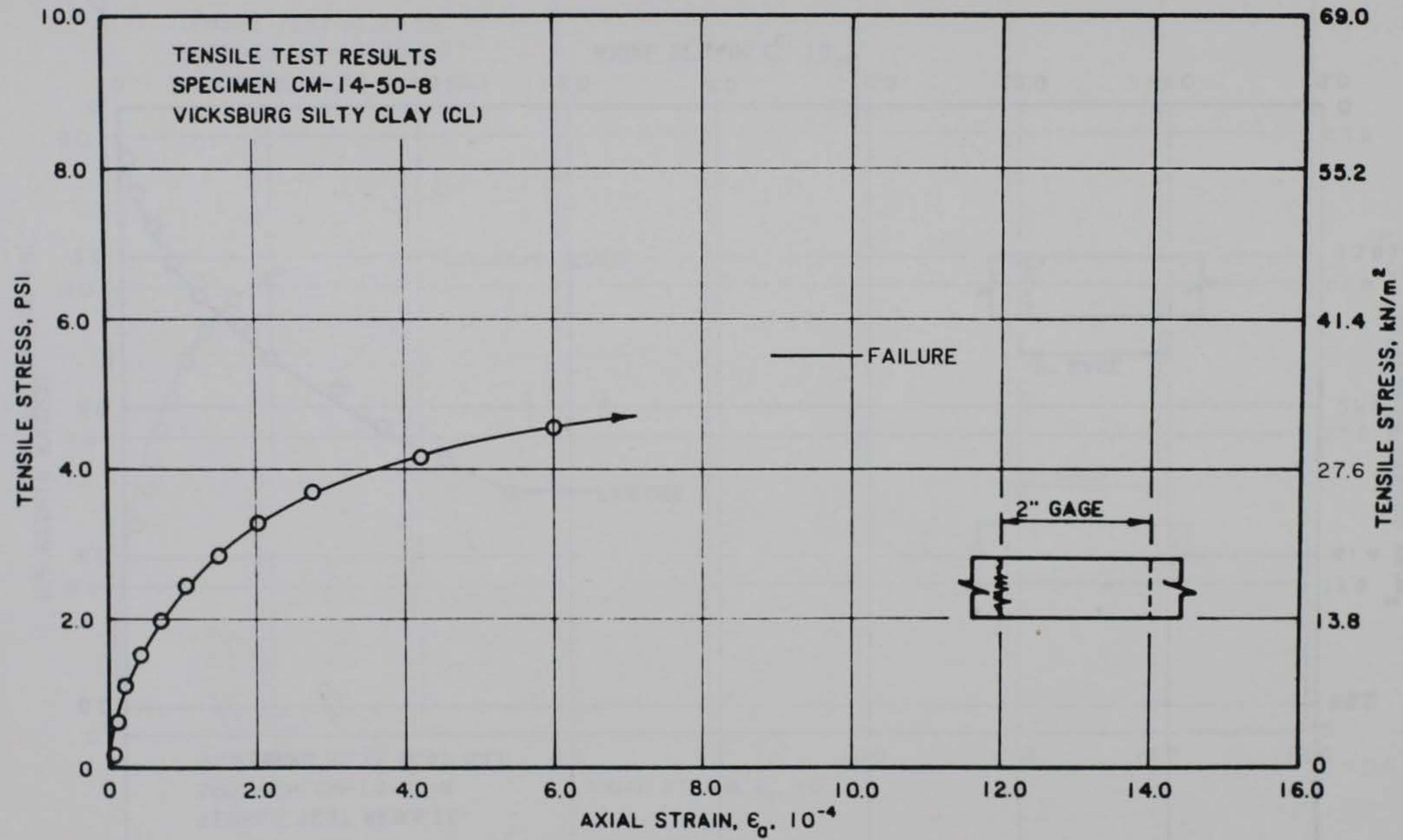


Figure B8. Stress-strain curve for tensile test CM-14-50-8

B10

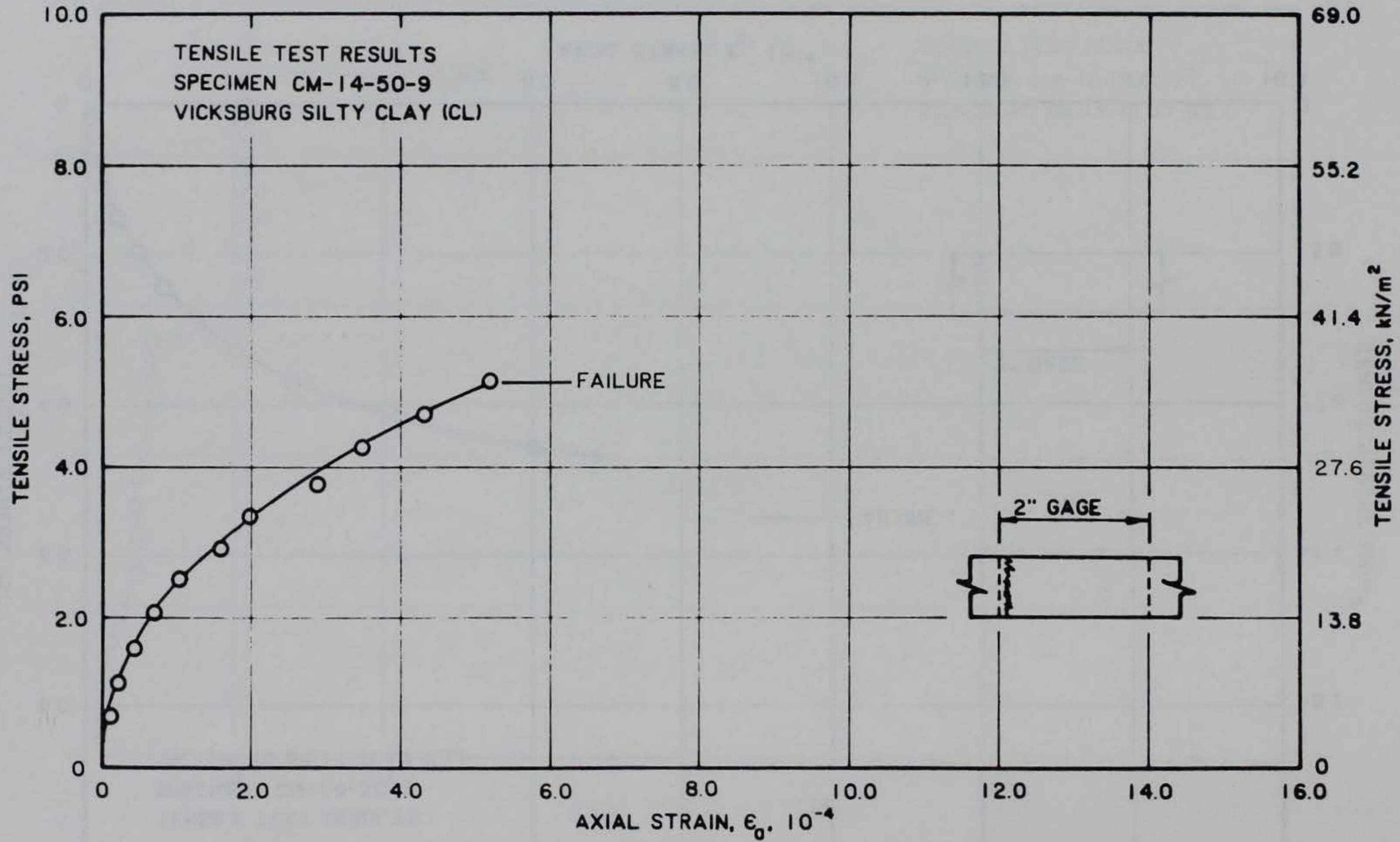


Figure B9. Stress-strain curve for tensile test CM-14-50-9

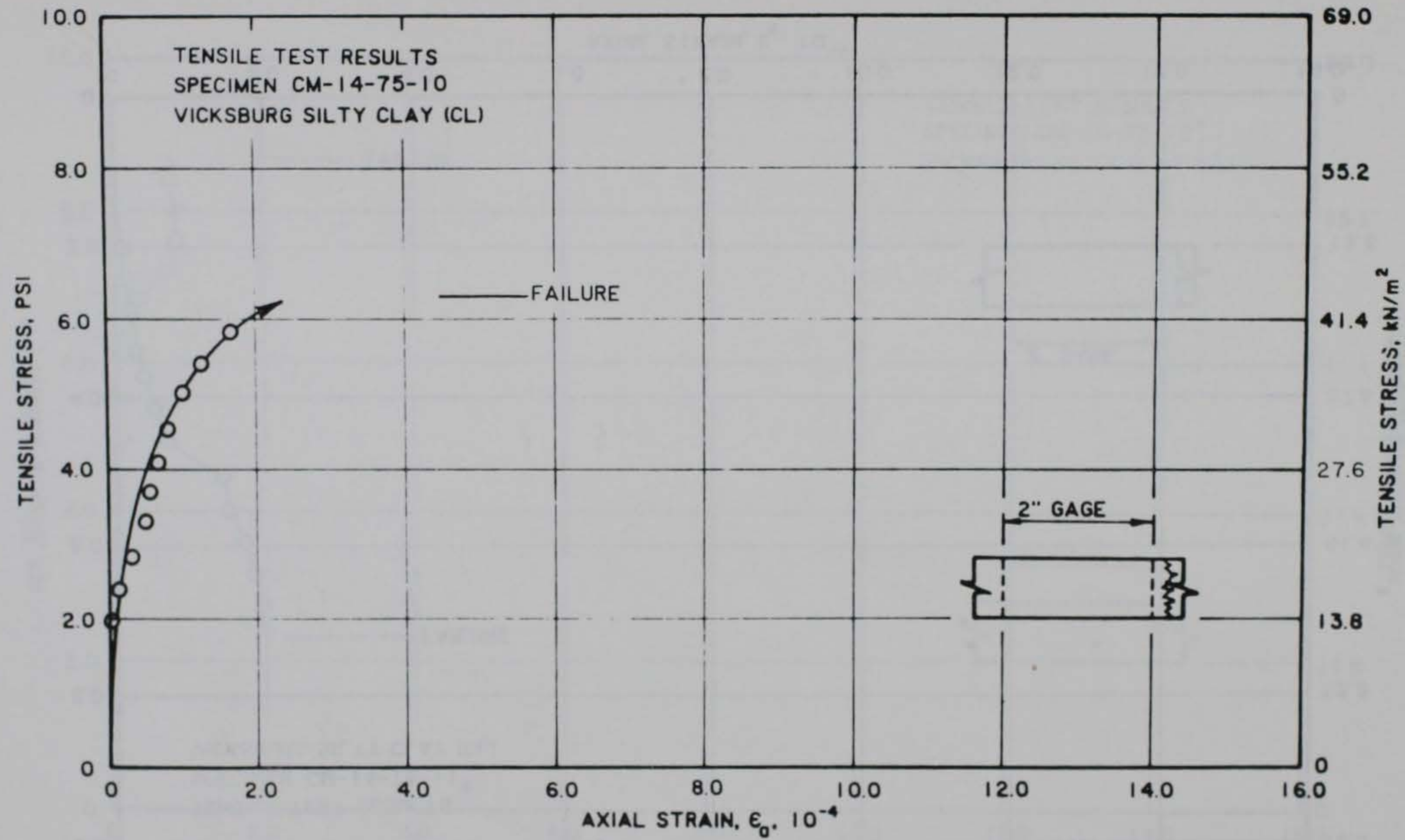


Figure B10. Stress-strain curve for tensile test CM-14-75-10

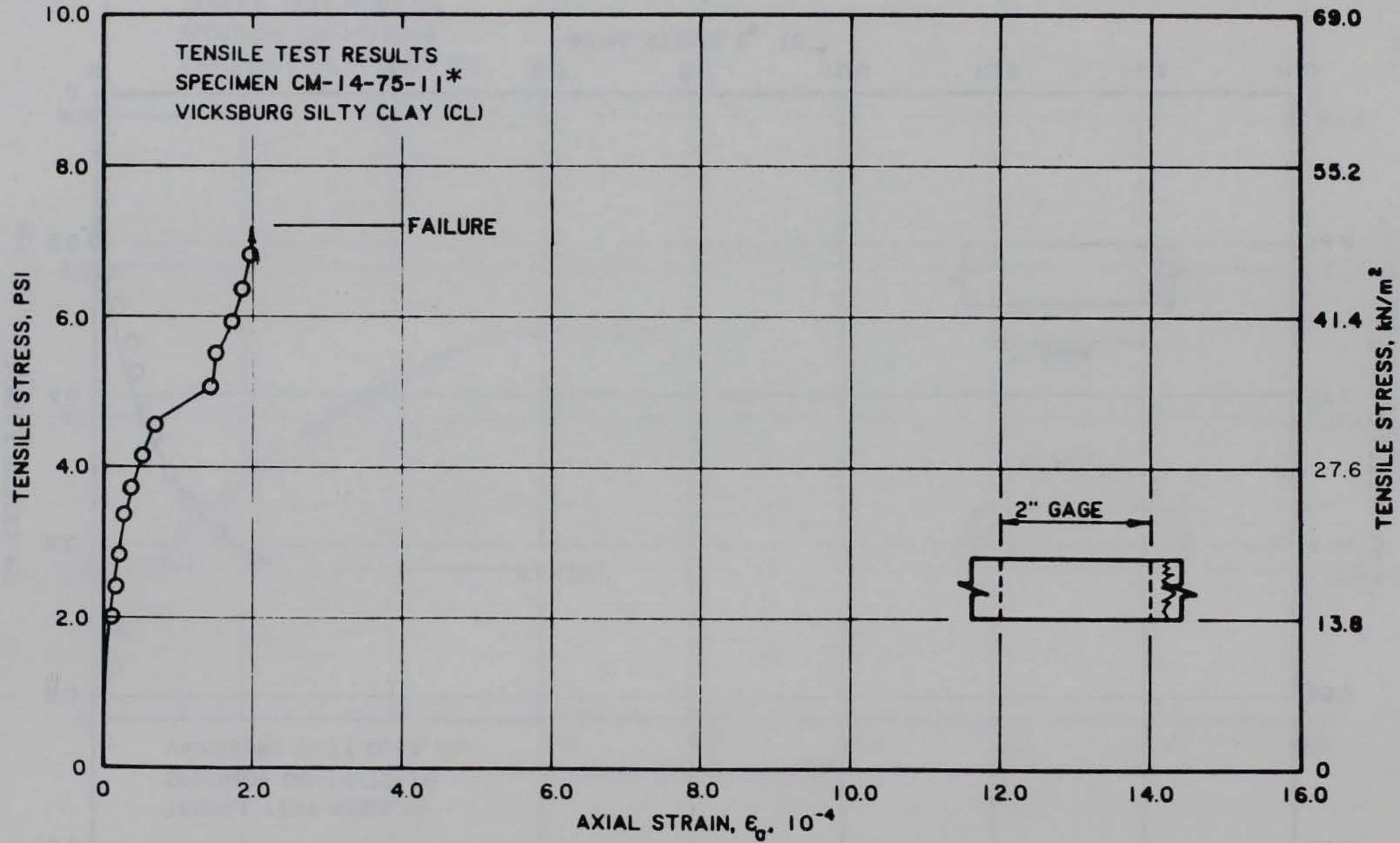


Figure B11. Stress-strain curve for tensile test CM-14-75-11*

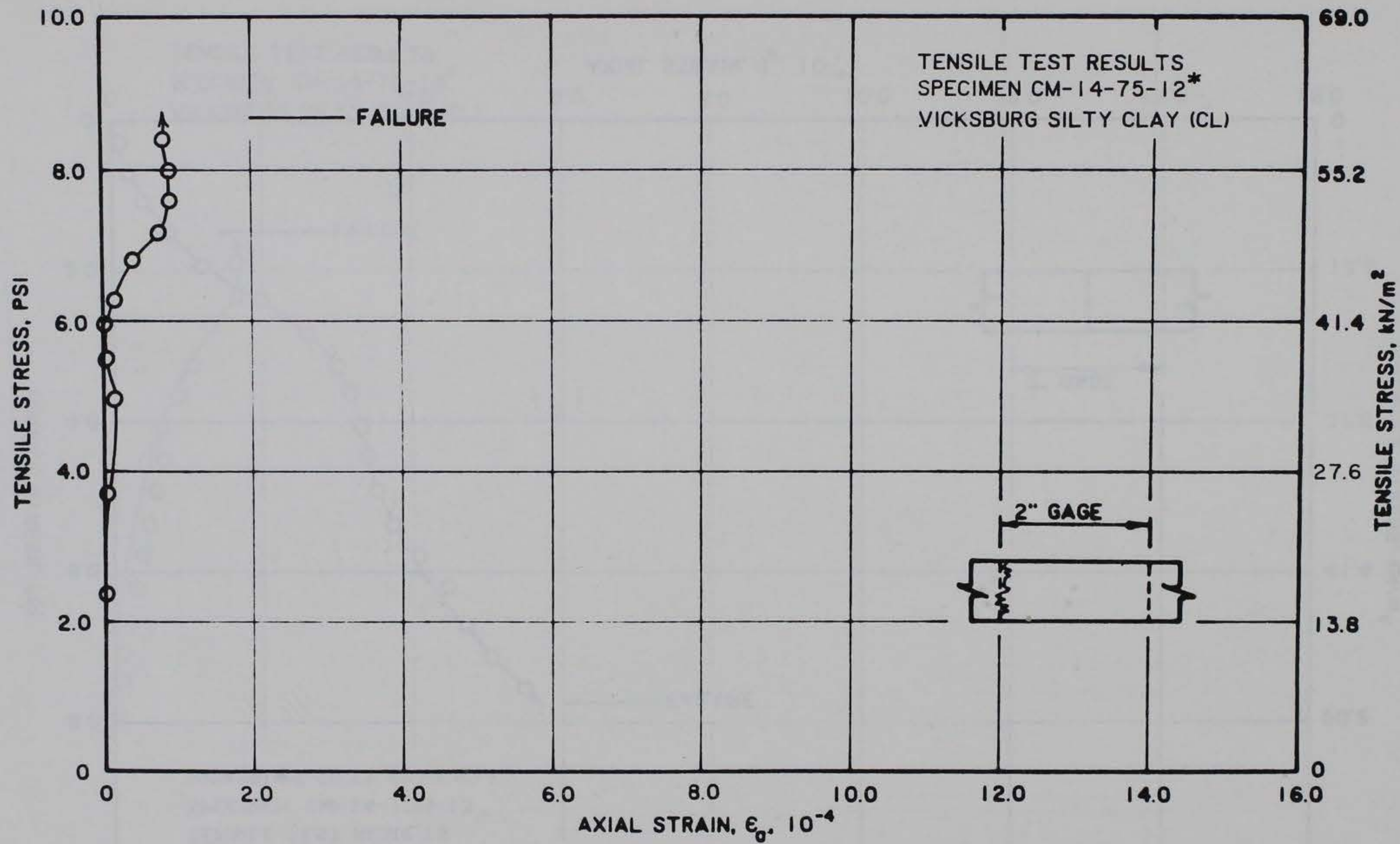


Figure B12. Stress-strain curve for tensile test CM-14-75-12*

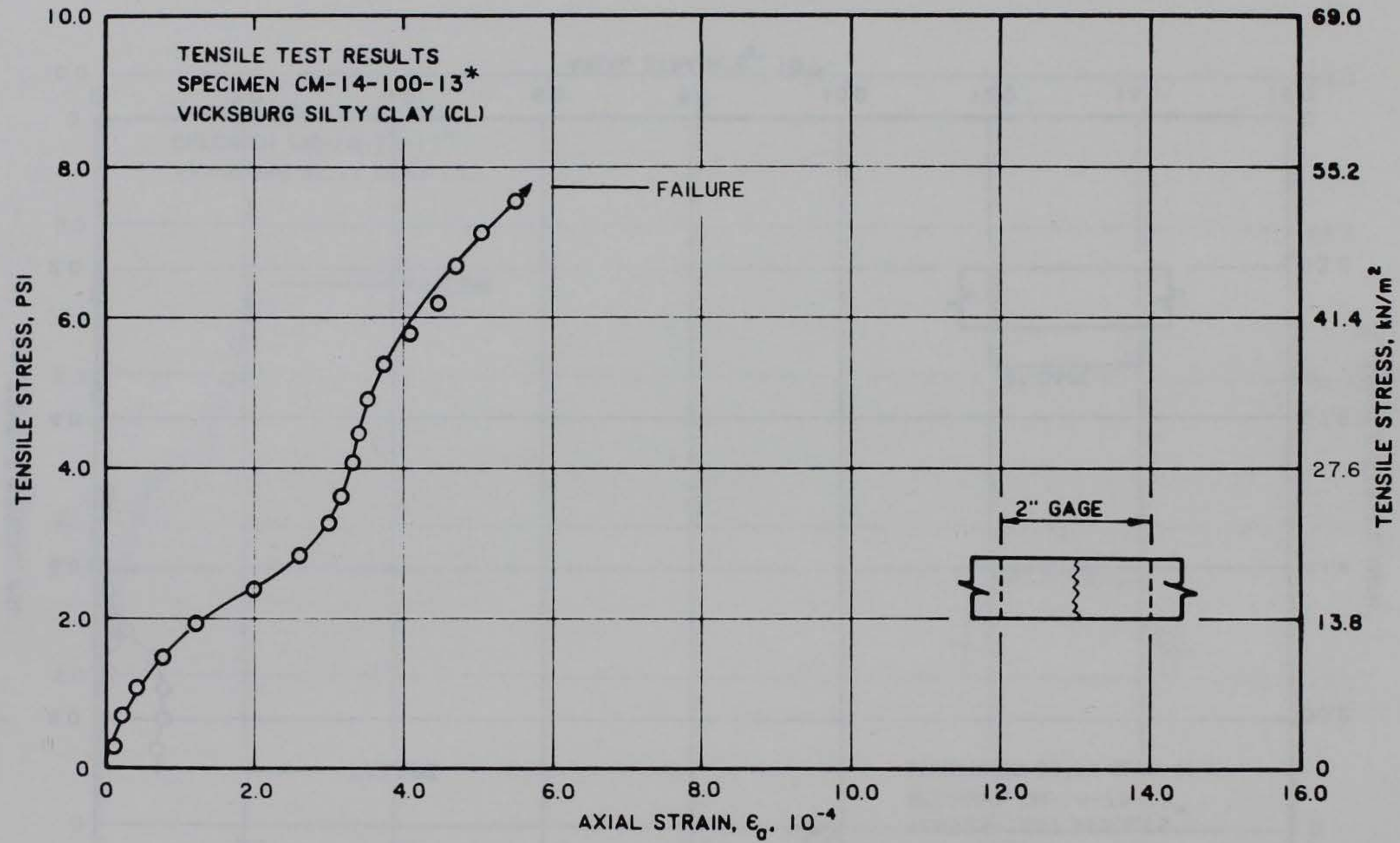


Figure B13. Stress-strain curve for tensile test CM-14-100-13*

B15

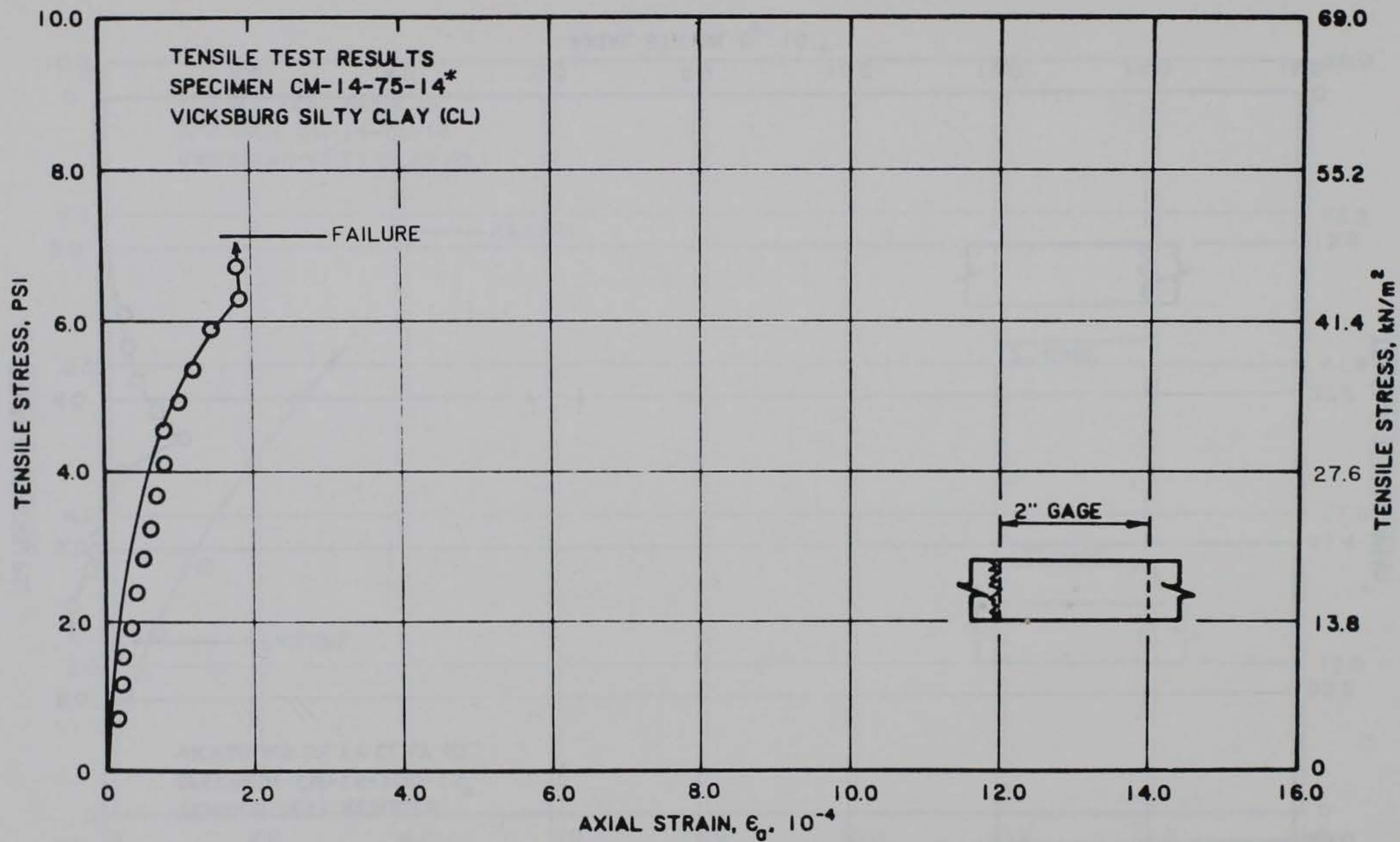


Figure B14. Stress-strain curve for tensile test CM-14-75-14

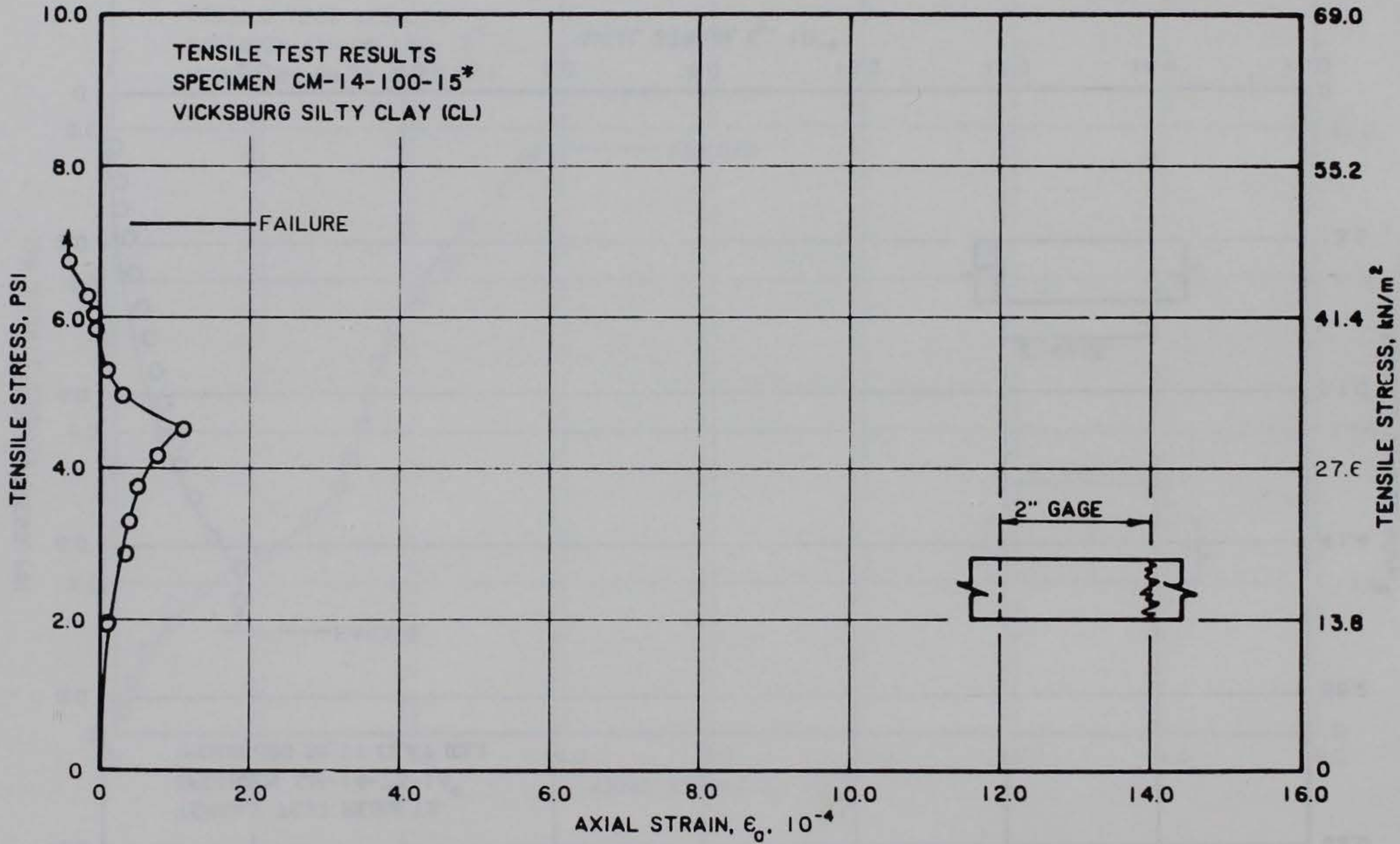


Figure B15. Stress-strain curve for tensile test CM-14-100-15*

B17

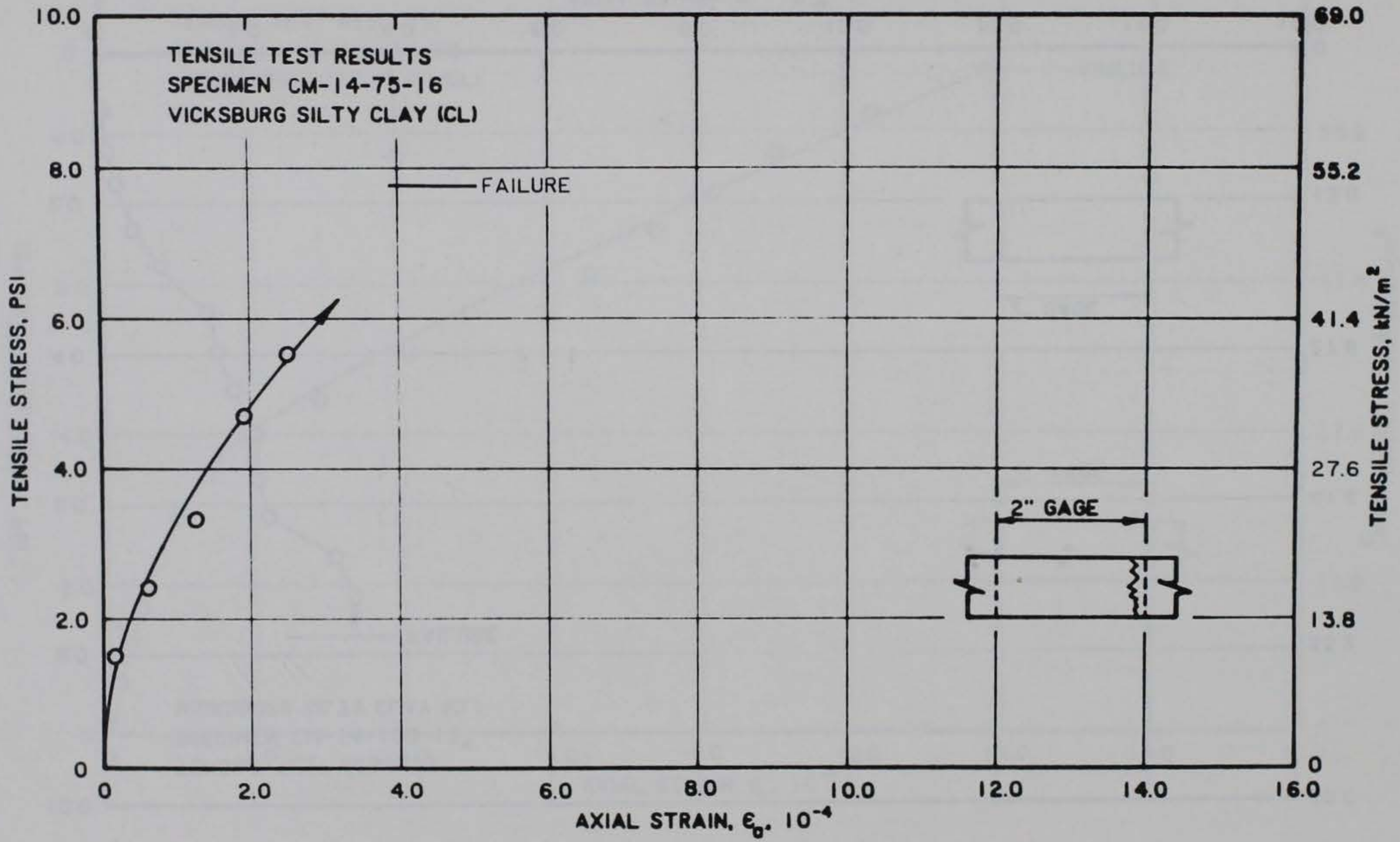


Figure B16. Stress-strain curve for tensile test CM-14-75-16

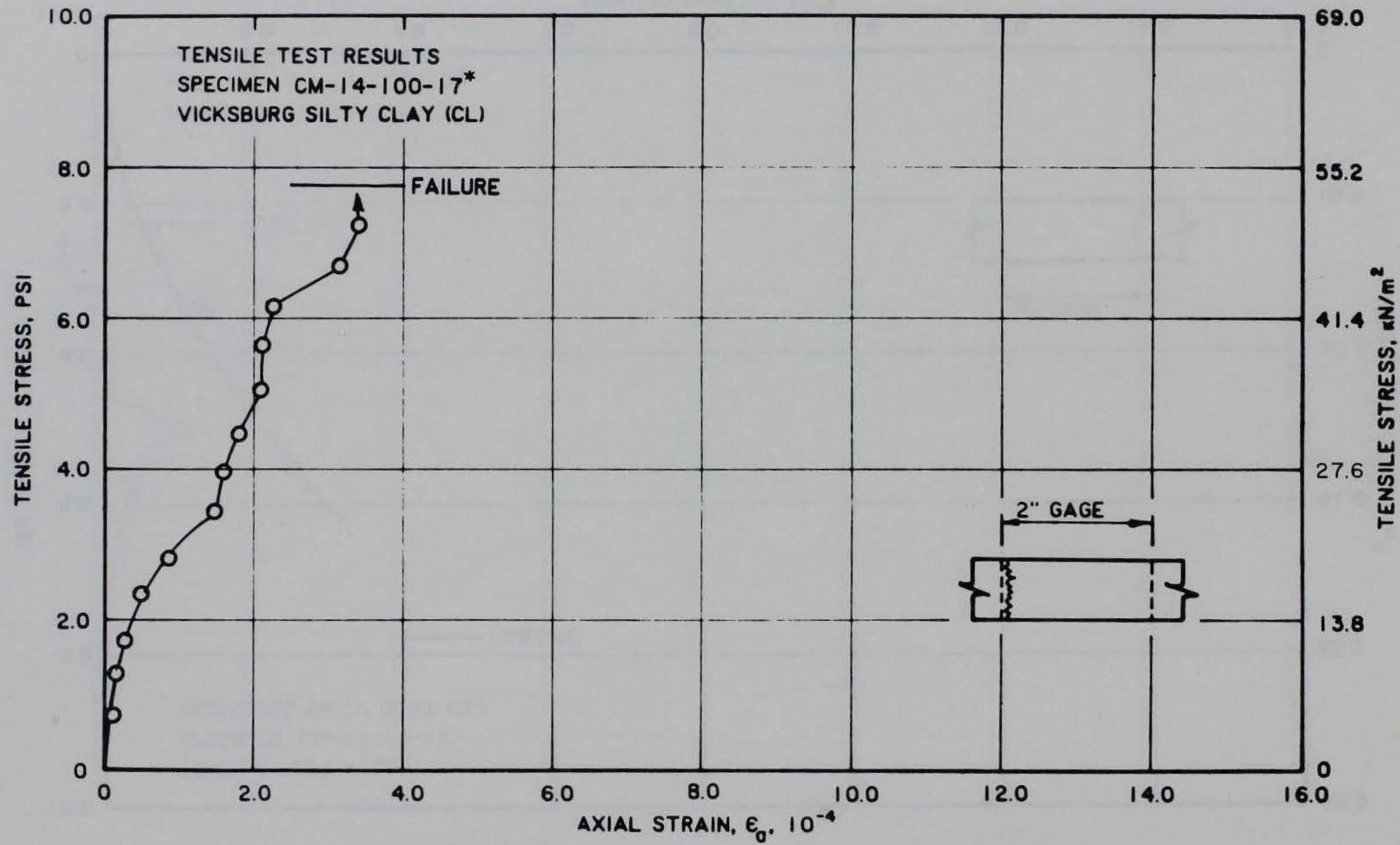


Figure B17. Stress-strain curve for tensile test CM-14-100-17*

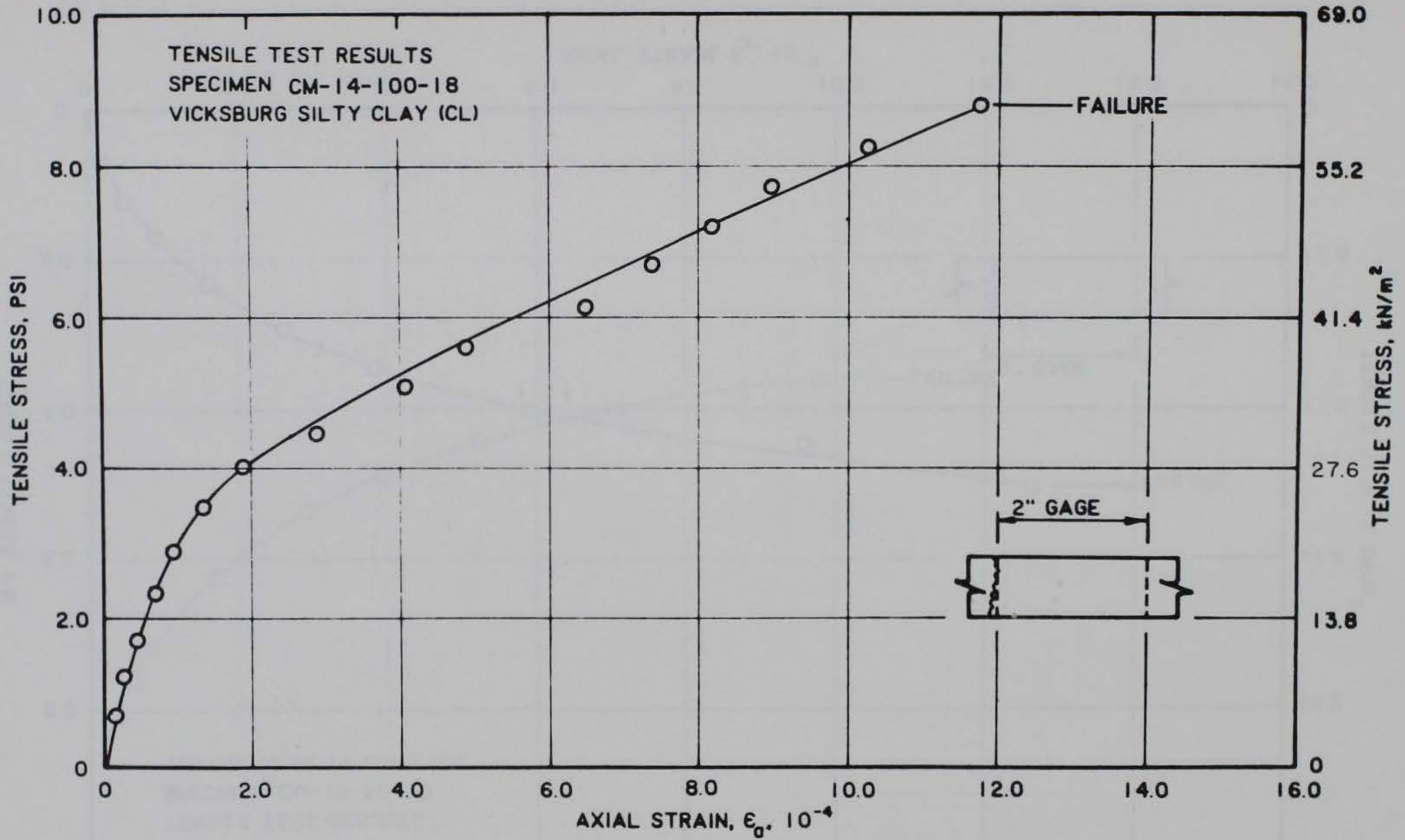


Figure B18. Stress-strain curve for tensile test CM-14-100-18

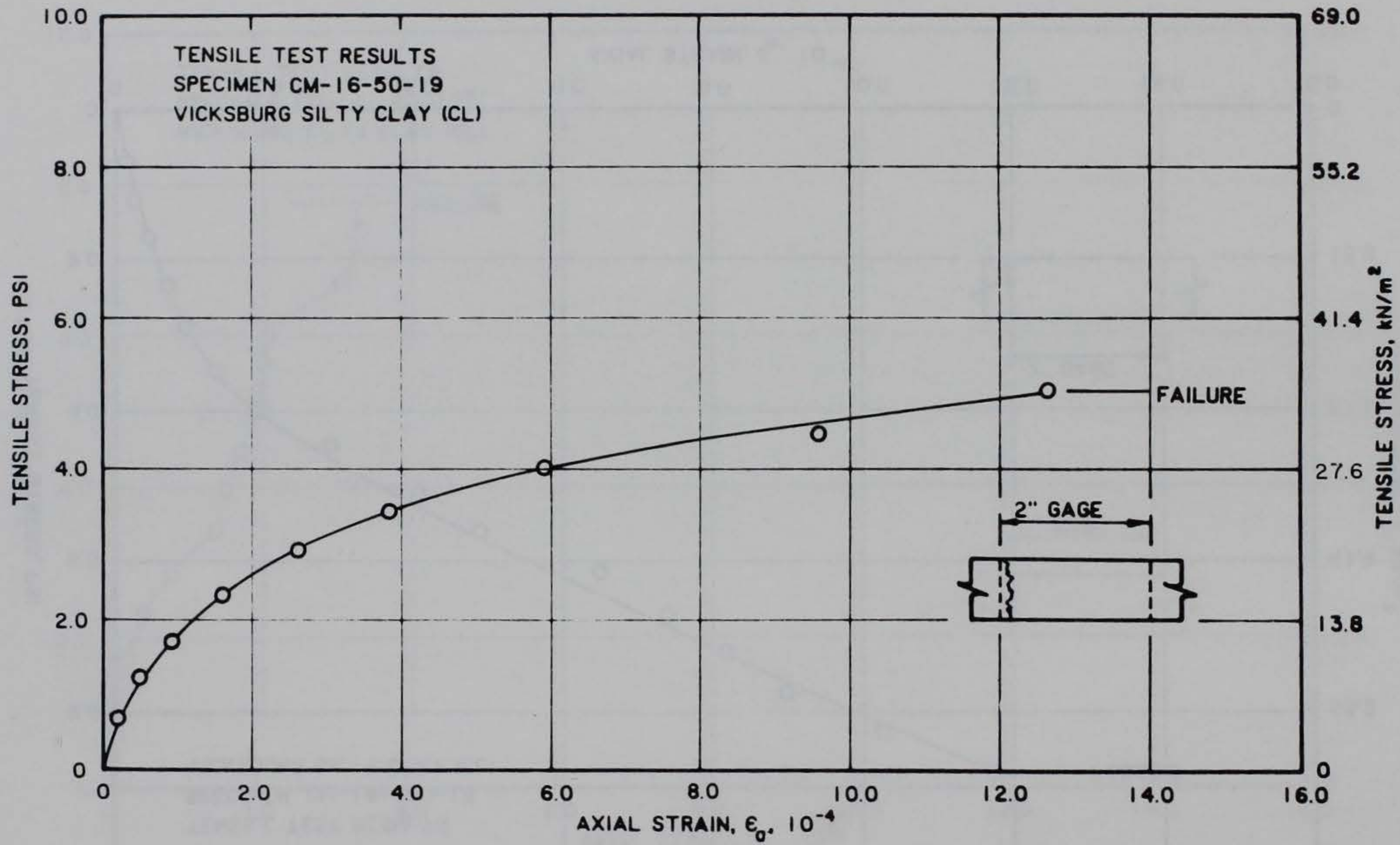


Figure B19. Stress-strain curve for tensile test CM-16-50-19

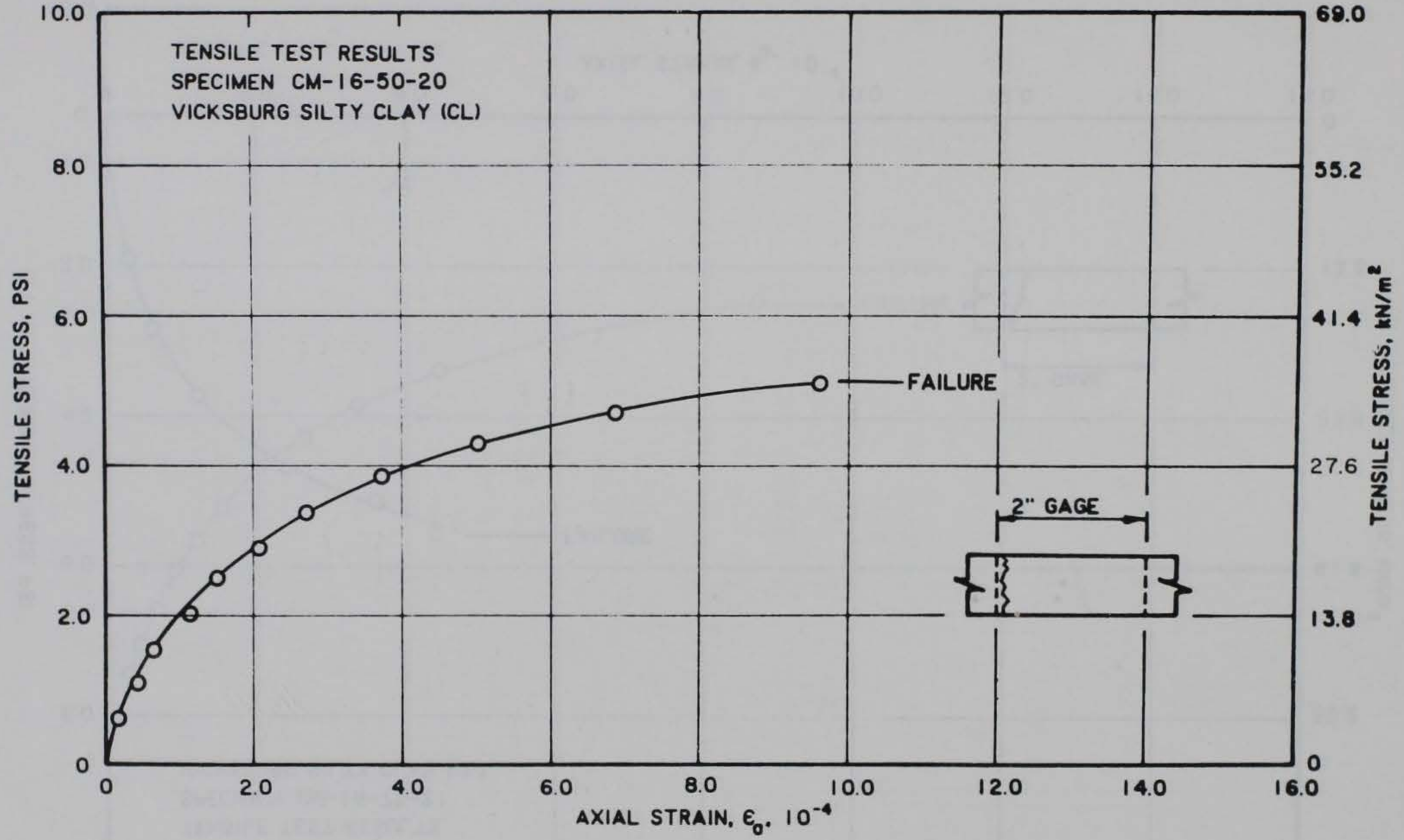


Figure B20. Stress-strain curve for tensile test CM-16-50-20

B22

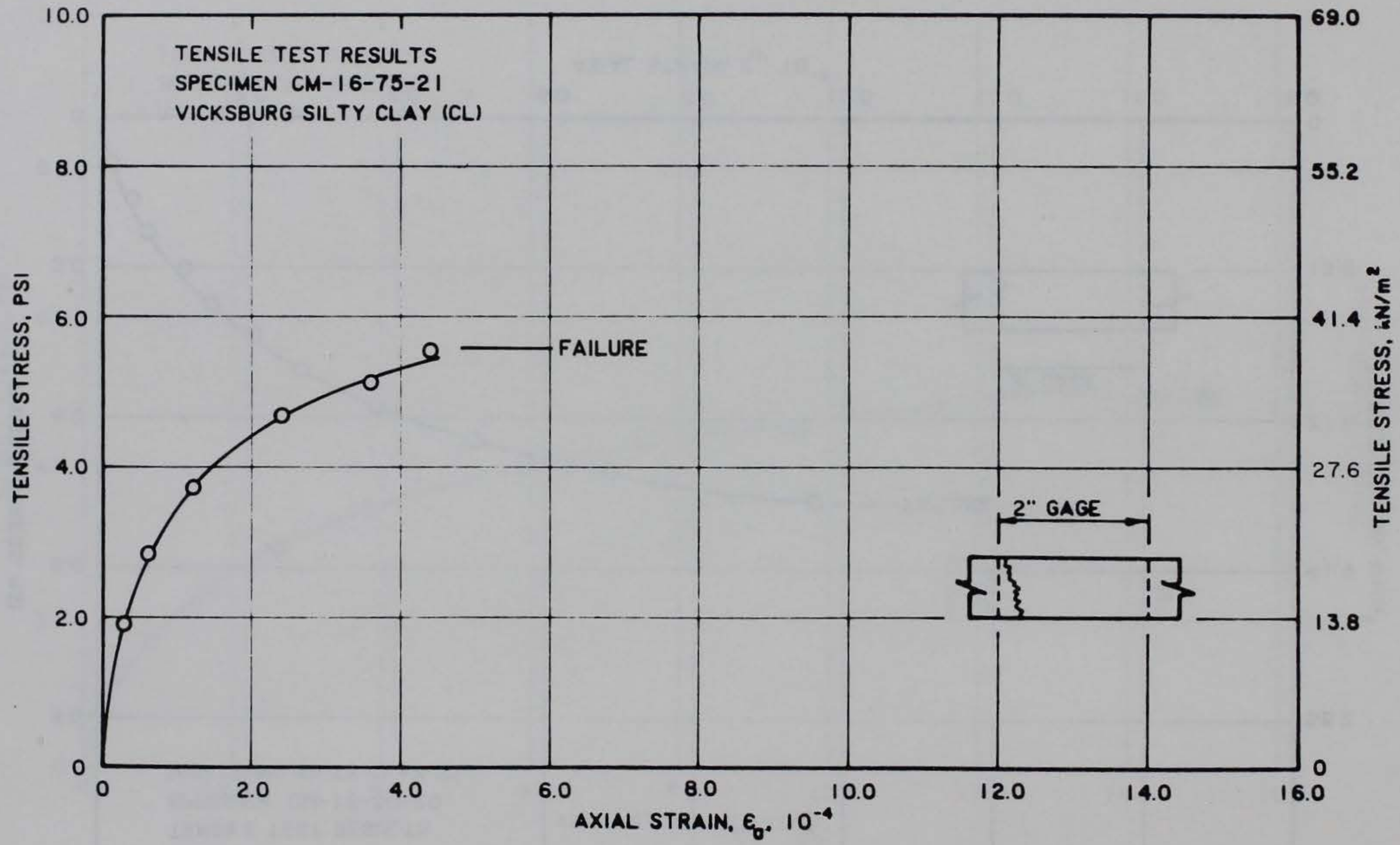


Figure B21. Stress-strain curve for tensile test CM-16-75-21

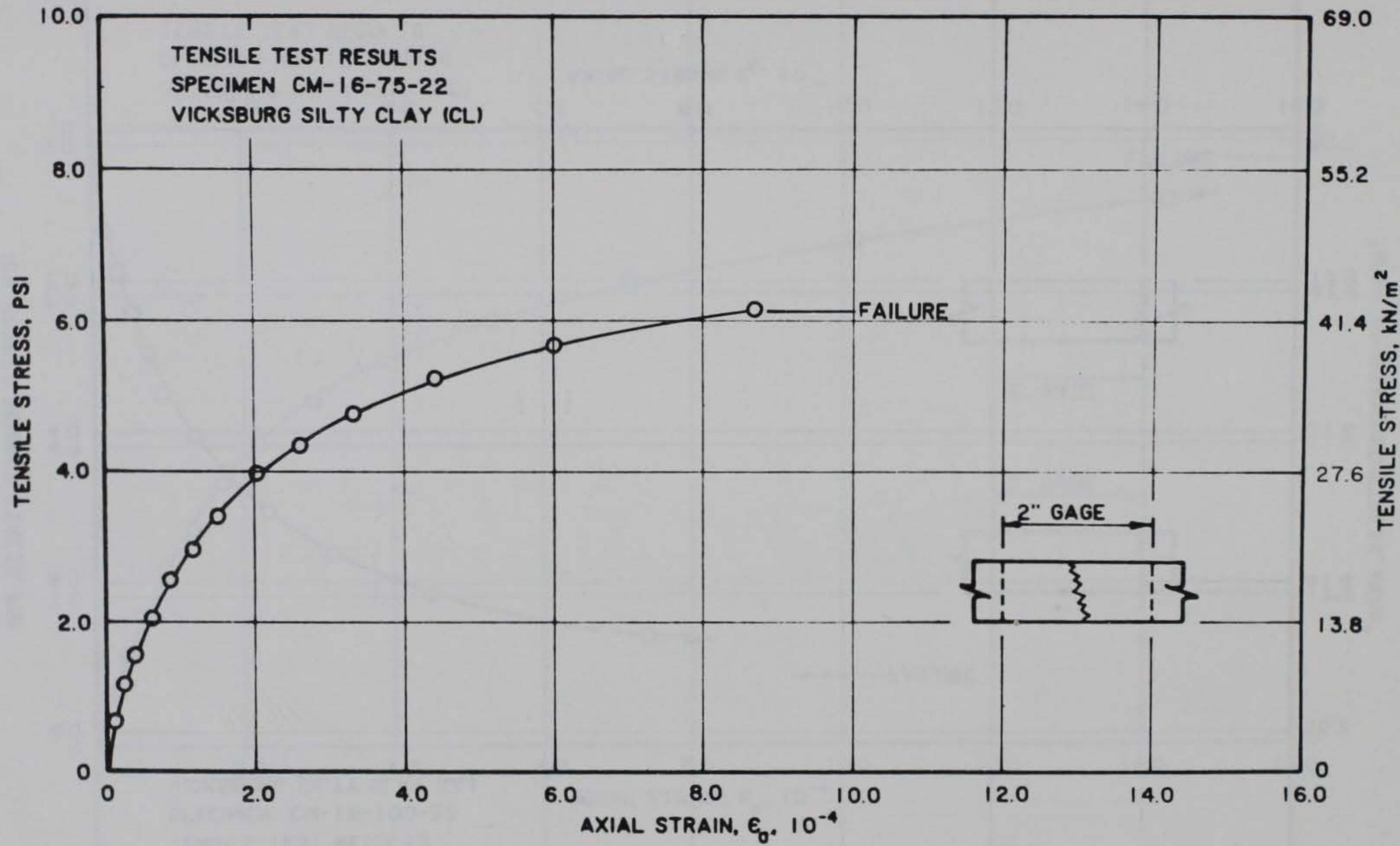


Figure B22. Stress-strain curve for tensile test CM-16-75-22

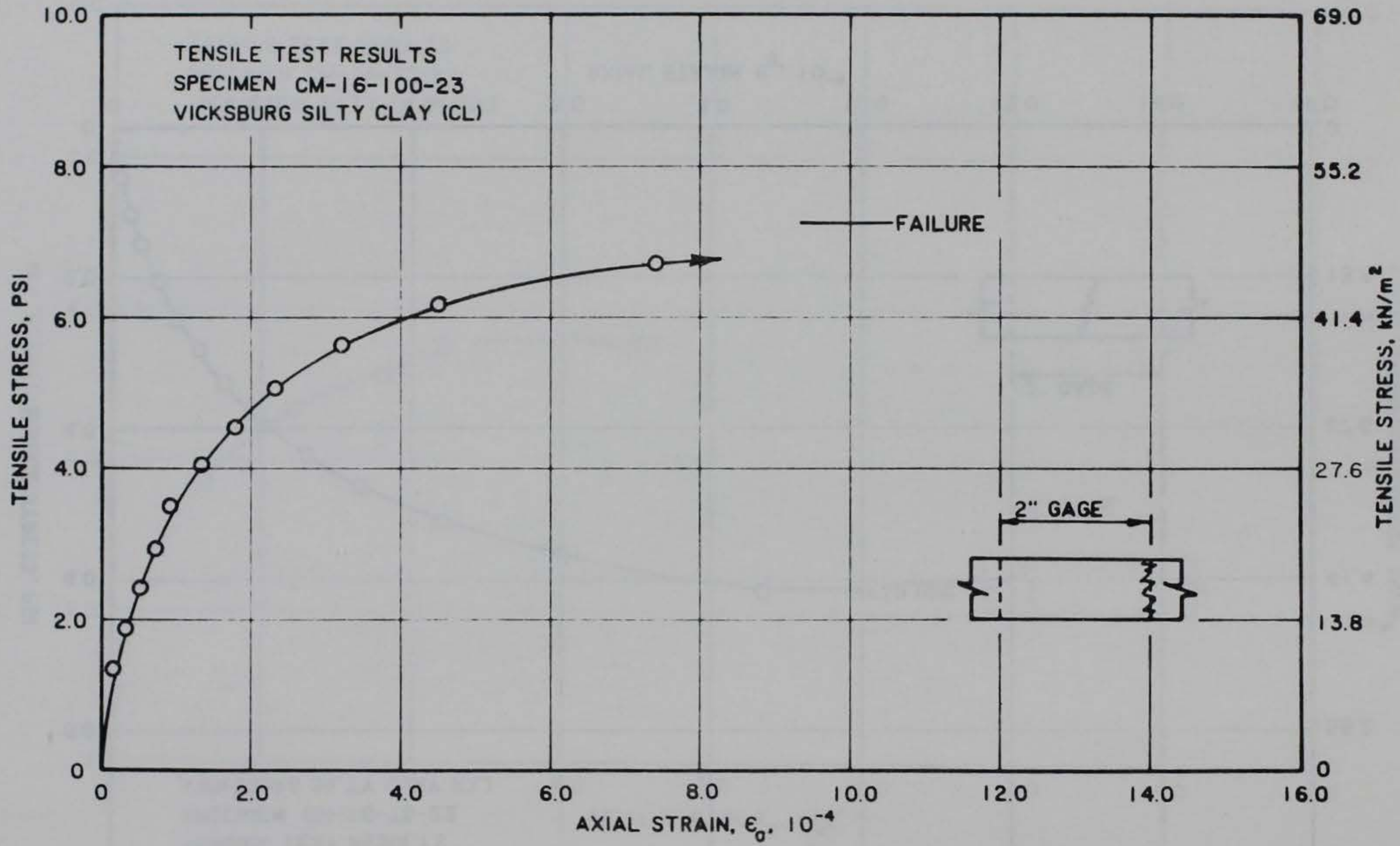


Figure B23. Stress-strain curve for tensile test CM-16-100-23

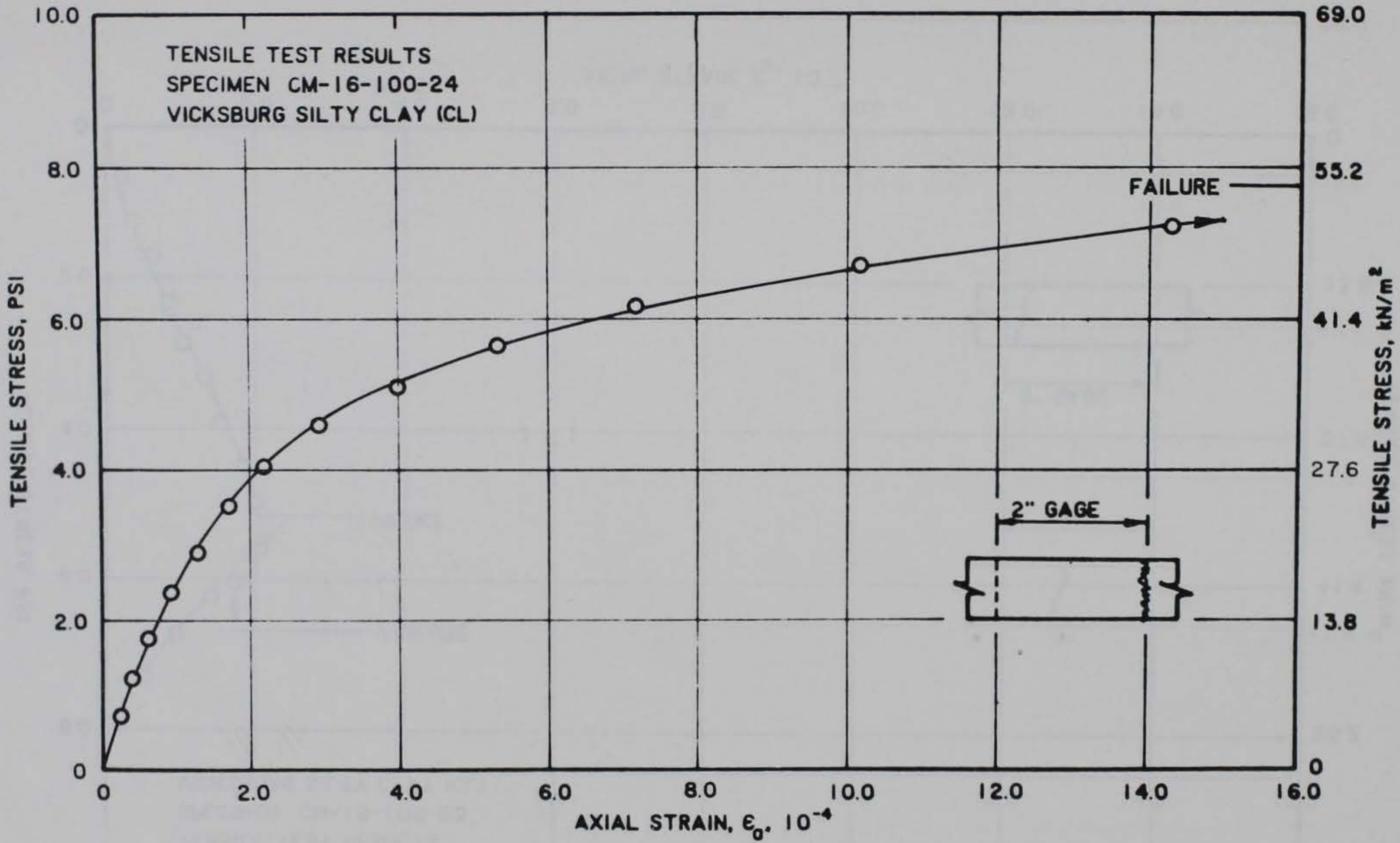


Figure B24. Stress-strain curve for tensile test CM-16-100-24

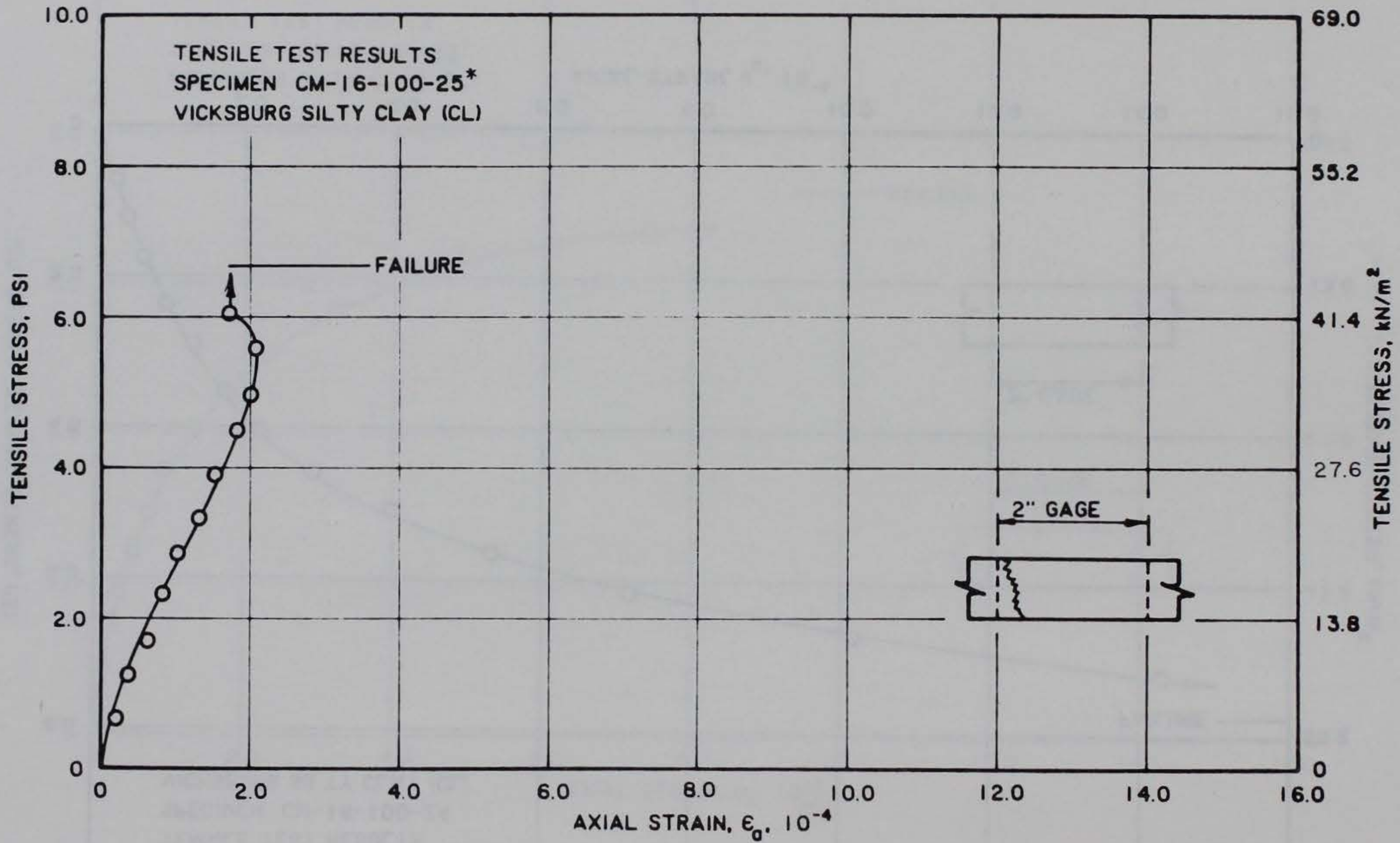


Figure B25. Stress-strain curve for tensile test CM-16-100-25*

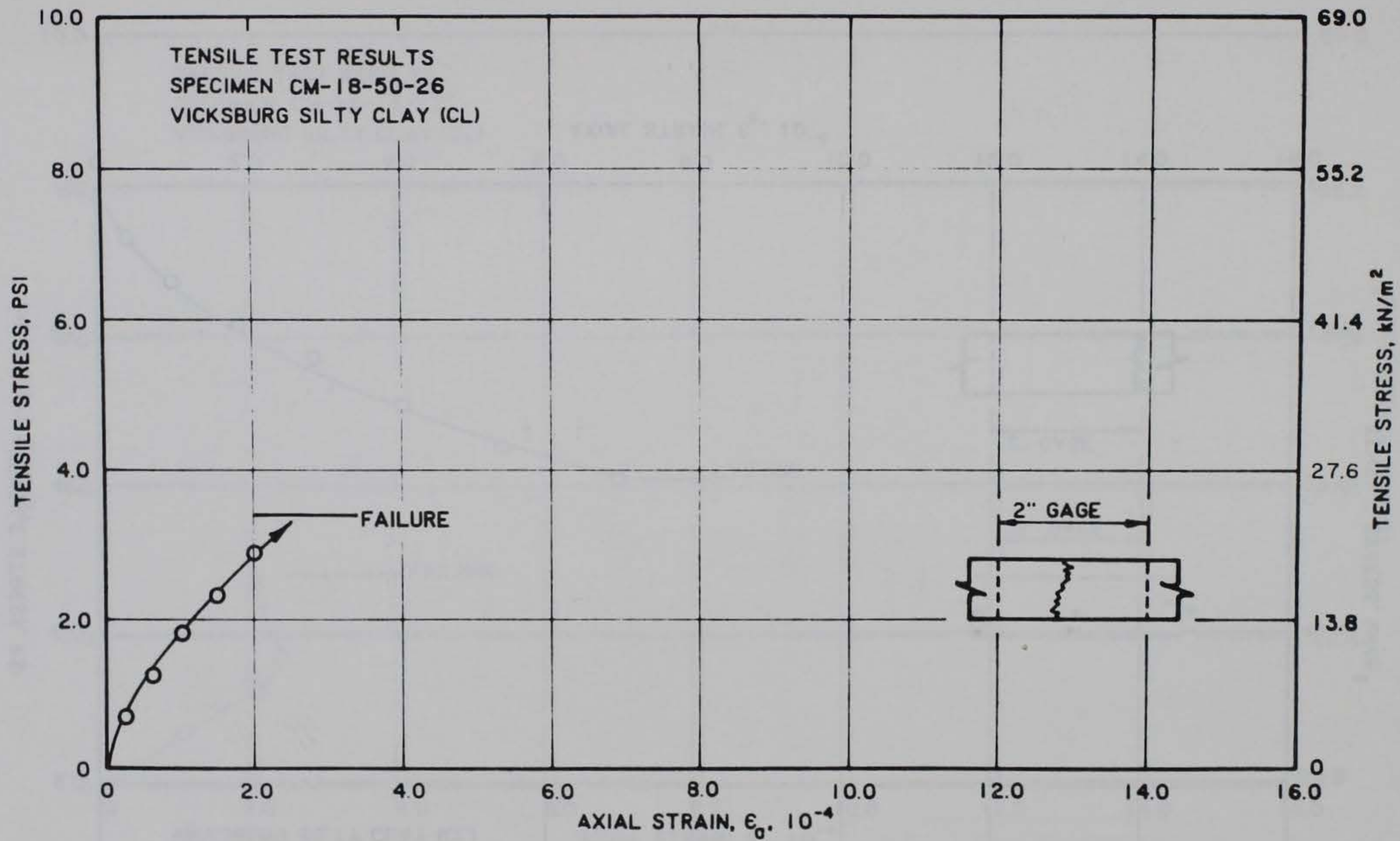


Figure B26. Stress-strain curve for tensile test CM-18-50-26

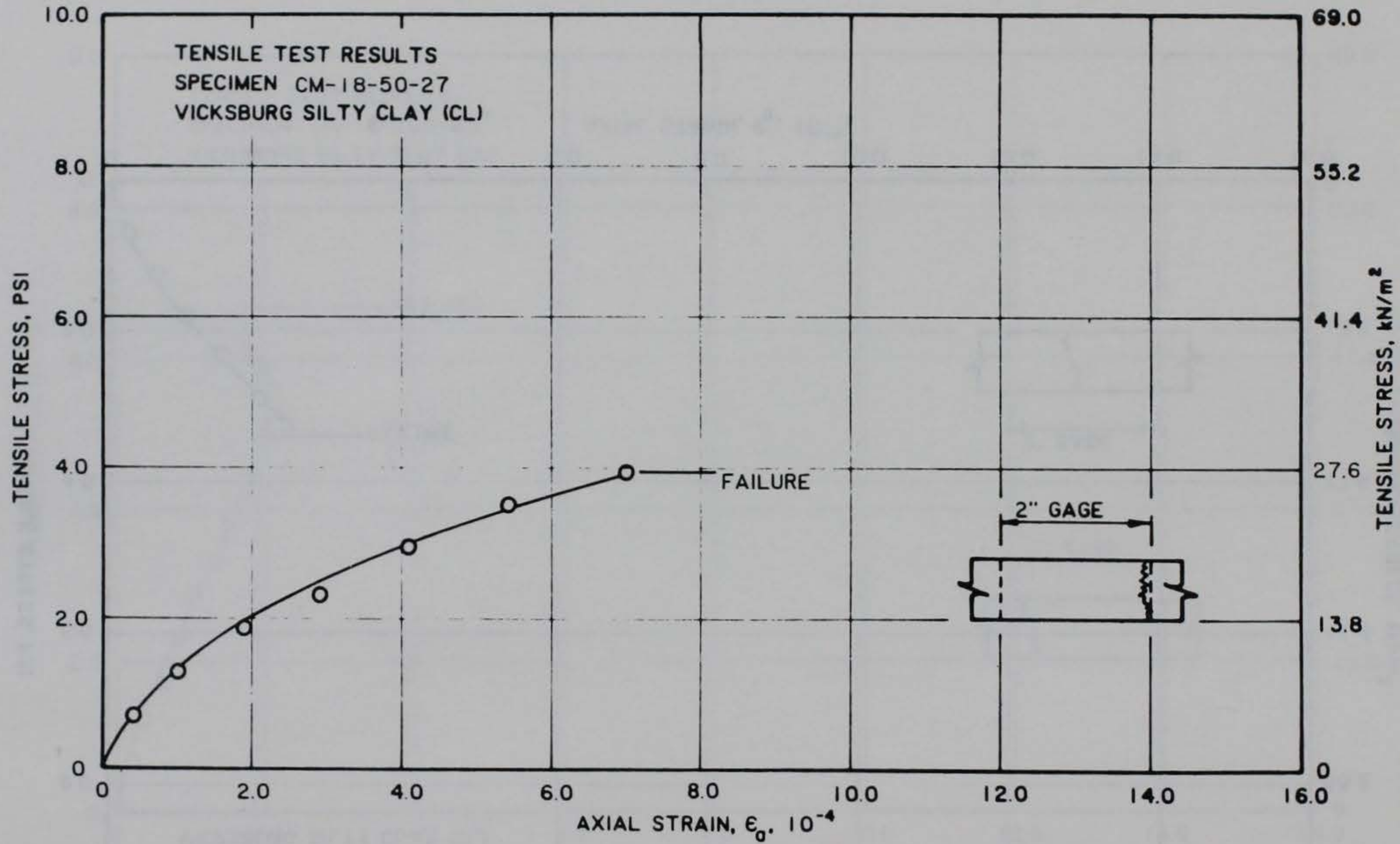


Figure B27. Stress-strain curve for tensile test CM-18-50-27

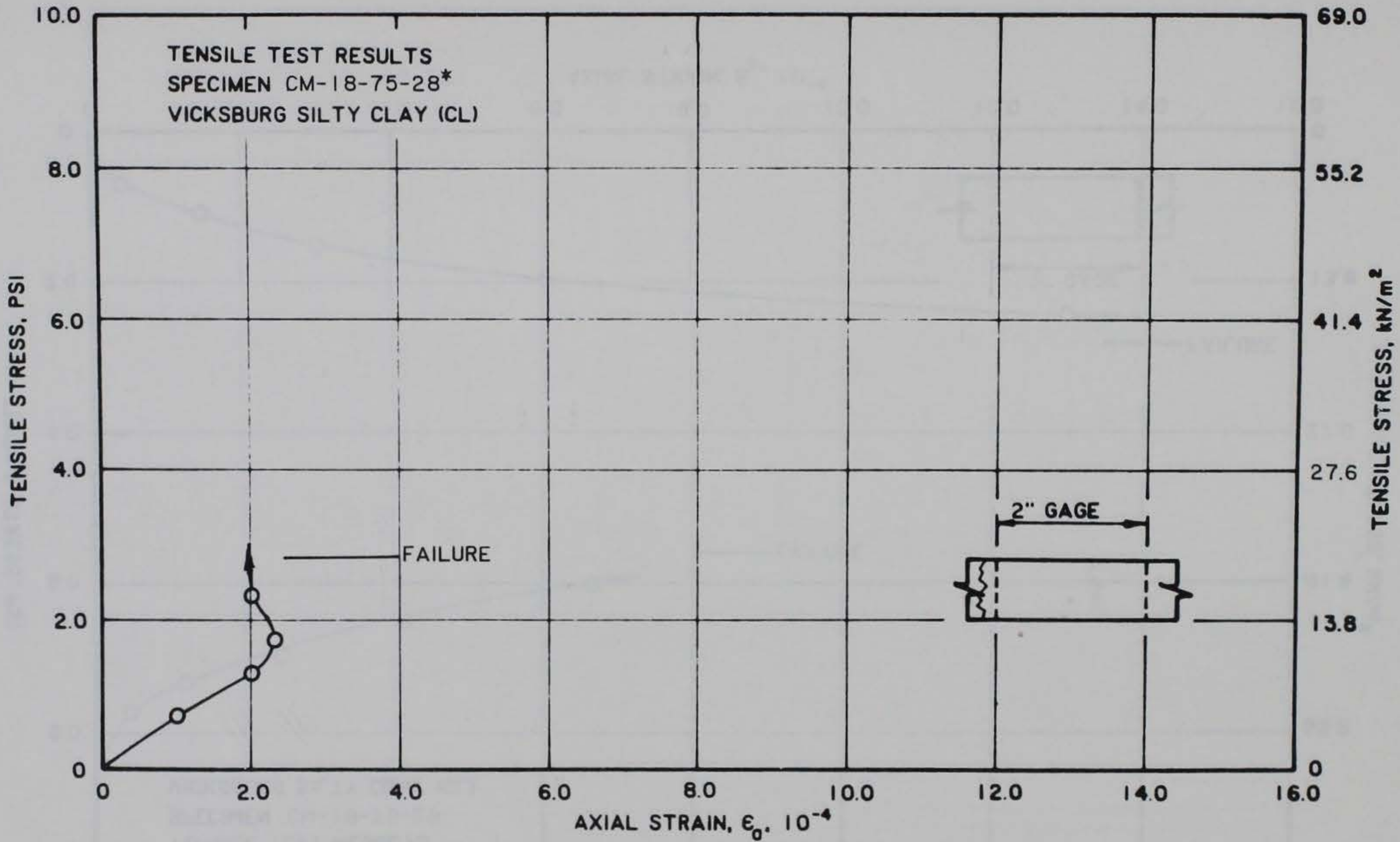


Figure B28. Stress-strain curve for tensile test CM-18-75-28*

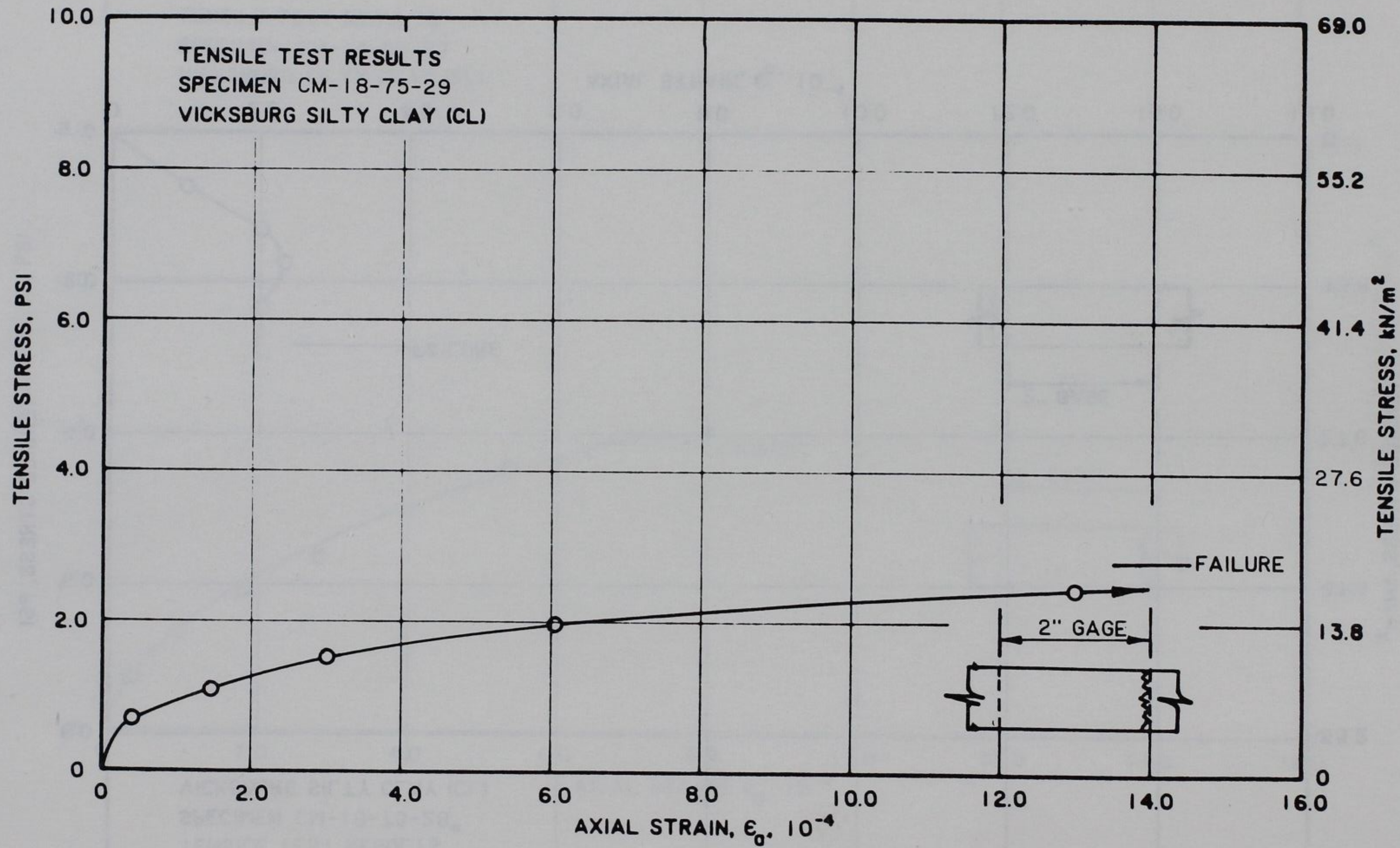


Figure B29. Stress-strain curve for tensile test CM-18-75-29

B31

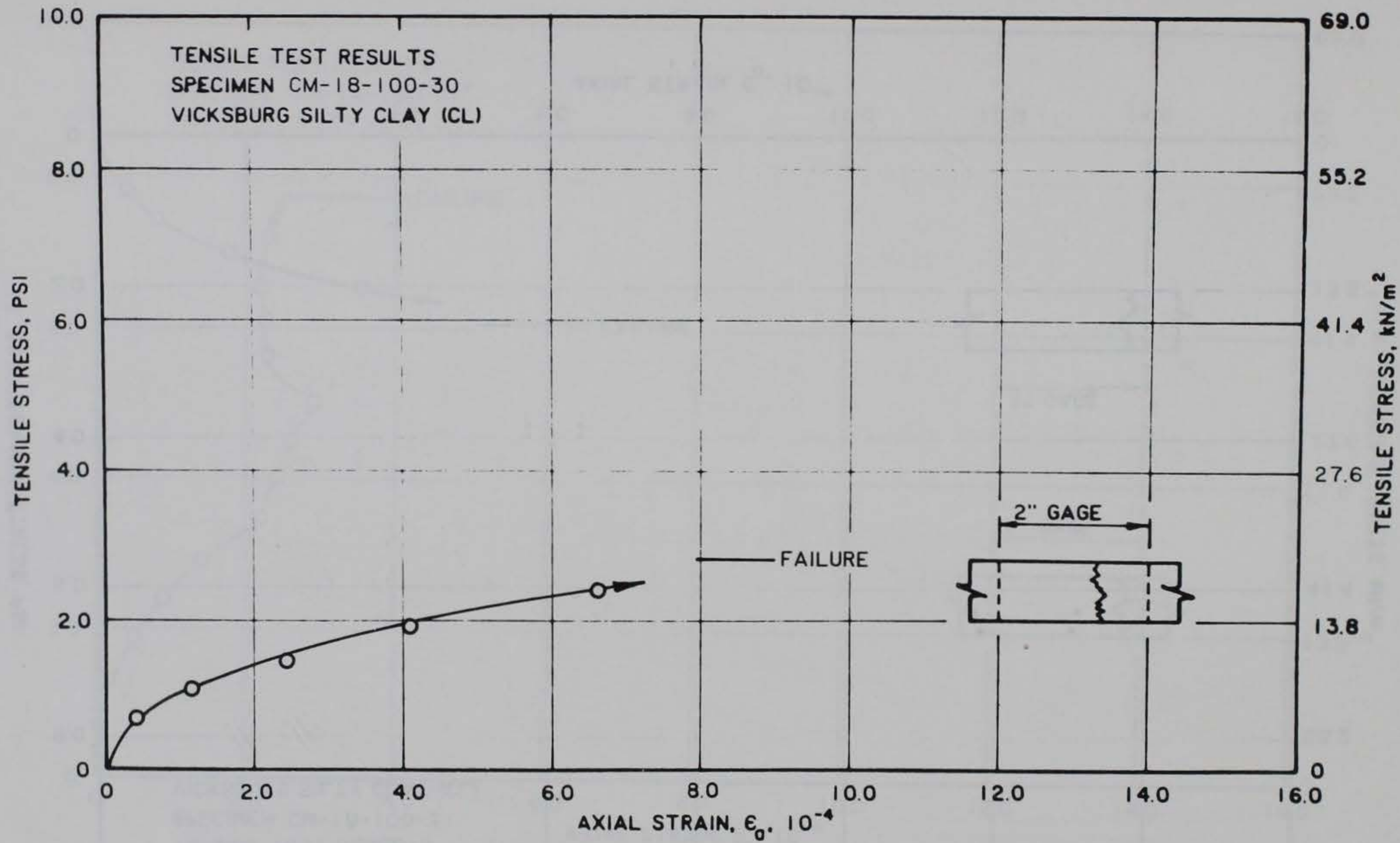


Figure B30. Stress-strain curve for tensile test CM-18-100-30

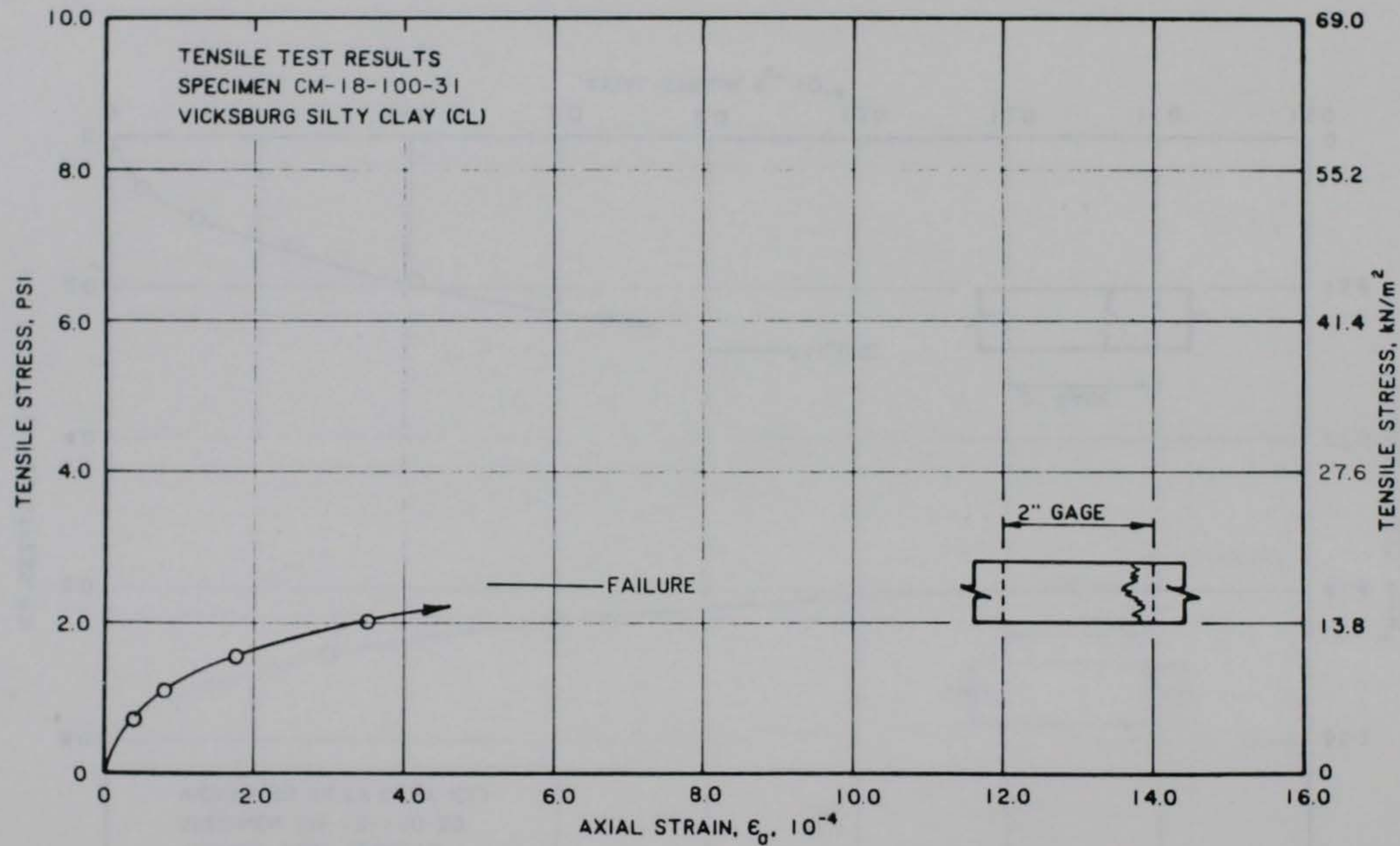


Figure B31. Stress-strain curve for tensile test CM-18-100-31

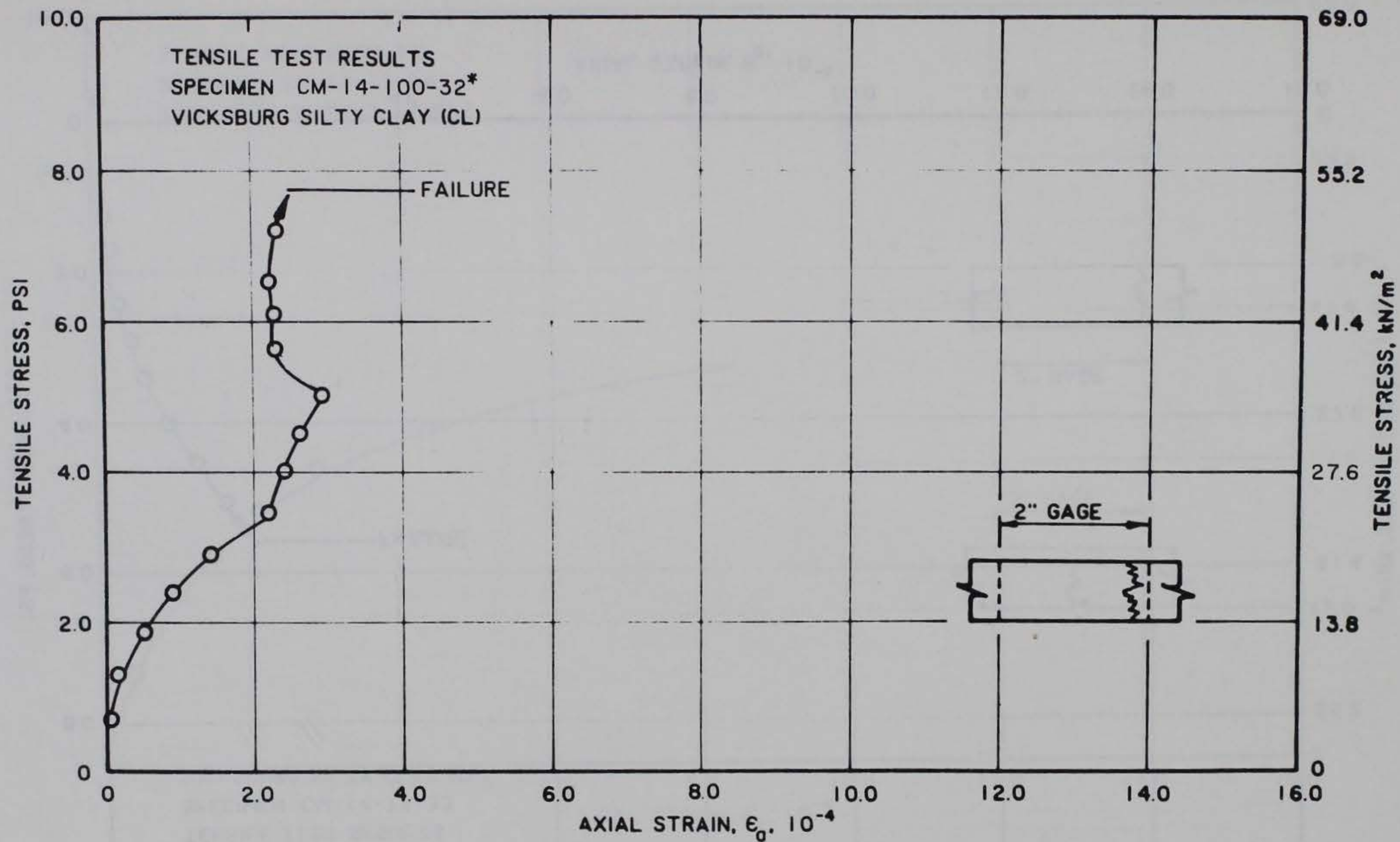


Figure B32. Stress-strain curve for tensile test CM-14-100-32*

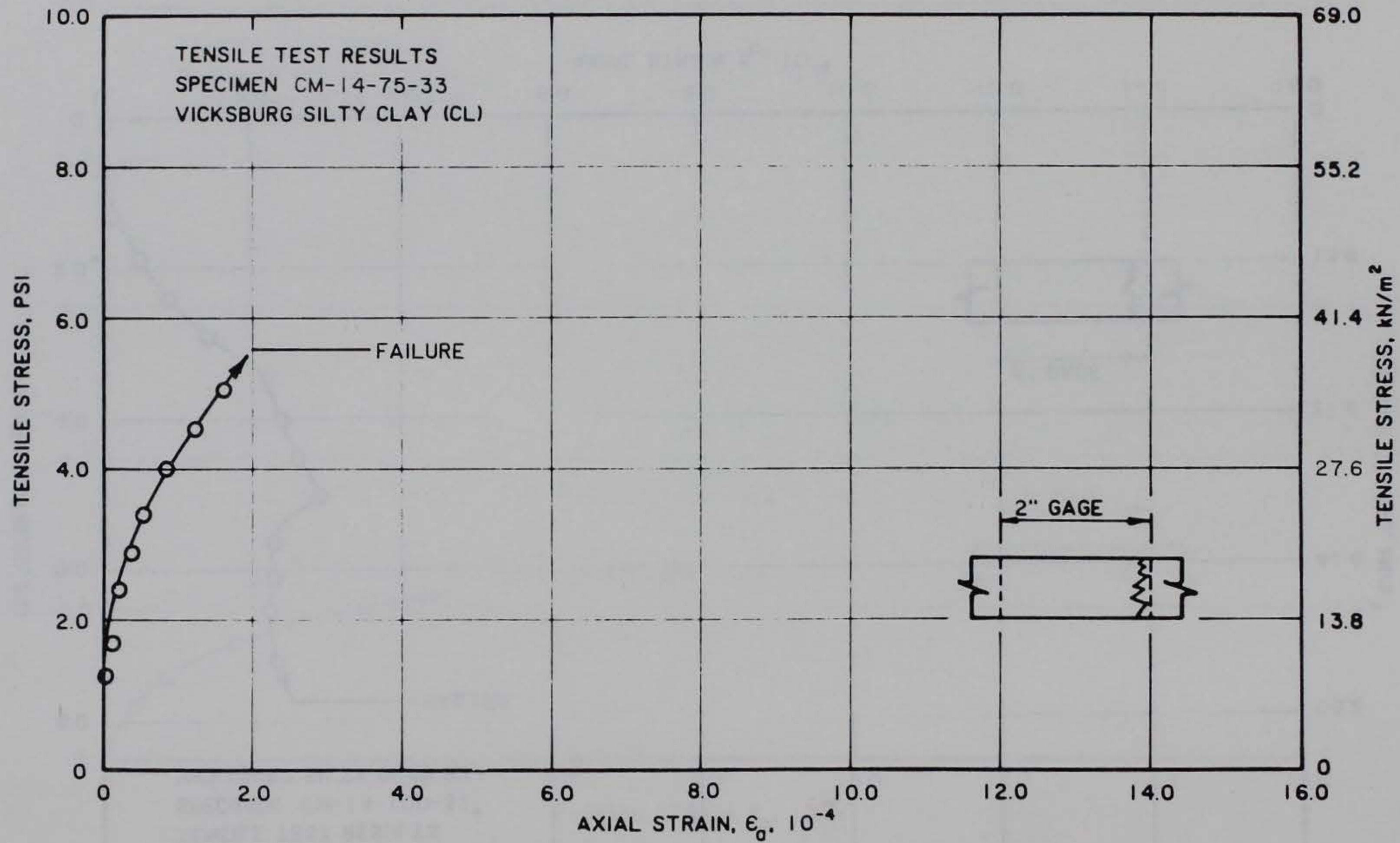


Figure B33. Stress-strain curve for tensile test CM-14-75-33

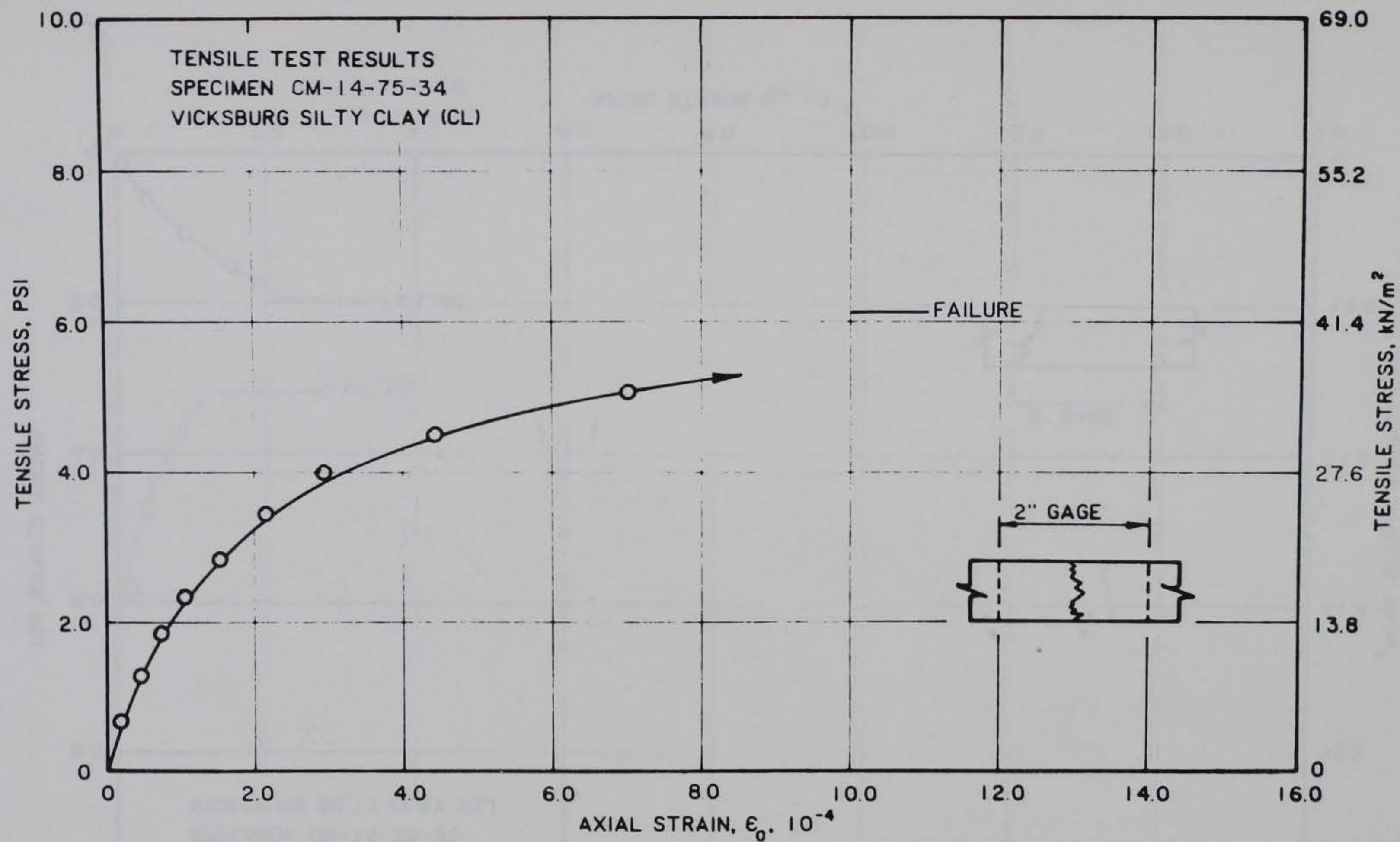


Figure B34. Stress-strain curve for tensile test CM-14-75-34

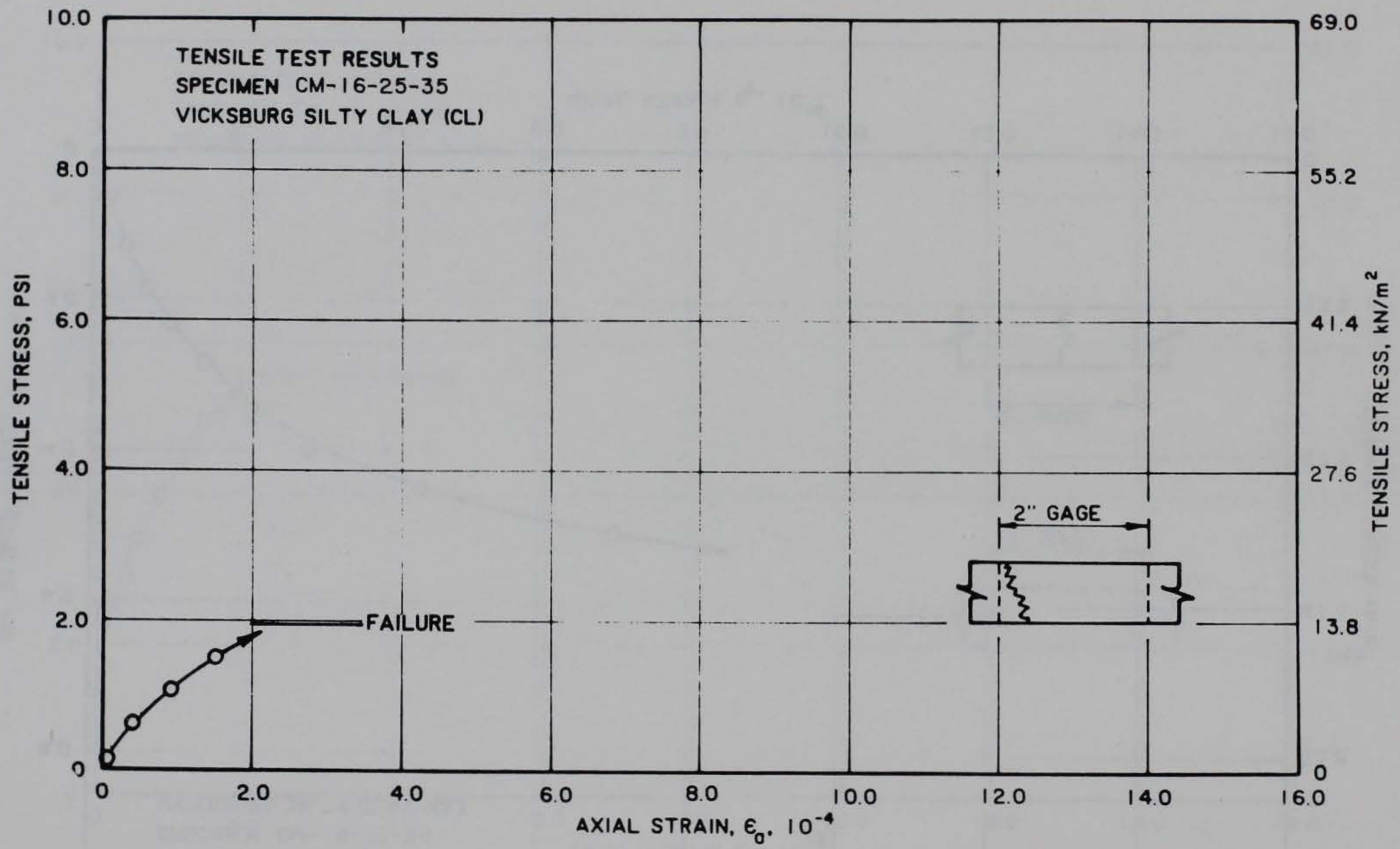


Figure B35. Stress-strain curve for tensile test CM-16-25-35

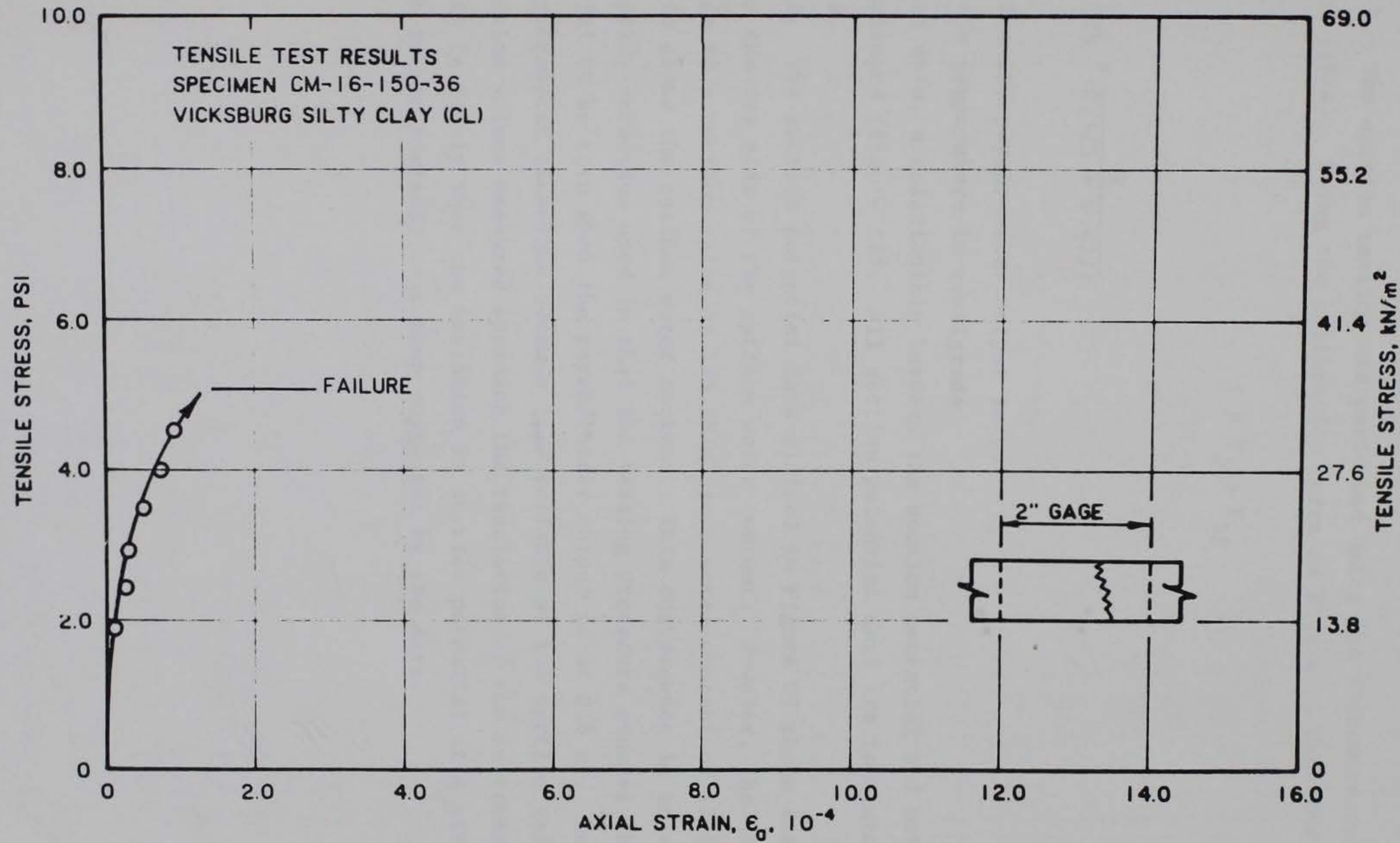


Figure B36. Stress-strain curve for tensile test CM-16-150-36

APPENDIX C: SUCTION DATA

1. The suction testing was performed using the procedure outlined by Johnson (1974). Using the calibration curve in Figure C1 with the equation

$$\tau = 2.55 E_{25} \quad (C1)$$

where

$$E_{25} = \frac{E}{0.325 + 0.027t}$$

and

E = the psychrometer output in μv

t = temperature in centigrade

and test data, a relationship between the suction potential and water content was developed (Figure C2). All suction potential data are tabulated in Table 3.

2. The suction potential data plotted in Figure C2 shows scatter in the data on the dry side of the optimum water content. However, the data tend to converge to a suction value of 175 kN/m^2 at a water content of 17.6 percent, which is above the optimum water content. This convergence is an artifact of the testing technique used in that the testing procedure assumes the suction potential to be zero when the psychrometer output is at $0.6 \mu\text{v}$. In general, the psychrometer technique becomes less reliable at low suction values, and the suction values measured approach the resolution of the instrument. Therefore, it is likely that the variation in suction potential at a given water content is considerably less than suggested by the data.

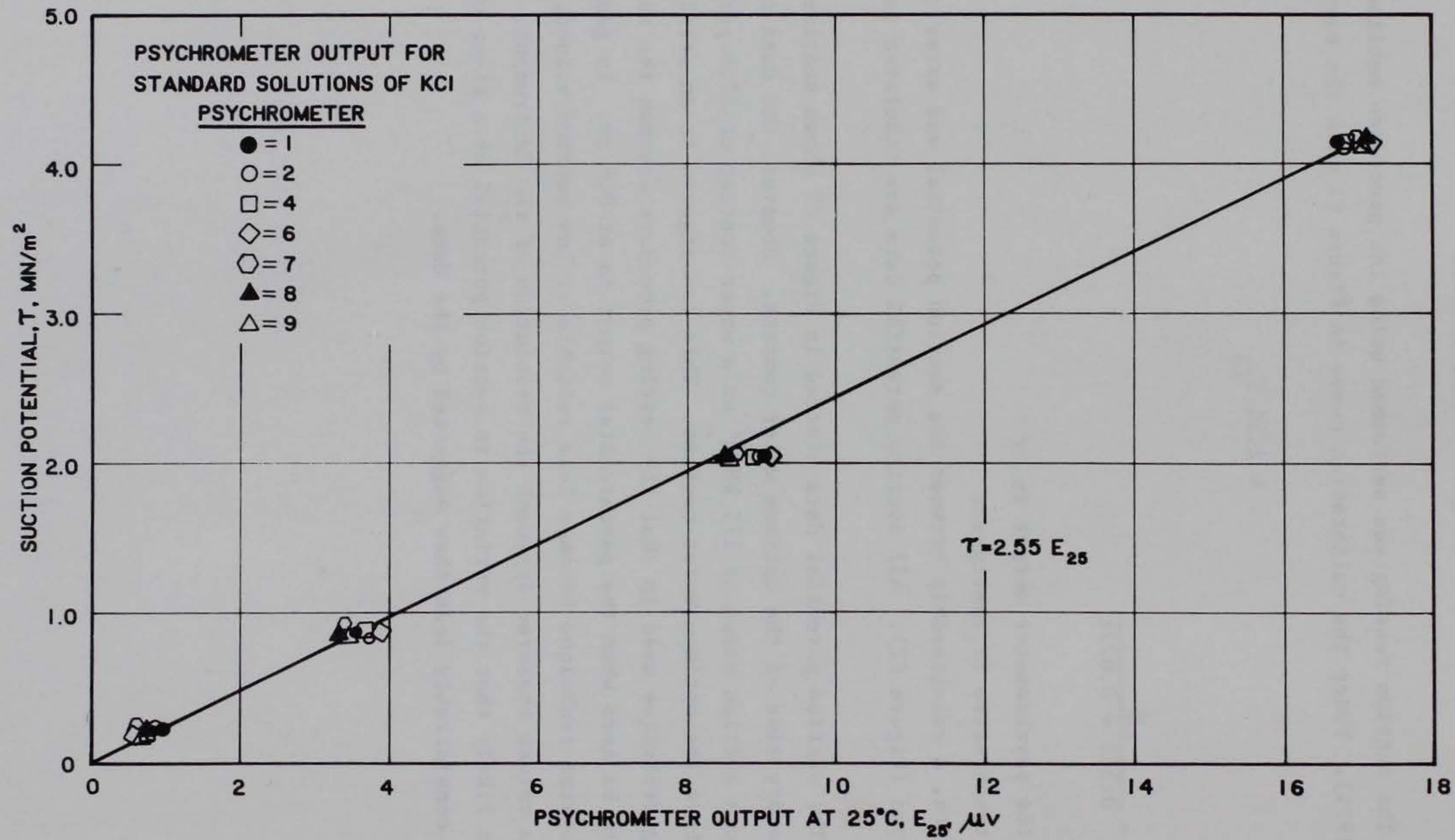


Figure C1. Calibration curve for psychrometers

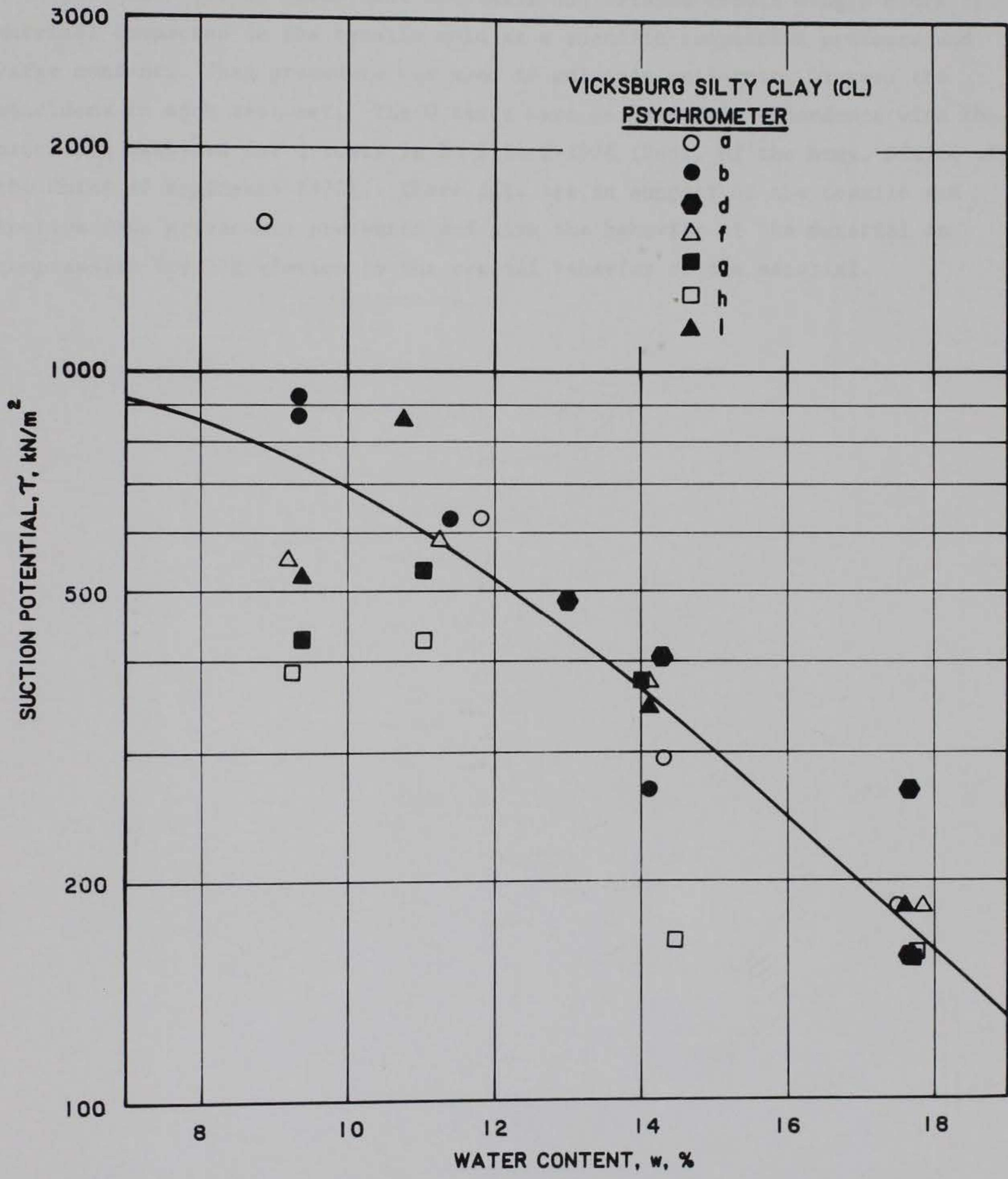


Figure C2. Suction potential versus water content for samples of Vicksburg silty clay (345 kN/m² compaction pressure)

APPENDIX D: TRIAXIAL COMPRESSION TEST DATA

1. Each set of three test specimens was trimmed from a single block of material compacted in the tensile mold at a specific compaction pressure and water content. This procedure was used to maintain uniformity between the specimens in each test set. The Q tests were performed in accordance with the procedure outlined for Q tests in EM 1110-2-1906 (Dept. of the Army, Office of the Chief of Engineers 1970). These data are in support of the tensile and suction data previously presented and give the behavior of the material in compression for correlation to the overall behavior of the material.

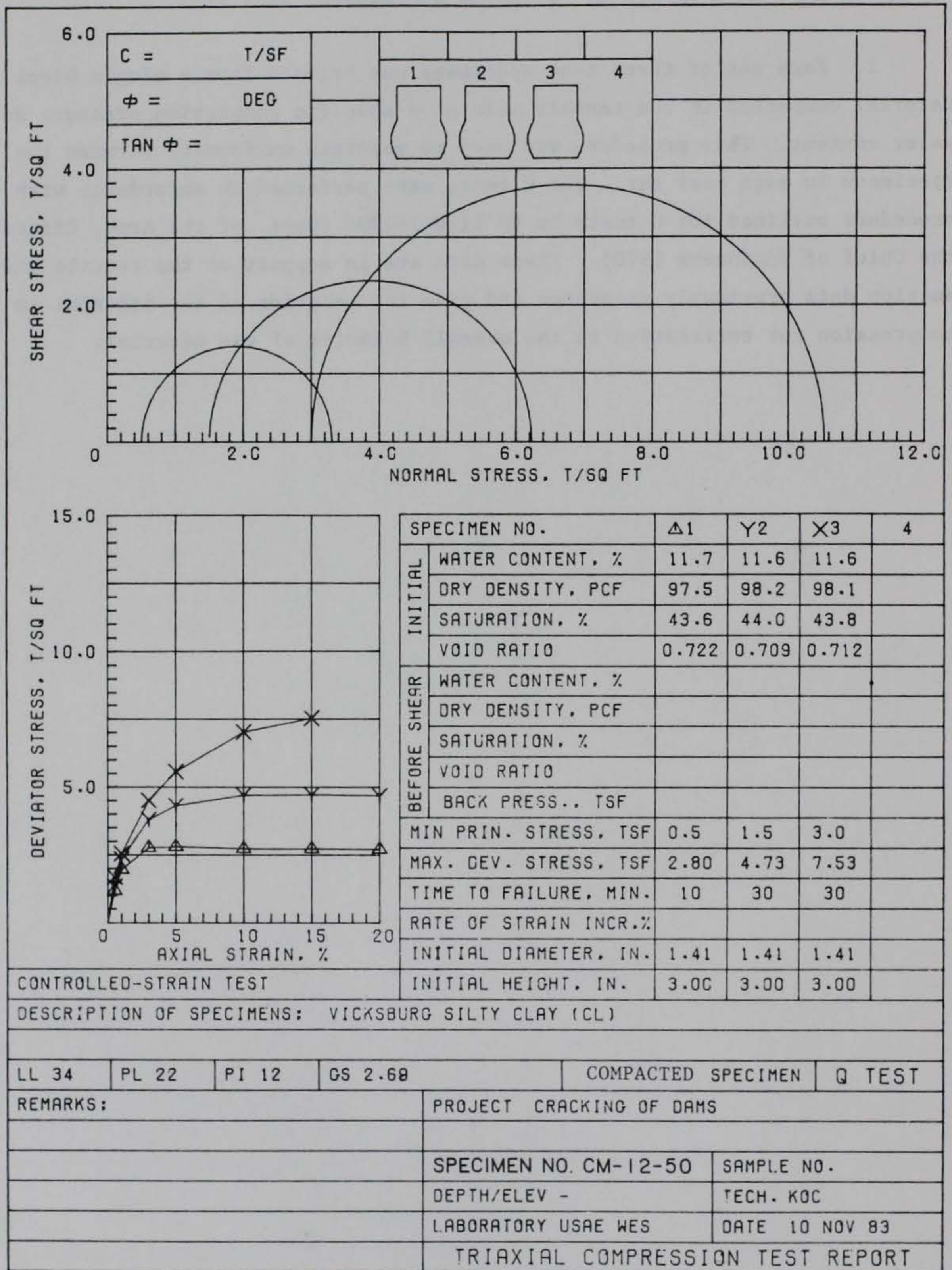


Figure D1. Triaxial compression test for specimen CM-12-50

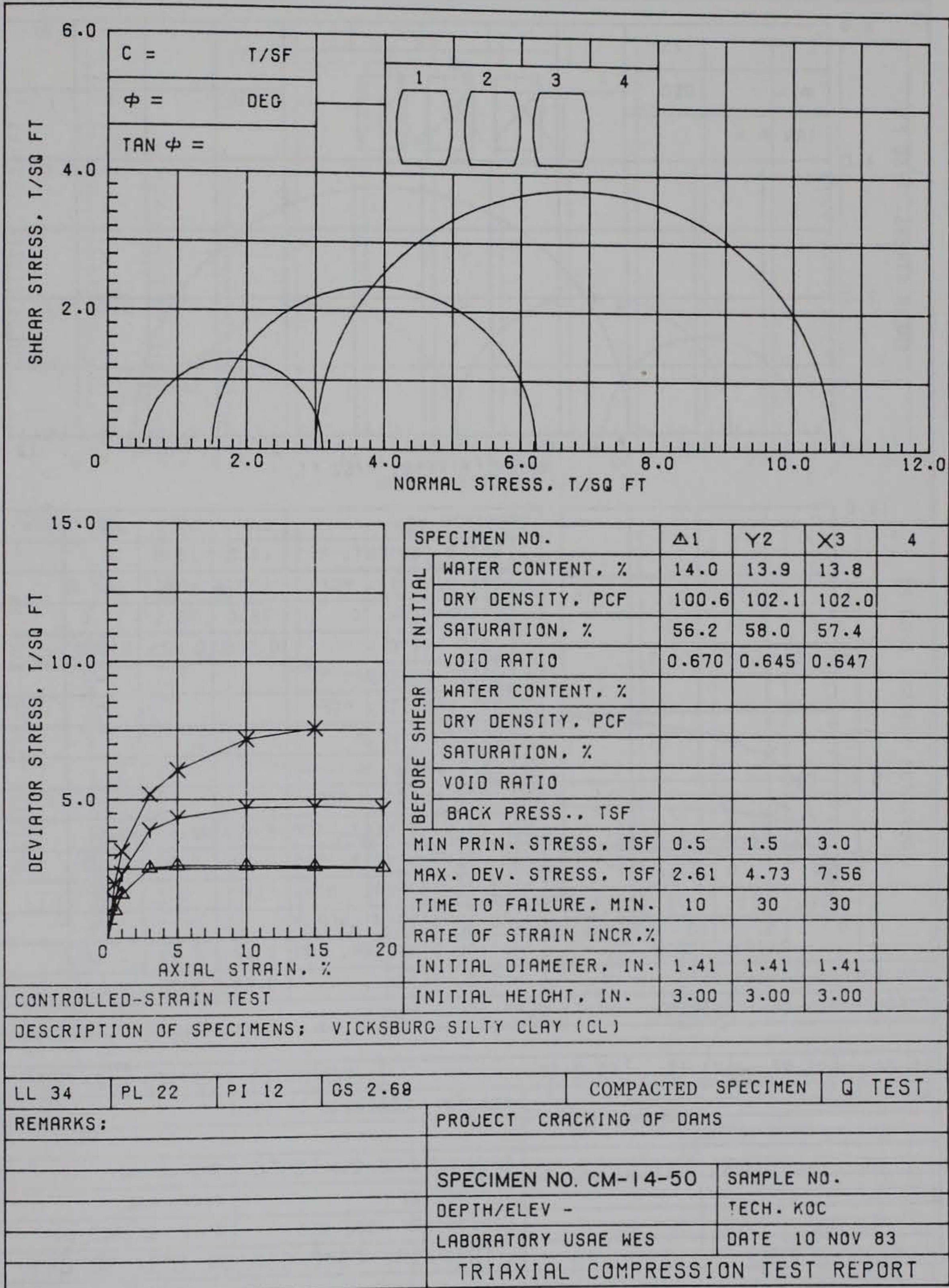


Figure D2. Triaxial compression test for specimen CM-14-50

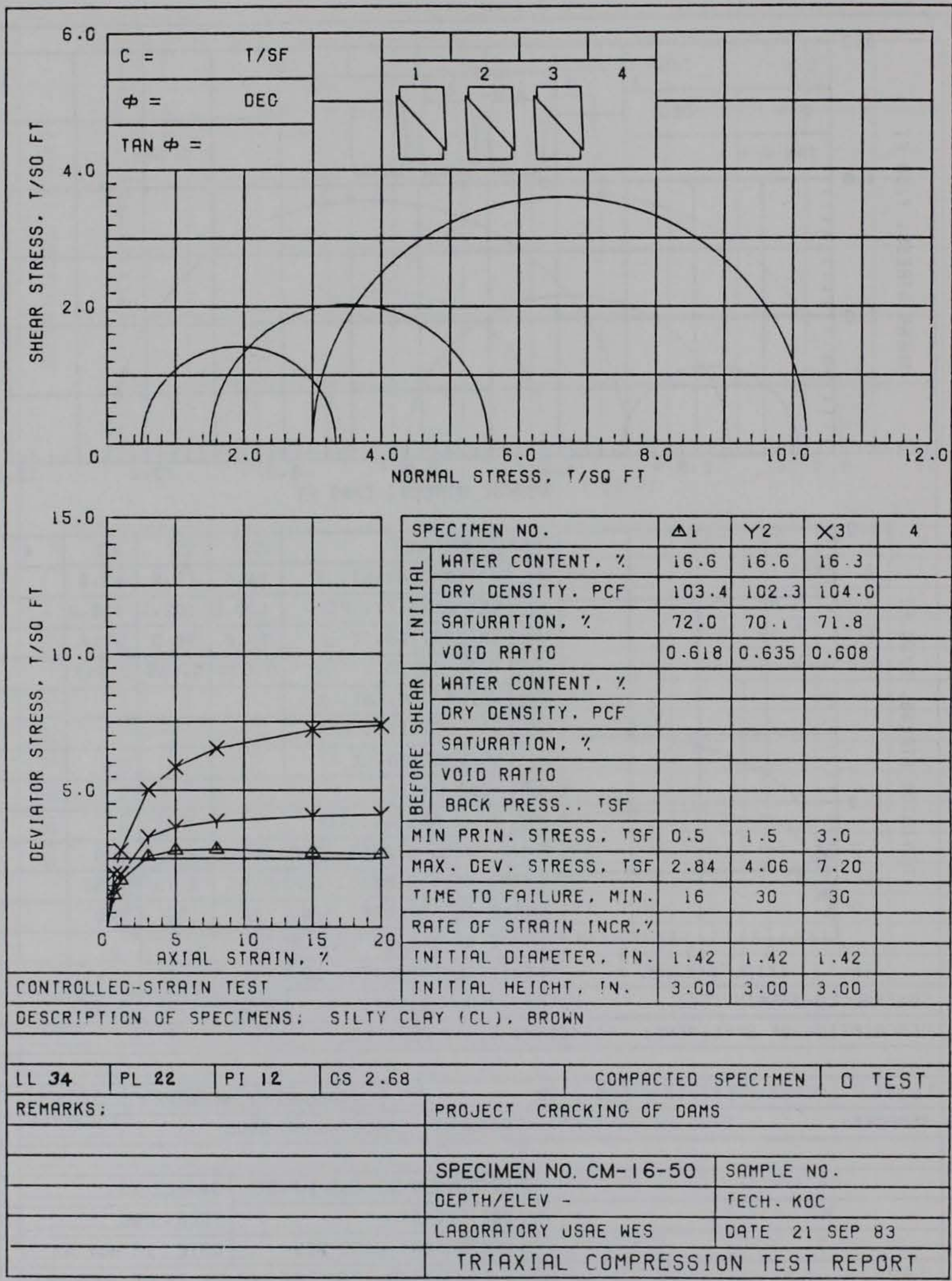


Figure D3. Triaxial compression test for specimen CM-16-50

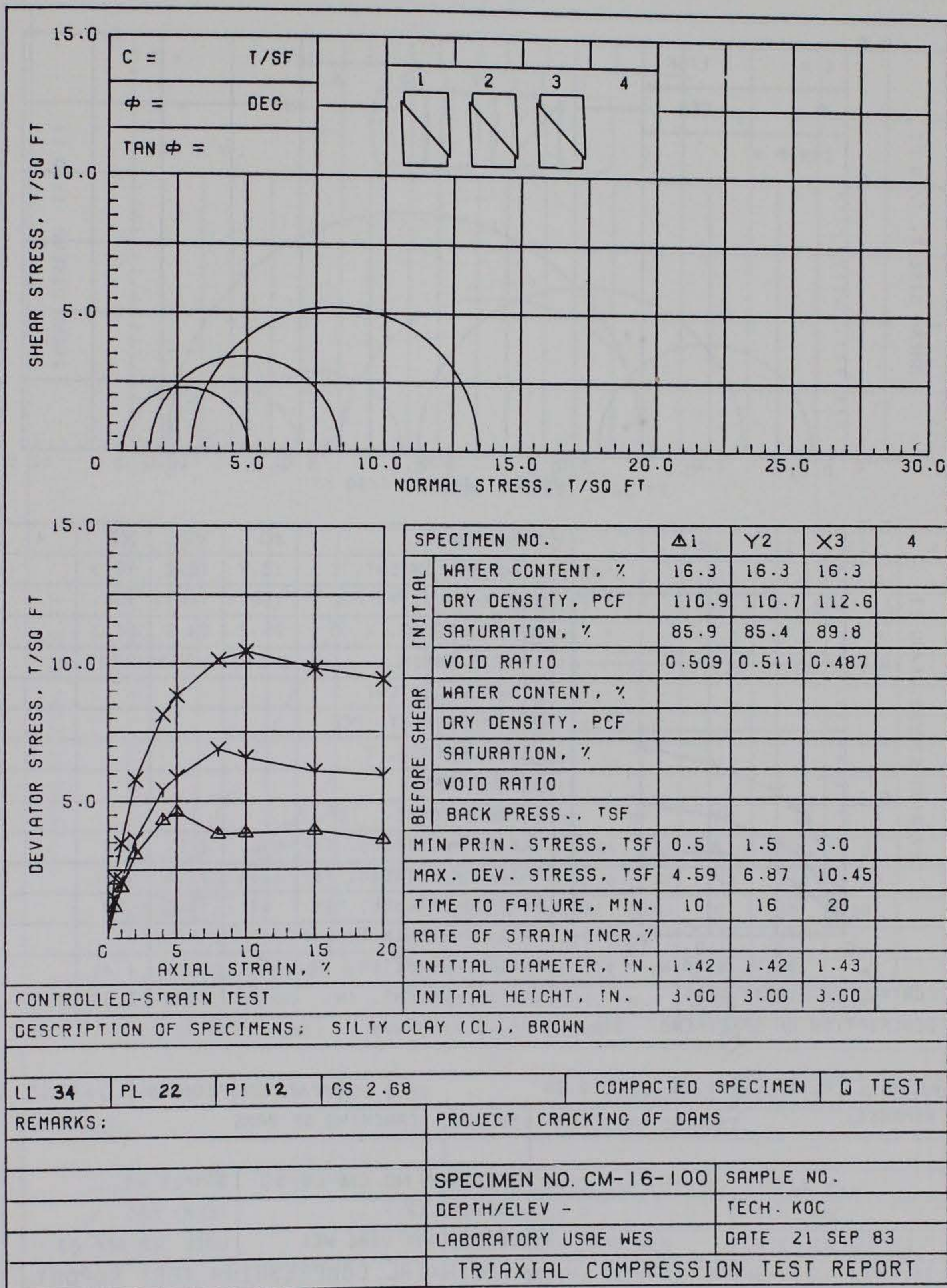


Figure D4. Triaxial compression test for specimen CM-16-100

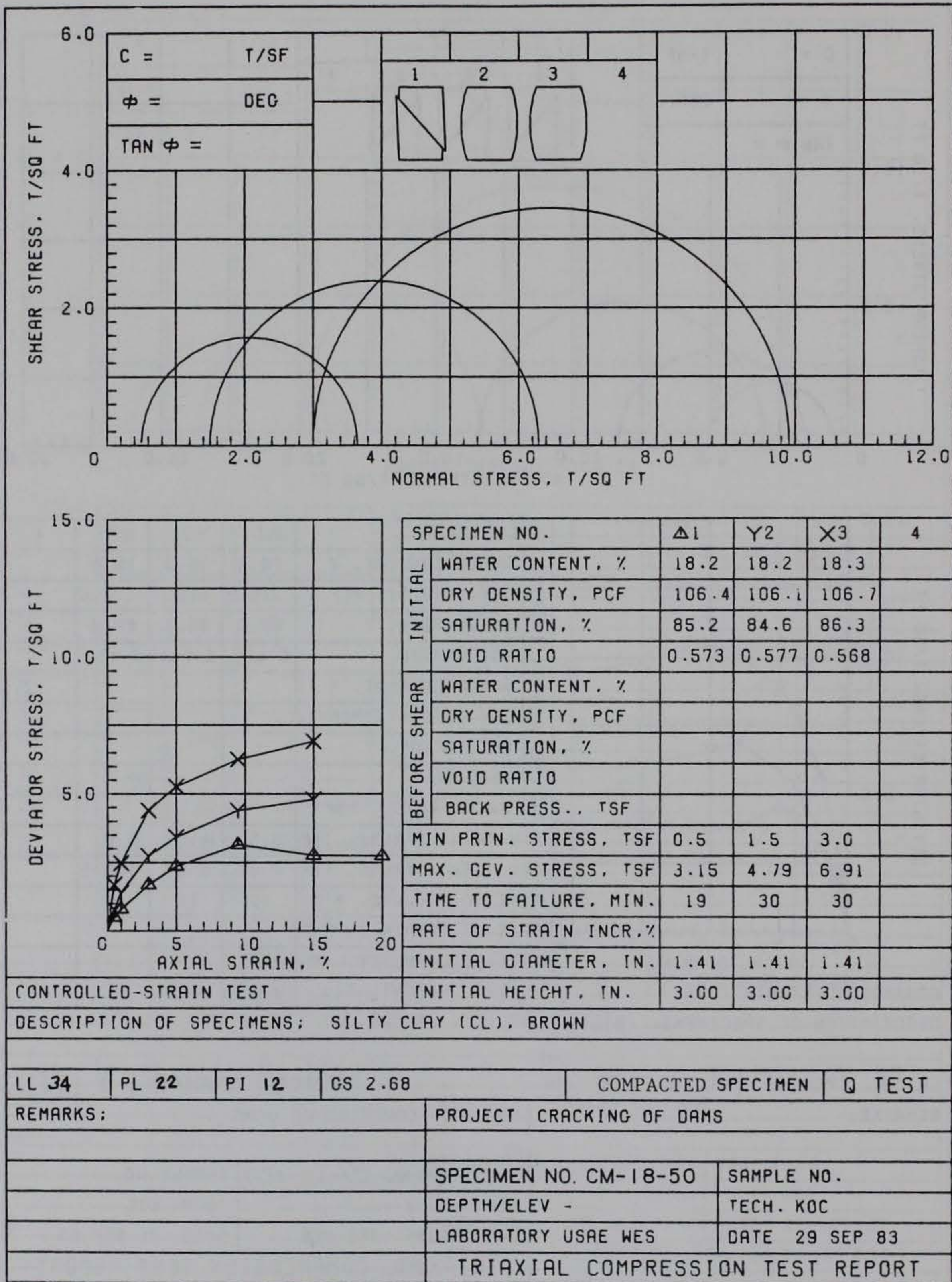


Figure D5. Triaxial compression test for specimen CM-18-50

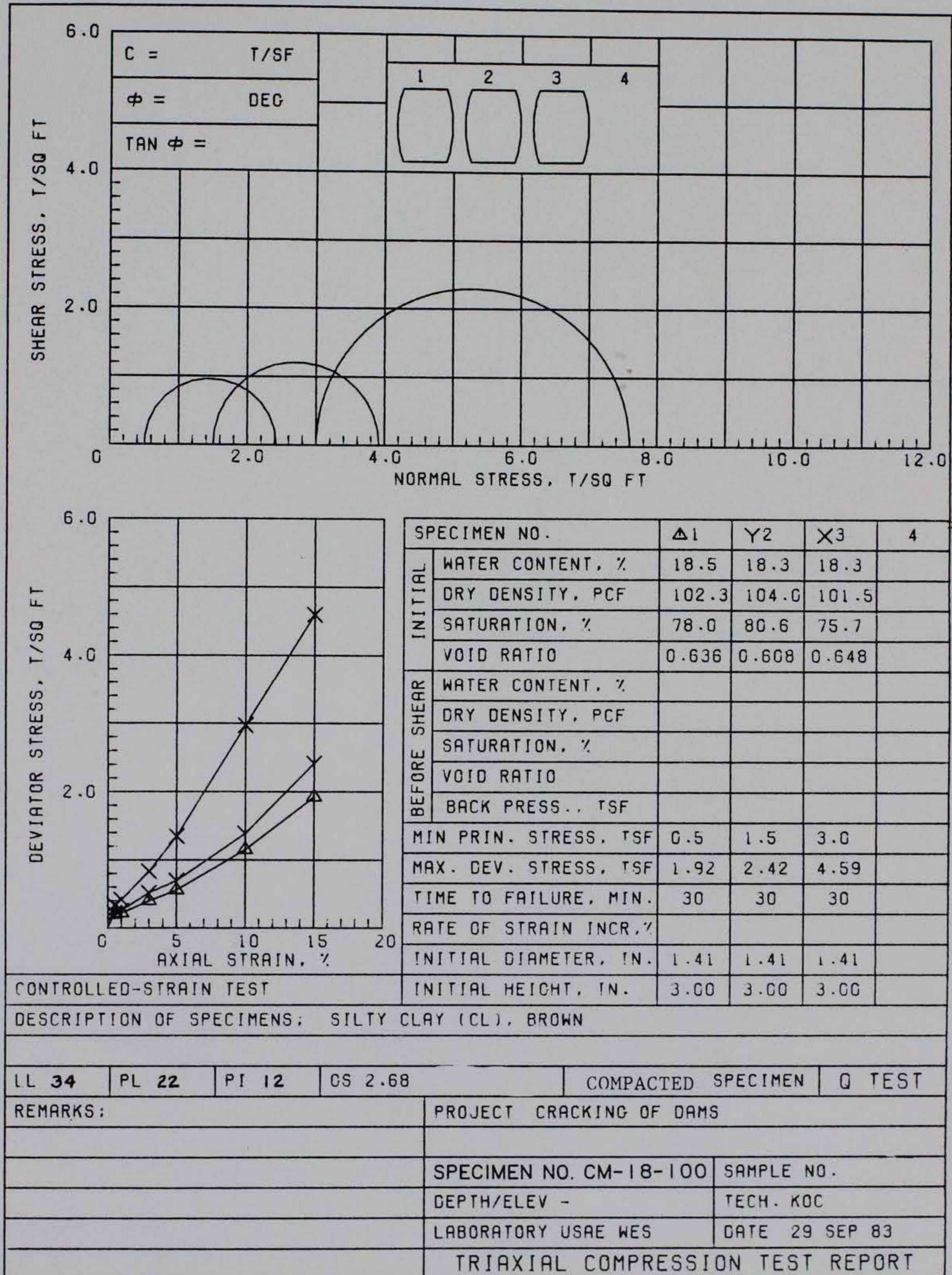


Figure D6. Triaxial compression test for specimen CM-18-100